Yuriy Romasevych, Viatcheslav Loveikin,
Alla Dudnyk, Vitaliy Lysenko, Natalia Zaets

SYNTHESIS OF ADVANCED AUTOMATIC CONTROL SYSTEMS

Monograph

Kõima 2020

Yuriy Romasevych, Viatcheslav Loveikin,
Alla Dudnyk, Vitaliy Lysenko, Natalia Zaets

SYNTHESIS OF ADVANCED AUTOMATIC CONTROL SYSTEMS

Monograph

Kõima 2020

ISBN 978-9916-4-0282-5

Synthesis of advanced automatic control systems.
Monograph, 2020, pp. 140, illus. 33, tabs. 25, bibls. 162.

Editorial Office Address: Keskuse tee, 11-29, Kõima, Pärnumaa, Estonia, 88305
e-mail: info@msdlab.eu

Recommended for publication:
by the Academic Council of Research Institute of Engineering and Technology
of National University of Life and Environmental Sciences of Ukraine
(Protocol No. 1 of September 17, 2020)
and
by the Academic Council of Research Institute of Electric Power Systems
of National University of Life and Environmental Sciences of Ukraine
(Protocol No. 6 of September 22, 2020)

Reviewers:
prof. Vladimir Kiselyov*, Educational & Scientific Institute of Municipal Governance and Municipal Economy of V.I. Vernadsky Taurida National University*
prof. Valentyn Mironenko*, National Scientific Centre „Institute for Agricultural Engineering and Electrification" of National Academy of agrarian Sciences of Ukraine*
prof. Mykola Zablodskiy*, National University of Life and Environmental Sciences of Ukraine*

Authors of Monograph
Yuriy Romasevych, Viatcheslav Loveikin,
Alla Dudnyk, Vitaliy Lysenko, Natalia Zaets

PREFACE

Modern industry, agriculture, transport are characterized by a high level of technological process automation. It is caused by requirements of obtaining quality products, exploitation of all the possible reserves of production, the substitution of man-involved work for automated one. All of these activities are connected with the application of the control systems. The monograph presents novel results in this area.

In the first chapter, authors have revealed the insights of optimal tuning of PI-controller for a wide verity of plants. Such calculations have been conducted based on the numerical optimization technique, which had been developed by the authors. In the chapter, the most used software for PID-controllers tuning is described, and the general criterion for PID-controller tuning is developed, as well.

Different modifications of controllers are studied in the second chapter. One of them is a simple modification of the integral component of the PI-controller, which leads to increase in controller performance (in terms of quality indicators). In the second chapter, a method of equalities meeting in the automated direct current drive and artificial neural network in problems of controllers' development are investigated.

In the third chapter, a method of fast controllers' synthesis has been developed. The outcome controller is characterized by advantages of the initial fuzzy-controller, (for some of the quality indicators the fast controller may outperform the initial one). The method consists of multistage procedures of tabulated function calculation, its approximation, and optimization of its parameters. The duration of executing all the necessary calculations in the algorithmic part of the fast controller is much faster than in the initial (original) fuzzy-controller.

In the fourth chapter, the features of biotechnical objects are described. As example, the poultry farms and greenhouses are considered. The control system of biotechnical objects allows providing the highest profit from the sale of products and to minimize energy costs by implementing the external disturbances forecasting. For example, the control system of growing vegetables in greenhouses allows providing the highest profit from the sale of products and to minimize energy costs by

implementing additional unit for neural network prediction of external disturbances and determine the control actions of optimal controller. The advantage of the developed control system is taking into account the effects of environmental parameters and the efficiency of decision-making based on previously obtained predictions.

The study results of noise filtering and synthesis of intelligent control systems for biotechnical objects are given in the fifth chapter. The Hilbert-Huang transformation for purifying the signal from noise is analyzed, a corresponding filter is created and the effectiveness of this approach is confirmed. The development of mathematical filters is needed to achieve the required precision of prediction. The implementation of the intelligent control system for controlling the operation modes of the electrotechnical equipment in poultry farms and greenhouses allows to reduce the cost of electricity by 25-30 %.

In the sixth chapter, the synergetic synthesis of the controller has been performed. The simulation results showed that the neural network controller, synthesized on the basis of a synergetic dynamic method, demonstrates when compared to conventional approaches, better quality indicators of transient processes and adaptation to parametric and external disturbances.

Most of the monograph's content has been obtained in the frame of scientific researches supported by the public grants for the young scientists of Ukraine „Development of high-efficient automatic controllers" (registration number 0119U100758) and "Development of resource-efficient regimes for growing vegetable products in greenhouse complexes" (registration number 0117U003966). It was conducted by scholars of National University of Life and Environmental Sciences of Ukraine: first, second and third chapters are prepared by Yuriy Romasevych and Viatcheslav Loveikin; fourth, fifth and sixth chapters are prepared by Alla Dudnyk, Vitaliy Lysenko and Natalia Zaets.

The monograph is useful for specialists in the area of automation and optimal control, scientists, workers, and operators of automated technological processes, students, and graduate students of higher technical institutions.

CHAPTER 1. PI-CONTROLLERS OPTIMAL TUNING

1.1 Analysis of software for PID-controllers tuning

In order to cope with the issues of PID-controllers tuning, manufacturers embed self-tuning features into them. However, there is a large segment of PID-controllers that do not have self-tuning functions, and therefore the issue of tuning proportional, integral and differential gains is important.

The aim of the current research is to establish functional features of state-of-the-art software for PID-controllers tuning.

INCA PID Tuner software by Inca [1] contains modules that connect to the most commonly used DCS, PLC, and RTDB systems using various OPCs. The software has state-of-the-art identification of the plants. The software calculates the optimal values of the PID gains, taking into account the limitations of DCS and PLC.

A PID-controller may be tuned with a free online service PID Tuner Controller [2]. In order to use it, one has to download the data of the plant: more than 50 samples „input-output" (the input is the steps of different magnitude, and the output is the response). The user selects the type of transfer function that matches the uploaded data. The resource automatically calculates the parameters of the transfer function and the gains of the PID-controller.

PID-Tuner by DOT X Control Solutions [3] may be used in on-line and off-line modes. On-line, it communicates with a computer or devices via OPC. These devices may be controllers Siemens, Allen Bradley, Arduino, and others. The software might use Matlab/Simulink, gProms, Aspen Technology.

Simcet software [4] by developer PiControl Solutions LLC is compatible with almost all of the world's DCS/MPC and PLC. This product performs multidimensional identification of the plants and uses obtained data to optimize gains of PID-controller.

The Protuner PID controller tuning system by Techmation Inc [5] converts the experimental data of the plant from the time domain to the frequency domain and calculates the PID-controller gains by using several different tuning methods.

PID-autotune software by Kevin Joly [6] provides automatic tuning of PID-controller with genetic algorithm. It allows building plots of a plant with open and closed loops.

In the engineering practice, one has a wide range of applications (software products) for PID-controllers tuning. They allow simplifying the process of controllers tuning. Most of the analyzed applications have advanced functionality. There is a tendency: free software has limited functions (however, it is enough for PID-controllers tuning), marketed applications allow controllers tuning and analyzing its performance.

1.2 PI-controller tuning optimization via PSO-based technique

Proportional-integral (PI) controllers are extremely common in many fields of industrial and agricultural production. A problem of PI-controller tuning has great practical meaning since it influences the efficiency of the automated process. There are hundreds of techniques for PI-controller tuning [7], but the researches in this sphere are continuing. They are caused by new requirements for automated processes, new constraints in tuning problems statements, and other reasons.

One of the approaches to the problem of PI- (or PID) controller tuning is connected with applying optimization methods, more specific – particle swarm optimization (PSO) method. Since PSO has great search abilities, it may be utilized for finding the optimal values of PI-controller coefficients. However, in already known scientific works [8-18] single-criterion optimization problems have been solved.

In these works transfer functions for heat [12], electrical [13-15], energy [16] and chemical [17] processes have been used. Note, that PSO-based PI-controller tuning may be used also for non-linear [17] or unstable [19] systems.

All of these works are related to the utilization of integral criteria. However, controlled processes are estimated with other important indicators (overshoot, settling time, etc.). Let us denote them as terminal criteria. For instance, in the article [19], the mentioned criteria were used as components of the cost function to minimize.

In order to achieve better controller performance, a complex criterion should be used, which concludes both integral and terminal criteria. In the current article, such criterion has been proposed and applied to the PI-controller tuning problem (we have considered only PI-controller because of its great spreading in practical applications).

As it was mentioned above, the most popular industrial controller is a PI-controller. That is why, in the research, a controlled with PI-controller process (plant) is under consideration. The scheme, which corresponds to it, may be presented as shown in Fig. 1.1.

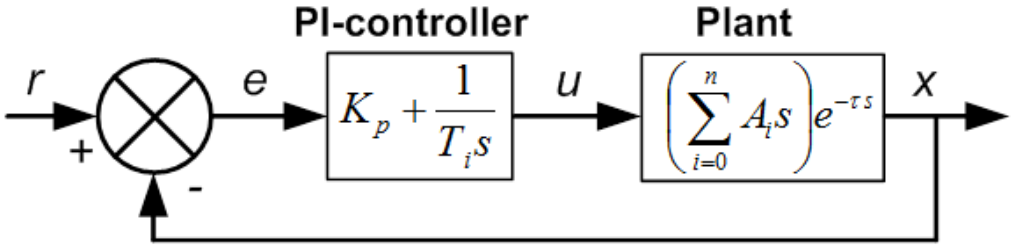

Fig. 1.1 Scheme of the closed-loop controlled process

In Fig. 1 we used followed denotations: A_i – coefficients, which depend on the parameters of the plant; n – the order of the plant; τ – time delay of the plant; u – control function (in the following we will denote it as „control”); K_p and T_i – proportional and integral coefficients of PI-controller respectively, e – error, which is defined as the reminder of the controlled variable x and set point r subtraction. Consequently, a mathematical model of PI-controller in the time domain is described with the following expression:

$$u = K_p e + T_i^{-1} \int_0^t e dt, \tag{1.1}$$

where t – time. Tuning of PI-controller is the process of finding the values K_p and T_i for a particular order of the plant n, and values A_i.

One of the most important demands of the PI-controller is providing the stability of the process. That demand may be expressed in the following manner:

$$\begin{cases} \lim\limits_{t\to\infty} x = r; \\ \lim\limits_{t\to\infty} \dfrac{d^i x}{dt^i} = 0, \quad i = (\overline{1,\ n}). \end{cases} \tag{1.2}$$

In practical calculations, infinity is substituted with some moment of time:

$$\begin{cases} x(T) = r \pm \Delta = r_\Delta; \\ \dfrac{d^i x(T)}{dt^i} \approx 0, \end{cases} \tag{1.3}$$

where Δ – acceptable process error, which for many cases is equal to $0{,}05r$ (such value has been used in the research), r_Δ – the acceptable value of the process variable, T – the moment when the conditions (1.3) are met. In the research we use the conditions (1.3), rather than other stability criteria, as they can be presented in the form of the following criteria to minimize:

$$Ter_E = \sqrt{(x(T) - r_\Delta)^2 + \sum_{i=1}^{n} \left(\frac{d^i x(T)}{dt^i} \right)^2} \to \min \tag{1.4}$$

or

$$Ter_M = \left| x(T) - r_\Delta \right| + \sum_{i=1}^{n} \left| \frac{d^i x(T)}{dt^i} \right| \to \min, \tag{1.5}$$

where Ter_E and Ter_M – Euclidian and Manhattan norms respectively. The absolute minima of the criteria (1.4) and (1.5) are equal to zero. Indeed, reducing of (1.4) or (1.5) to zero allows to meet conditions (1.3). Such an approach to satisfy the stability satisfaction brings the foundation for reducing the initial problem to the problem of unconstrained optimization. In the opposite case, using Hurwitz or another similar

criterion involves constraints in the optimization problem statement and substantially that complicates it.

The choice of a particular criterion depends on its effectiveness. In the current investigation, better performance has revealed criterion (1.5) and all the further numerical data which are related to its applying.

The quantity of the numbers K_p and T_i, which allow to minimize criterion (1.5), is equal to infinity. It provides the possibility of utilizing additional requirements. Such requirements may be presented as minimization of widely spread in the practice *IAE* (Integral Absolute Error) or *ISE* (Integral Square Error) criteria. The use of these, for low order transfer functions, allows finding analytical expressions for K_p and T_i [7]. However, *IAE* or *ISE* reflects only one aspect of control quality, which is connected with the error.

In the research, we have taken into consideration more general criterion, which includes other important indicators of the PI-controller exploitation. It can be presented as follows:

$$Cr = \delta_1 \cdot t_s^{-1} \int_0^{t_s} |e| dt + \delta_2 \cdot t_s^{-1} \int_0^{t_s} |u| dt + \delta_3 \cdot \frac{e_{\max}}{r} + \delta_4 \cdot t_s, \qquad (1.6)$$

where $\delta_1 ... \delta_4$ – weight coefficients (each of these coefficients shows the impact of the particular summand), $e_{\max}$ – maximum of error, t_s – settling time.

The first summand in the expression (1.6) corresponds to the mean integral error (it is proportional to *IAE*). The second summand is the similar value of control *u*. It shows "the cost" of the system control. The third summand is proportional to the overshoot and the fourth one is proportional to the settling time. All of these indicators are undesirable, which causes the need of criterion (1.6) minimization.

Thus, we have reduced the PI-controller tuning problem to the optimization problem. It may be expressed in such a manner:

$$Cr + \delta_T \cdot Ter_M \rightarrow \min_{K_p \in P;\ T_i \in I}, \qquad (1.7)$$

where P and I – search domains for proportional and integral coefficients of PI-controller respectively, δ_T – terminal weight coefficient, which shows the requirement of conditions (1.3) satisfaction. Expression (1.7) shows, that the minimization of the sum $Cr+\delta_T \cdot Ter_M$ should be performed with respect to the coefficients K_p and T_i. Their values may be varied in domains P and I respectively.

One of the important issues in problem solving is the choice of an appropriate method. In the research, the modification of particle swarm optimization (PSO) was used. It is called multi-epoch PSO (ME-PSO) [20].

In the ME-PSO method, a swarm is a set of particles which move on the surface of minimized function (1.7). The position of a particle is described by a set of its coordinates ($K_{p,j}$, $T_{i,j}$) in the search domains P and I. At the initial stage of ME-PSO algorithm, the particles' positions are randomly initialized. During subsequent iterations, the components of the position vector of a particle are updated according to the formulas:

$$\begin{cases} K_p^j = K_p^{j-1} + c_1 r_1 (p_{K_p} - K_p^{j-1}) + c_2 r_2 (g_{K_p} - K_p^{j-1}); \\ T_i^j = T_i^{j-1} + c_1 r_1 (p_{T_i} - T_i^{j-1}) + c_2 r_2 (g_{T_i} - T_i^{j-1}), \end{cases} \quad (1.8)$$

where K_p^j and T_i^j – are components of the position vector of the particle on j-th iteration (the previous iteration is denoted with (j-1) superscript); p_{K_p} and p_{T_i} – coordinates of the best position of a particle, that has been found on the previous iterations (personal best); g_{K_p} and g_{T_i} – coordinates of the best position, that has been found by the swarm on the previous iterations (global best); c_1 and c_2 – cognitive and social coefficients respectively; r_1, r_2 – random numbers that are generated on the interval [0, 1]. An iteration of PSO algorithm includes applying the formulas (1.8) and updating the global and personal bests according to the rules:

$$\begin{cases} p_{K_p} = K_p^j, \ if \ \ Cr(K_p^j) + \delta_T \cdot Ter_M(K_p^j) < Cr(p_{K_p}) + \delta_T \cdot Ter_M(p_{K_p}); \\ p_{T_i} = T_i^j, \ if \ \ Cr(T_i^j) + \delta_T \cdot Ter_M(T_i^j) < Cr(p_{T_i}) + \delta_T \cdot Ter_M(p_{T_i}); \\ g_{K_p} = p_{K_p}, \ if \ \ Cr(p_{K_p}) + \delta_T \cdot Ter_M(p_{K_p}) < Cr(g_{K_p}) + \delta_T \cdot Ter_M(g_{K_p}); \\ g_{T_i} = p_{T_i}, \ if \ \ Cr(p_{T_i}) + \delta_T \cdot Ter_M(p_{T_i}) < Cr(g_{T_i}) + \delta_T \cdot Ter_M(g_{T_i}). \end{cases} \quad (1.9)$$

During the execution of classical PSO, particles may trap into a local minimum of the function (1.7). In this case, the swarm tends to stagnation: its exploration features are considerably declining. A stagnant swarm is unable to find the global minimum of the criterion (1.7).

The novelty of the ME-PSO technique is in the reinitialization of the stagnant swarm. The indicator of the swarm stagnation is as follows:

$$AR \geq \frac{Cr(g_{T_i}^{j}) + \delta_T \cdot Ter_M(g_{T_i}^{j}) - Cr(g_{T_i}^{j-1}) - \delta_T \cdot Ter_M(g_{T_i}^{j-1})}{Cr(g_{T_i}^{j}) + \delta_T \cdot Ter_M(g_{T_i}^{j})}, \qquad (1.10)$$

where AR – is an acceptable rate of the global best reduction. If condition (1.10) is required, then swarm should be reinitialized: positions of all particles become random. Such an approach allows to continue the exploration procedure and to find the global minimum of the criterion (1.7).

In the conducted research we have used parameters of ME-PSO, which are given in Table 1.1.

Table 1.1 Parameters of optimization algorithm ME-PSO

Parameters	Value
social coefficient c_1	2.1
cognitive coefficient c_2	0.1
swarm population	50
connection topology	full
acceptable rate AR	0.1
number of iterations	50

In order to investigate the impact of the values $\delta_1 \ldots \delta_4$ on the PI-controller tuning efficiency, they have been varying through numerical experiments. Used $\delta_1 \ldots \delta_4$ values are given in Table 1.2.

In order to prove the superiority of the developed tuning technique, all the results were compared with the results of tuning PI-controller, with other well-known in the engineering practice methods:

1) Ziegler-Nichols [21];
2) Kappa-Tau [22];
3) AMIGO [23];
4) Chien-Hrones-Reswick [24];
5) Cohen-Coon [25];
6) Lambda Tuning [26];
7) Skogestad [27];
8) Tyreus-Luyben [28].

Table 1.2 Values of coefficients $\delta_1 \ldots \delta_4$

Notation	Weight coefficients values				
	δ_T	δ_1	δ_2	δ_3	δ_4
ME-PSO-Error	1000	1000	1	5	1
ME-PSO-Control	1000	1	1000	5	1
ME-PSO-Duration	1000	1	1	5	1000

The indicators, which have been used for determination of control quality are: mean integral error $t_s^{-1}\int_0^{t_s}|e|dt$ (MIE), mean integral control $t_s^{-1}\int_0^{t_s}|u|dt$ (MIC), overshoot (OS), and settling time t_s.

In order to prove the superiority of the developed PI-controller tuning technique, five benchmark transfer functions have been used. They are proposed by K.J. Åström and T. Hägglund in the work [29]. For each transfer function the search domains for proportional and integral coefficients were different (Table 1.3).

Table 1.3 Conditions of the experiments

Transfer function	Search domain	
	P	I
1	2	3
$G_1(s)=1/(s+1)^2$	0…10	0…10
$G_2(s)=1/(s+1)^3$	0…10	0…10

Table 1.3 continuation

1	2	3
$G_3(s)=(1-0.1s)/(s+1)^3$	0…10	0…10
$G_4(s)=1/(s+1)(1+0.1s)(1+0.01s)(1+0.001s)$	0…50	0…10
$G_5(s)=e^{-s}/(0.5s+1)^2$	0…10	0…20

All the obtained results are given in Table 1.4. The best values in Table 1.4 are in bold.

Table 1.4 Results of numerical experiments

Tuning method	Parameters		MIE	MIC	OS, %	t_s, sec
	K_p	T_i				
1	2	3	4	5	6	7
First experiment						
Ziegler-Nichols	2.173	0.899	0.33	1.39	9.2	3.0
Kappa-Tau	0.436	2.238	0.50	0.93	3.2	4.6
AMIGO	0.495	2.559	0.44	0.90	0.0	5.7
Chien-Hrones-Reswick	1.449	1.618	0.25	1.07	0.0	6.0
Cohen-Coon	3.001	0.350	0.22	1.30	37.2	5.8
Lambda Tuning	0.293	4.828	0.35	0.80	0.0	13.2
Skogestad	1.500	1.000	0.31	1.27	9.3	3.9
ME-PSO-Error	10.000	1.313	0.14	1.62	29.3	6.6
ME-PSO-Control	0.000	9.701	0.38	0.69	0.0	24.3
ME-PSO-Duration	1.257	1.336	0.51	1.30	1.9	2.5
Second experiment						
Ziegler-Nichols	1.229	3.438	0.25	0.98	0.0	12.2
Kappa-Tau	0.245	4.836	0.49	0.81	0.6	9.7
AMIGO	0.295	5.637	0.40	0.81	0.0	13.6
Chien-Hrones-Reswick	0.820	6.188	0.25	0.88	0.0	22.9

Table 1.4 continuation

1	2	3	4	5	6	7
Cohen-Coon	2.057	0.831	0.22	1.12	55.7	20.3
Lambda Tuning	0.268	6.464	0.38	0.80	0.0	16.4
Skogestad	0.500	3.000	0.37	1.00	5.8	9.0
Tyreus-Luyben	2.500	3.225	0.17	1.01	13.6	17.7
ME-PSO-Error	2.450	3.100	0.17	1.01	12.8	17.0
ME-PSO-Control	0.000	7.730	0.51	0.68	0.6	15.2
ME-PSO-Duration	0.718	2.834	0.56	1.06	2.0	5.0
Third experiment						
Ziegler-Nichols	1.135	4.025	0.23	0.95	0.0	15.6
Kappa-Tau	0.229	5.184	0.49	0.80	0.4	10.5
AMIGO	0.280	5.974	0.40	0.81	0.0	14.5
Chien-Hrones-Reswick	0.757	7.245	0.25	0.86	0.0	26.8
Cohen-Coon	1.963	0.900	0.20	1.09	55.2	24.0
Lambda Tuning	0.264	6.558	0.38	0.80	0.0	16.5
Skogestad	0.469	3.200	0.56	0.96	4.9	6.0
Tyreus-Luyben	1.923	4.702	0.17	0.94	1.0	23.4
ME-PSO-Error	3.271	3.556	0.15	1.04	30.8	25.6
ME-PSO-Control	0.000	7.900	0.51	0.68	0.6	15.4
ME-PSO-Duration	0.944	2.558	0.59	1.18	4.2	4.2
Fourth experiment						
Ziegler-Nichols	8.536	0.041	0.28	2.68	40.2	0.9
Kappa-Tau	2.199	0.235	0.25	1.47	13.4	1.9
AMIGO	2.651	0.236	0.24	1.54	9.5	1.7
Chien-Hrones-Reswick	5.691	0.074	0.32	2.15	27.8	0.9
Cohen-Coon	9.364	0.031	0.25	2.74	48.9	1.2
Lambda Tuning	6.380	0.035	0.25	2.22	53.1	1.6
Skogestad	8.606	0.057	0.35	2.93	31.2	0.6

Table 1.4 continuation

1	2	3	4	5	6	7
Tyreus-Luyben	34.409	0.013	0.22	7.78	70.2	1.3
ME-PSO-Error	27.836	0.259	0.21	5.99	44.0	0.8
ME-PSO-Control	1.804	0.547	0.38	1.39	0.0	1.4
ME-PSO-Duration	13.419	0.085	0.26	3.62	28.0	0.7
Fifth experiment						
Ziegler-Nichols	0.492	8.755	0.26	0.80	0.0	30.9
Kappa-Tau	0.130	4.352	0.46	0.75	0.0	9.3
AMIGO	0.216	3.767	0.44	0.79	0.0	8.3
Chien-Hrones-Reswick	0.328	15.760	0.28	0.76	0.0	53.6
Lambda Tuning	0.207	18.728	0.29	0.74	0.0	60.0
Skogestad	0.300	2.500	0.63	0.87	4.9	4.1
Tyreus-Luyben	0.544	14.922	0.25	0.79	0.0	56.2
ME-PSO-Error	0.782	2.822	0.26	0.93	0.0	9.4
ME-PSO-Control	0.000	5.393	0.52	0.66	0.0	9.7
ME-PSO-Duration	0.508	2.344	0.66	0.94	1.7	2.4

Analysis of the figures that are given in Table 1.4 shows that the used approach is effective for minimization of the undesirable indicators. For example, the optimal settling time for the first experiment is 1.20…5.28 times smaller than similar values of other PI-controller tuning methods. For the second experiment, it ranges from 1.80 to 4.58, for the third is from 1.43 to 6.38, and for the fifth one is from 1.7 to 25.0. For all results of ME-PSO-Duration approach, the overshoot is no more than 4.2% (Fig. 1.2, a, c, e).

Obtained results confirm the suggestion about an invariant property of the developed approach. Indeed, as the calculations of coefficients K_p and T_i are performed numerically, more complicated transfer functions will not make significant obstacles for technique application.

Minimization of indicator MIE allowed us to reduce mean values of error during transition mode. However, criterion MIE utilizing has a disadvantage, which is connected with quite big overshoot (Fig. 1.2, b). In fact, that effect to a greater or a lesser extent has been revealed almost for all experiments (except the fifth one). For instance, the minima of indicator MIE for the transfer functions $G_1(s)$, $G_2(s)$, $G_3(s)$, $G_4(s)$ vary in the range 12.8…44.0%. It means that using single indicator MIE does not lead to a good quality of tuned PI-controller performance. Indicator MIE should be used only as a part of the complex optimization criterion.

Using in the calculations criterion MIC is connected with minimization of control mean value and reducing the overshoot (Fig. 1.2, d). In the frame of the research, the obtained values of the overshoot were 0.0…0.6%. From this point of view, criteria MIE and MIC are the opposite.

The use of the proposed approach (ME-PSO-Control) allowed us to find the smallest values of MIC for all experiments. They are less by 1.20…5.59 times than those that related to the eight engineering PI-controller tuning methods.

For the fourth numerical experiment, we have obtained zero overshoot (Fig. 1.2, d) while for the rest of the results that indicator varies from 9.5% to 70.2%.

Positive results have been received for the transfer function with delay $G_5(s)$. These data support the previous suggestion about the invariability of the technique towards the complexity of the system under PI-control.

In order to estimate the obtained results, graphics for the most popular tuning methods as well as for ME-PSO-based method have been plotted (Fig. 1.2). They support the previous conclusion about the superiority of the developed technique over known in engineering practice PI-controller tuning methods.

Analysis of the figures in Table 1.4 allows us to state that the developed technique of PI-controller tuning is effective. Indeed, almost all undesirable indicators are smaller than those that have been calculated with the known PI-controller tuning methods.

Varying the values of the weight coefficients $\delta_1...\delta_4$ provides technique flexibility. That is why a user of the algorithm may obtain desirable results (in terms

of minimization of criterion (1.6) components) by setting the values of weight coefficients.

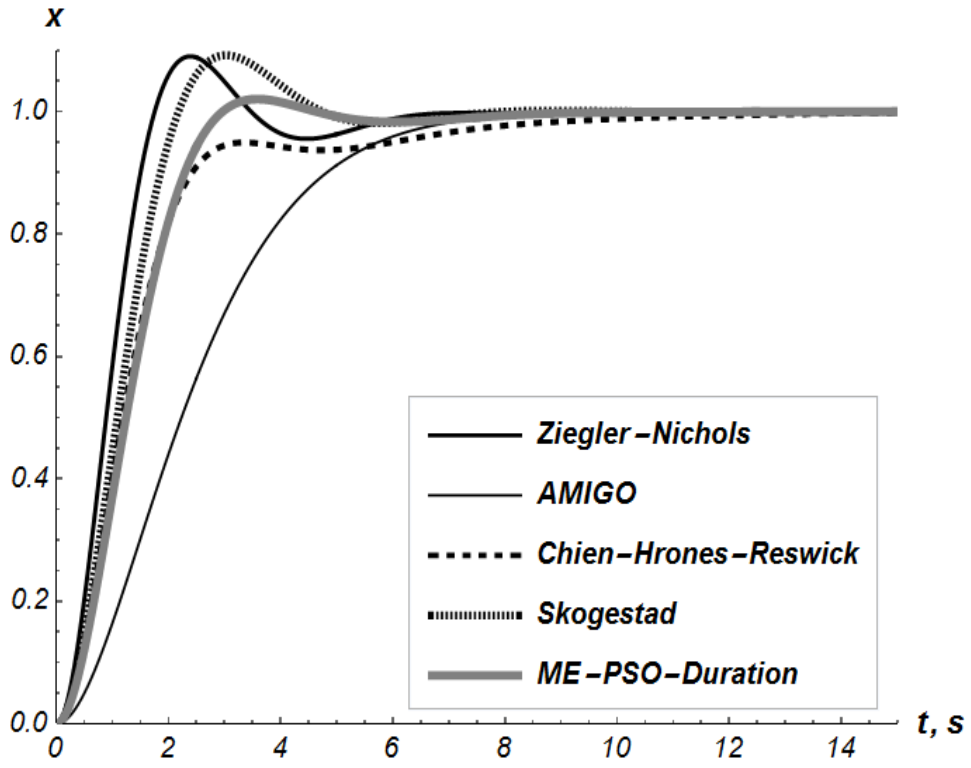

a)

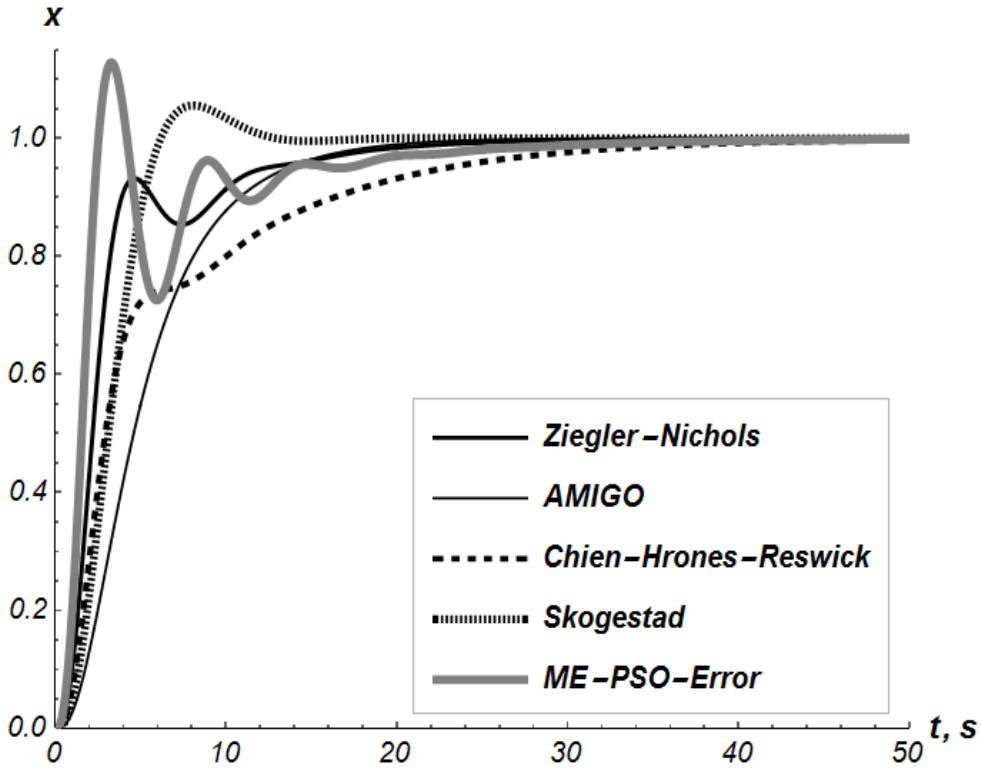

b)

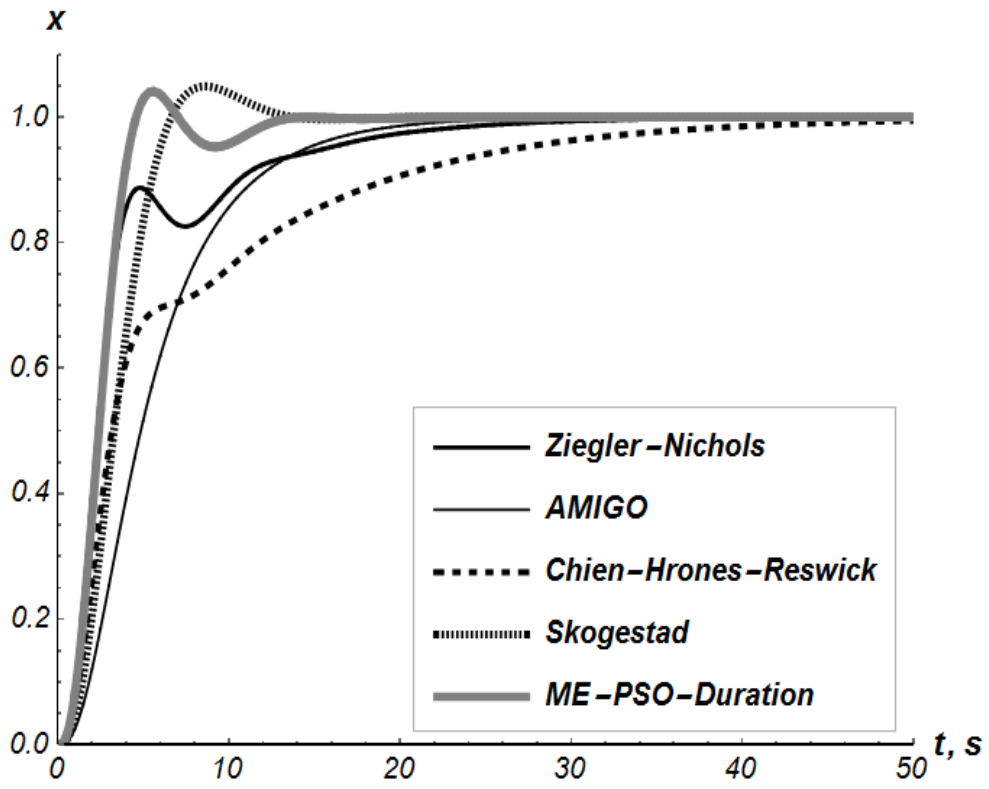
x
1.0
0.8
0.6
0.4
0.2
0.0
0
10
20
30
40
50
t, s
Ziegler–Nichols
AMIGO
Chien–Hrones–Reswick
Skogestad
ME–PSO–Duration

c)

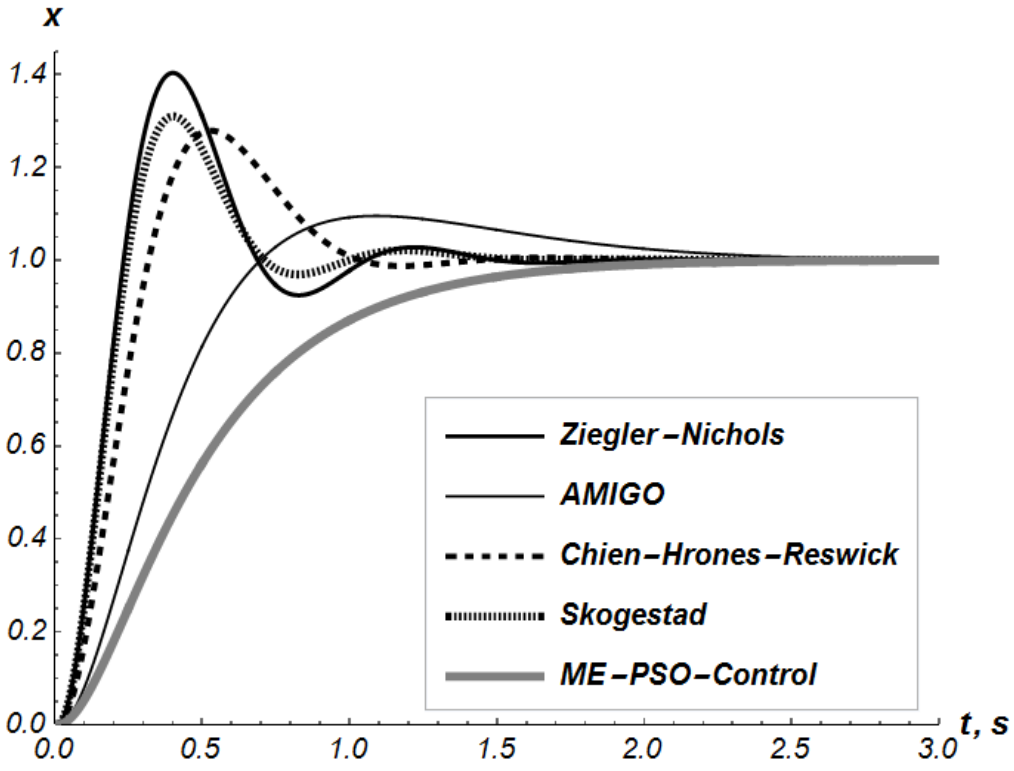
x
1.4
1.2
1.0
0.8
0.6
0.4
0.2
0.0
0.0
0.5
1.0
1.5
2.0
2.5
3.0
t, s
Ziegler–Nichols
AMIGO
Chien–Hrones–Reswick
Skogestad
ME–PSO–Control

d)

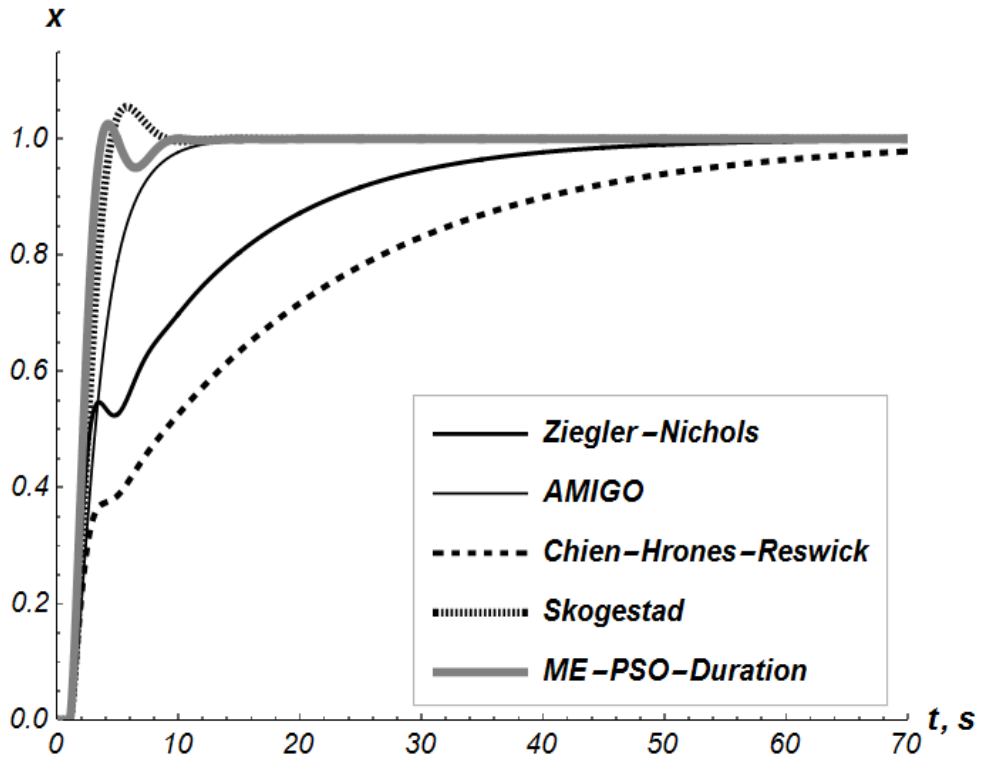

e)

Fig. 1.2. Systems' responses for experiments: a) first; b) second; c) third; d) fourth; e) fifth

Implementing of the proposed tuning algorithm requires special software development. It may help engineers to tune and retune PI-controllers. Another way of using the technique is connected with its implementation in the intelligent algorithms for PI-controllers self-tuning.

The developed technique may be generalized for the systems which are described by MIMO mathematical models (including non-linear ones) [30].

1.3 Optimization of PI-controller by a new criterion

1.3.1 Development a general criterion for PID-controller tuning

Proportional-integral-derivative (PID) controllers are widely spread in many fields of industry. They are used in electrical, heat, mechanical, and other processes.

Note, that in order to effectively exploit a PID-controller it should be properly tuned. That problem has been attracting scientists for decades. It is still important nowadays.

In the frame of the research, we will consider PID-controller, which is connected with its simplicity, efficiency, and extremely wide spreading.

In order to reflect the PID-controller performance a lot of criteria have been developed. In the current research, we will focus on the time-domain criteria, more specific – on the integral type criteria. Tuning a PID-controller in relation to values of these criteria allows to improve dynamical features of the PID-controller. Thus, the selection of criterion for PID-controller tuning – is a very important problem, which influences the tuned controller efficiency.

The main purpose of the study is to develop a novel criterion for purposes of PID-controllers tuning. Note, that proposed in the research indicator (criterion) may be used for P-, PD- or PI-controllers.

In order to achieve the stated purpose, the following objectives should be accomplished: 1) to carry out an analysis of the integral criteria that are exploited in the controllers tuning procedures; 2) proposed criterion which takes into account the values of error, control and settling time.

In many scientific researches, in order to tune coefficients of a PID-controller following values have been used:

ITAE (Integral of Time multiplied by Absolute Error):

$$I_{ITAE} = \int_0^T t|e|dt, \tag{1.11}$$

where e – the current error (difference of set-point and controlled parameter values); t – time; T – settling time;

IAE (Integral of Absolute Magnitude of the Error):

$$I_{IAE} = \int_0^T |e|dt; \tag{1.12}$$

ISE (Integral of the Square of the Error):

$$I_{ISE} = \int_0^T e^2 dt; \tag{1.13}$$

ITSE (Integral of Time multiplied by the Square of the Error):

$$I_{ITSE} = \int_0^T te^2 dt. \tag{1.14}$$

Similar criteria may be designed for control estimation. In order to do this in the formulas (1.11)-(1.14) the character „*e*" should be substituted to the „*u*" (control or output function of a PID-controller). In these cases, we will obtain the following criteria: *ITAC* (Integral of Time multiplied by Absolute Control); *IAC* (Integral of Absolute Magnitude of the Control); *ISC* (Integral of the Square of the Control); *ITSC* (Integral of Time multiplied by the Square of the Control).

As we have seen, there is no single value which takes into account the main features of the controller performance. Such criterion may be presented as the *IPTEC* (Integral of Powered of Time multiplied by the Error multiplied by the Control) value:

$$I_{IPTEC} = \int_0^T t^\tau \left(\sqrt{e^2}\right)^\varepsilon \left(\sqrt{u^2}\right)^\nu dt, \tag{1.15}$$

where τ, ε, and ν – indexes of power of time, error, and control.

Note, that the proposed value (1.15) is a quite general criterion for PID-controller tuning. Indeed, one can state relations between *IPTEC* and known criteria. They are presented in Table 1.5.

Table 1.5 Relations between *IPTEC* and known criteria

Values of indexes τ, ε and ν in *IPTEC*			Criterion
τ	ε	ν	
1	2	3	4
1	1	0	*ITAE*
0	1	0	*IAE*

Table 1.5 continuation

1	2	3	4
0	2	0	*ISE*
1	2	0	*ITSE*
1	0	1	*ITAC*
0	0	1	*IAC*
0	0	2	*ISC*
1	0	2	*ITSC*
0	0	0	*T*

The further directions for investigation are connected with the study of influence the values of indexes τ, ε, and ν to performance of the tuned PID-controller [32].

1.3.2 PI-controller tuning optimization

Proportional-integral (PI) controllers are used in many fields of industry. The tuning of PI-controller is a very important issue, which has a great influence on quality indicators of automated technological processes. There are hundreds of tuning techniques [7]. Among them, optimization-based approaches allow finding the best (in a sense) values of proportional and integral coefficients of PI-controller.

One of the main elements in such optimization techniques is the criterion. Another point of the problem is the optimization method. It is used for the calculation of optimal values of proportional and integral coefficients of PI-controller. Successful selection of the criterion and method provides effective tuning of a PI-controller. Thus, its further exploitation will be effective.

The main purpose of the study is to develop the technique of calculation of PI-controller optimal parameters, which is based on the metaheuristic method. In order to achieve the stated purpose, the following objectives should be accomplished: 1) to justify the optimization criterion for PI-controller tuning; 2) to conduct calculation of

PI-tuning for a set of benchmark transfer functions. One of the criteria which takes into account the settling time, cost of error and control, may be presented in the form (1.15). In order to illustrate the advantages of the proposed criterion, the numerical experiments have been conducted. In the experiments, we have used three benchmark transfer functions (they are proposed by K.J. Åström and T. Hägglund in the work [29]). The limits of the search domains for calculation of optimal values of PI-controller coefficients (Table 1.6) have been stated as well.

Table 1.6 Conditions of the experiments

Search domain		Benchmark transfer functions	Values of indexes			Number of experiment
P	*I*		τ	ε	ν	
0...10	0...10	$1/(s+1)^2$	1	2	2	1
			2	1	2	2
			2	2	1	3
0...10	0...10	$1/(s+1)^3$	1	2	2	4
			2	1	2	5
			2	2	1	6
0...10	0...10	$(1-0,1s)/(s+1)^3$	1	2	2	7
			2	1	2	8
			2	2	1	9

For solving optimization problems ME-PSO [20] technique was used. The obtained results have been given in Table 1.7. The smallest numbers in Table 1.7 are in bold.

Table 1.7 Results of optimization of PI-controller tuning

Number of experiment	Coefficients		*IPTEC* value	*T*, sec	Overshoot, %	*ISE** value	*ISC*** value
	P	*I*					
1	2	3	4	5	6	7	8
1	1.36	0.63	1.04	5.30	0.00	0.92	6.50
2	2.05	0.95	2.27	4.62	4.90	0.70	7.75

Table 1.7 continuation

1	2	3	4	5	6	7	8
3	4.52	2.55	0.32	3.66	29.3	0.50	15.66
4	0.31	0.22	3.99	9.50	0.00	3.18	6.95
5	0.65	0.34	15.57	5.28	2.10	2.19	5.62
6	0.64	0.34	6.40	5.33	1.90	2.20	5.63
7	0.59	0.31	3.30	5.79	1.00	2.34	5.73
8	0.64	0.33	16.42	5.40	1.80	2.24	5.67
9	0.64	0.33	6.74	5.42	1.70	2.24	5.68

* Integral of the Square of the Error ($I_{ISE} = \int_0^T e^2 dt$);

** Integral of the Square of the Control ($I_{ISC} = \int_0^T u^2 dt$).

Analysis of the data, that is in Table 1.7, shows that adjusting τ=1, ε=2 and ν=2 leads to the high performance of control (in terms of overshoot). For the second and the third transfer functions found values of coefficients for proportional and integral terms are almost equal. Although, the values of criterion (1.15) are different. Thus, in the frame of the research performances of PI-controller for cases τ=2, ε=1, ν=2 and τ=2, ε=2, ν=1 are similar [32].

Conclusions to chapter 1

1. In the study, PI-controller tuning technique, which is based on a metaheuristic optimization algorithm, has been developed. It consists in the reduction of the initial problem to the problem of minimization of the devised complex criterion. Using the advanced optimization technique ME-PSO allowed us to find the coefficients of PI-controller for five benchmark transfer functions.
2. In the carried out research we have used as a criterion the weighted sum of mean integral error, mean integral control, overshoot, and settling time. The brief analysis of the impact of weight coefficients $\delta_1 \ldots \delta_4$ to the performance of the tuned PI-controller has been given. The developed PI-controller tuning technique shows its superiority over other well-known methods. It should be noted, that the proposed approach is not limited by used in the research indicators; the optimization criterion may include other important indicators.
3. In the study, we have developed criterion IPTEC, which naturally takes into account the cost of the error, control, and duration of the controlling process. Thus, it is a general form of many known criteria. IPTEC may be used as a cost function in state-of-the-art techniques of PID-controllers tuning which are based on the optimization approaches.
4. In the work, the optimization of PI-controller tuning has been carried out. Obtained results show high efficiency of the developed approach which is based on novel integral type criterion and metaheuristic optimization technique. Quality indicators for three benchmark transfer functions reveal that tuned in such a way PI-controllers might be exploited quite effectively.

References to chapter 1

1. PID tuner. Robust advanced PID control. URL: https://19lz9c16l9mt45jwvkt81p14-wpengine.netdna-ssl.com/wp-content/uploads/2015/08/INCA_A4_PID-Tuner_04-2013.pdf (date of access 29.08.2019).
2. Tune your PID. URL: https://pidtuner.com/ (date of access 29.08.2019).
3. PID Tuner Software. URL: https://pid-tuner.com/software/ (date of access 29.08.2019).
4. PID Tuning and APC Design & Optimization. URL: https://www.picontrolsolutions.com/ (date of access 29.08.2019).
5. Optimization of Regulatory Control Systems. URL: http://www.protuner.com/on-site-optimization.html (date of access 29.08.2019).
6. PID controller auto-tuning using genetic algorithm. URL: https://kevinjoly25.wordpress.com/ (date of access 29.08.2019).
7. O'Dwyer Handbook of PI and PID controller tuning rules (3rd edition). Ireland: Imperial College Press, 2009, p. 623.
8. Anil K., Gupta R. Tuning Of PID Controller Using PSO Algorithm And Compare Results Of Integral Errors For AVR System. International journal of innovative research and development. 2013, Vol 2, Issue 4, pp. 58-68.
9. Lakshmi K.S., Srinivas R. Tuning of PID controllers using particle swarm optimization. International Journal of Industrial Electronics and Electrical Engineering. 2015, Vol 3, Issue 2, pp. 17-22.
10. Solihin M.I., Fook L.T., Kean M.L. Tuning of PID Controller Using Particle Swarm Optimization (PSO). Proceeding of the International Conference on Advanced Science, Engineering and Information Technology. 2011, pp. 458-461.
11. Bassi S.J., Mishra M.K., Omizegba E.E., Automatic tuning of proportional-integral-derivative (PID) controller using particle swarm optimization (PSO)

algorithm. International Journal of Artificial Intelligence & Applications. 2011, Vol.2, No.4, pp. 25-34.

12. Sungthonga A., Assawinchaichoteb W. Particle Swarm Optimization based Optimal PID Parameters for Air Heater Temperature Control System. Procedia Computer Science. 2016, 86, pp. 108-111.
13. Nasri M., Nezamabadi-pour H., Maghfoori M. A PSO-Based Optimum Design of PID Controller for a Linear Brushless DC Motor. International Science Index, Electrical and Information Engineering. 2007, Vol 1, No 2, pp. 179-183.
14. Aranza M.F., Kustija J., Trisno B. and Hakim D.L. Tunning PID controller using particle swarm optimization algorithm on automatic voltage regulator system. International Conference on Innovation in Engineering and Vocational Education. IOP Conf. Series: Materials Science and Engineering. 2016, 128, pp. 1-9.
15. Ansu E.K., Koshy Th. Comparison of Adaptive PID controller and PSO tuned PID controller for PMSM Drives. International Journal of Advance Engineering and Research Development. 2018, Vol 5, Issue 03, pp. 812-820.
16. Jau-Woei P., Guan-Yan C., Shan-Chang H. Optimal PID Controller Design Based on PSO-RBFNN for Wind Turbine Systems. Energies. 2014, 7, pp. 191-209.
17. Mercy D., Girirajkumar S.M., Design of PSO-PID controller for a nonlinear conical tank process used in chemical industries. ARPN Journal of Engineering and Applied Sciences. 2016, Vol. 11, No. 2, pp. 1147-1153.
18. Latha K., Rajinikanth V., Surekha, P.M. PSO-Based PID Controller Design for a Class of Stable and Unstable Systems. ISRN Artificial Intelligence. 2013, pp. 1-11.
19. Pourhossein H., Zare A., Monfared M., Hybrid Modeling and PID-PSO Control of Buck-Boost Chopper. Przegląd elektrotechniczny. 2012, 88(8), pp. 187-191.

20. Romasevych Yu., Loveikin V. A Novel Multi-Epoch Particle Swarm Optimization Technique. Cybernetics and Information Technologies. 2018, 18(3), pp. 62-74.
21. Ziegler J.G., Nichols N.B., Optimum Settings for Automatic Controllers. Transaction of the ASME. 1942, Vol. 64, pp. 759-768.
22. Åström K.J., Hägglund T. PID Controllers: Theory, Design and Tuning. Instrument Society of America NC.: Research Triangle Park, 2 edition, 1995, p. 344.
23. Åström K.J., Hägglund T., Revisiting the Ziegler-Nichols step response method for PID control. Journal of Process Control. 2004, 14, pp. 635-650.
24. Chien K.L., Hrones J.A., Reswick J.B., On the automatic control of generalized passive systems. Transaction of the ASME. 1952, Vol. 74, No. 2, pp. 175-185.
25. Cohen G.H., Coon G.A., Theoretical Consideration of Retarded Control. Transaction of the ASME. 1953, Vol. 75, pp. 827-834.
26. Eriksson L., Control Design and Implementation of Networked Control Systems. Licentiate thesis' Department of Automation and Systems Technology. Helsinki University of Technology. 2008, p. 118.
27. Skogestad S., Simple analytic rules for model reduction and PID controller tuning. J. Process Control. 2003, 13(4), pp. 291-309.
28. Luyben W.L, Luyben M.L. Essentials of Process Control, McGraw-Hill, 1997, p. 624.
29. Åström K.J., Hägglund T., Benchmark Systems for PID Control. International Federation of Automatic Control, 2000, pp. 165-166.
30. Romasevych, Y., Loveikin V., Usenko S. PI-controller tuning optimization via PSO-based technique. Przeglad Elektrotechniczny. 2019, R. 95 NR 7, p. 33-37.
31. Romasevych Y.O., Loveikin V.S., Liashko A.P. Development a general criterion for PID-controller tuning. Collection of scientific works of XII international scientific and practical conference «Infirmation technologies and automation – 2019», Part II, Odessa. 2019, pp. 99-100.

32. Romasevych Y.O., Loveikin V.S., Krushelnytskyi V.V. PI-controller tuning optimization. Collection of scientific works of XII international scientific and practical conference «Infirmation technologies and automation – 2019», 2019, Part II, Odessa, pp. 11-12. (in Ukrainian)

CHAPTER 2. MODIFICATIONS OF CONTROLLERS

2.1 PI-controller modification

There is a hudge area of PI-controllers' applications. The classical structure of PI-controller is characterized by good performance for simple plants. However, there are requirements for increasing PI-controller features in terms of quality indicators. One of the possible ways – is to modify its structure. In the current section, one of the PI-controller modifications has been developed. The carried out calculations were performed for the example of the robot platform, which is operated in a greenhouse [1].

In order to ensure good positioning of the mobile robot platform at given points, increasing the energy efficiency of using the battery of its power supply, increasing the performance of monitoring and eliminating undesirable phenomena during its movement (fluctuation of structural elements, possible abnormal situations, etc.), it is necessary to implement a synthesis of algorithms of motion control at the executive level.

To ensure the above-mentioned requirements, it is necessary to modify the structure of the PI-controller. Its essence can be illustrated by the following equation:

$$u = k_P e + k_I f\left(e,\ e_{\partial on},\ \int_0^t e dt\right), \tag{2.1}$$

where u – system moving control function; k_P and k_I – proportional and integral gains of PI-controller respectively; e and $e_{\partial on}$ – current and permissible error of the angular speed regulation of the robot drive motor ($e=\omega_y-\omega$, $e_{\partial on}=0{,}05\omega_y$) respectively; ω_y and ω are the given and actual values of the angular speed of robot drive motor respectively; f – nonlinear discontinuous function of its arguments.

To illustrate the suggested modification of the PI-controller structure, let's do calculations for the robotic complex, the parameters of which are given in Table 2.1.

The drive voltage control is performed by pulse-width modulation of the signal coming from the PI-controller.

Table 2.1 Parameters of the robotic system

Parameter	Parameter value
Mechanical parameters	
Robot weight, kg	$1.51 \cdot 10^{1}$
Robot wheel radius, m	$1.50 \cdot 10^{-1}$
A gear ratio of the drive	$4.98 \cdot 10^{1}$
Drive efficiency	$7.10 \cdot 10^{-1}$
The coefficient of static resistance of the robot motion	$5.00 \cdot 10^{-2}$
Electrical parameters	
Battery voltage, V	$1.20 \cdot 10^{1}$
Carrier frequency PWM, Hz	$5.00 \cdot 10^{1}$
Armature windings resistance, Ohm	$7.10 \cdot 10^{-1}$
Armature inductance, Gn	$9.43 \cdot 10^{-3}$
Coefficient of the engine torque, Nm/A	$2.30 \cdot 10^{-2}$

Taking into account the data shown in Table 4.1, we calculated the process transfer function on the channel “power supply voltage – the angular speed of the drive”. It may be presented as follows:

$$G(s) = \frac{1}{2.30 \cdot 10^{-2} + 6.17 \cdot 10^{-3} s + 8.20 \cdot 10^{-5} s^2}. \qquad (2.2)$$

In order to determine the effectiveness of the proposed modification (2.1), let’s perform an estimate of the quality of automatic control of the robot speed for two modes: set-point mode (acceleration of the robot to the steady speed) and neutralizing the external disturbances (providing the fixed speed under stochastic disturbances on the robot).

The selected duration of the simulation of the first mode is equal to one second (T_{SPM}=1 s). For evaluating the quality of control during the set point mode, we use the following indicators:

1) integral error

$$\bar{e}_{SPM} = T_{SPM}^{-1} \int_0^{t_p} |e| dt, \tag{2.3}$$

where t_p – response time;

2) integral control quality index

$$\bar{u}_{SPM} = T_{SPM}^{-1} \int_0^{t_p} |u| dt; \tag{2.4}$$

3) overshoot

$$e_{\max .SPM} = \left(1 - \frac{\max(e)}{\omega_y}\right) \cdot 100\%; \tag{2.5}$$

4) response time (time of the output angular speed of the drive in the area where the error does not exceed the permissible value)

$$t_p = \arg(\omega(t) \le \omega_y \pm e_{\partial on}). \tag{2.6}$$

The subscript of indicators (2.3)-(2.5) denotes the set point mode.

The indicators (2.3)-(2.6) were calculated for the set point mode of the angular speed of the drive for the methods of the PI-controller tuning: Ziegler-Nichols [2], Kappa-Tau [3], AMIGO (Approximate M-constrained integral gain optimization) [4], Chien-Hrones-Reswick [4], Cohen-Coon [6], Lambda [7], Skogestad [8] (Table 2.2).

Analysis of the results presented in Table 2.2 shows that the modified controller has significant advantages over the classical ones. This applies to all values. The $\bar{e}_{SPM}$ indicator for the modified structure of the controller decreased by

1.84-3.05 times, which allows to provide a more qualitative reaching the steady mode of movement.

Table 2.2 Automatic control quality indicators for set point processing

Method of setting the PI-controller	The structure of the PI-controller							
	Classical				Modified			
	$\bar{e}_{SPM}$, rad/s	$\bar{u}_{SPM}$, V	$e_{\max.SPM}$, %	t_p, s	$\bar{e}_{SPM}$, rad/s	$\bar{u}_{SPM}$, V	$e_{\max.SPM}$, %	t_p, s
Ziegler-Nichols	24.75	3.16	65.83	0.47	9.66	1.32	4.92	0.11
Kappa-Tau	19.42	2.78	53.31	0.39	10.54	2.00	8.36	0.25
AMIGO	19.22	2.93	47.98	0.41	9.97	1.46	7.68	0.15
Chien-Hrones-Reswick	22.34	2.93	62.67	0.42	9.66	1.32	4.92	0.11
Cohen-Coon	26.32	3.19	67.89	0.46	9.66	1.32	4.92	0.11
Lambda	29.52	3.62	70.44	0.58	9.66	1.32	4.92	0.11
Skogestad (SIMC)	22.10	2.95	62.14	0.43	9.66	1.32	4.92	0.11

The $\bar{u}_{SPM}$ indicator decreased by 1.39-2.39 times. This signifies that the use of the modified structure of the PI-controller provides a less stressful mode of operation of the battery. The advantage of the PI-controller with a modified structure also lies in the significant reduction of overshoot $e_{\max.SPM}$ and time of control (settling time) t_p by 1.56-5.27 times (Fig. 2.1).

The graphs shown in Fig. 2.1, reflect the function of the relative power supply voltage $\tilde{U}$ of the motor (black line) and the relative angular speed $\tilde{\omega}$ of the electric drive robot (gray line). They are built for the Ziegler-Nichols tuning method, which is one of the most widespread in practice. The graphs shown in Fig. 2.1, confirm that the modification of the structure of the PI-controller allows to obtain much better control quality, a less stressful mode of battery operation and a significantly shorter duration of the transient operation of the electric drive.

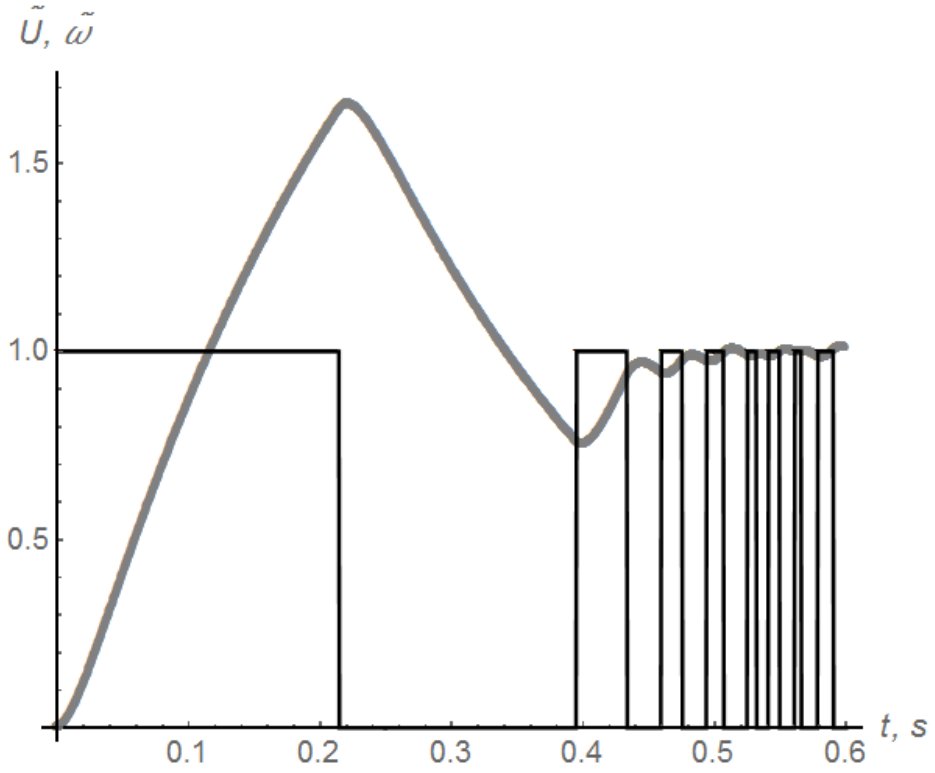

a)

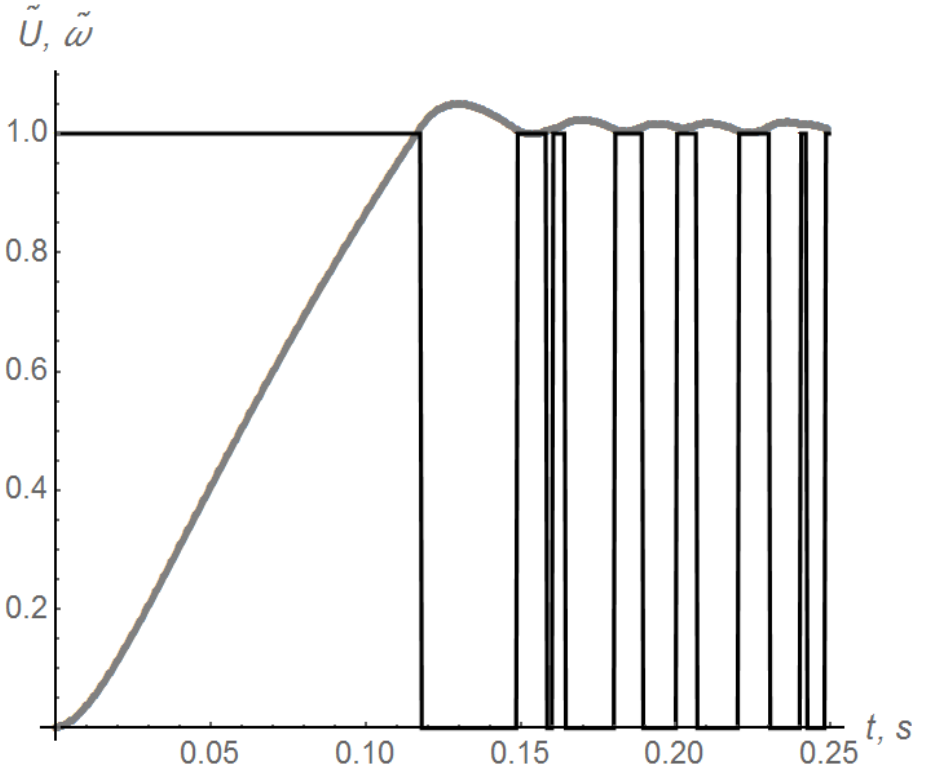

b)

Fig 2.1 Plots of the function obtained by simulating the set-point mode of the PI-controller with: a) classical; b) modified structure

The latter factor makes it possible to increase the energy efficiency of its operation. In addition to the set point mode, calculations were made for the mode of neutralization of disturbances. In this operating mode, the PI-controller is used to maintain the robot steady speed under stochastic disturbances on the robot's motion. In the framework of this study, the disturbance function is physically represented as force acting on the platform of the robot, diverting its speed from the set one. The disturbance function is identical for all performed calculations, the values of its aggregated parameters are given in Table 2.3. The duration of simulation of the disturbances neutralization mode is selected at one minute (T_{DNM}=60 s).

Table 2.3 Integrated parameters of the random disturbance function*

Parameter	Value
Maximum value	9.80
Minimum value	-7.59
Median RMS value	4.87
Universal mean	0.00

* the numerical values of the combined parameters, which are presented in Table 2.2, are obtained as the ratio of the actual value of the parameter to the fixed value of the moment of resistance of the robot platform movement.

The following indicators were used to evaluate the quality of the control process during the disturbances neutralization mode:

1) integral error

$$\bar{e}_{DNM} = T_{DNM}^{-1} \int_0^T |e| dt; \tag{2.7}$$

2) integral control quality index

$$\bar{u}_{DNM} = T_{DNM}^{-1} \int_0^T |u| dt; \tag{2.8}$$

3) maximum relative error

$$e_{\max.DNM} = \left(1 - \frac{\max(e)}{\omega_y}\right) \cdot 100\%; \quad (2.9)$$

4) minimum relative error

$$e_{\min.DNM} = \left(1 - \frac{\min(e)}{\omega_y}\right) \cdot 100\%. \quad (2.10)$$

The subscript of the indicators (2.7)-(2.10) denotes the disturbances neutralization mode. The indicators (2.7)-(2.10) were calculated for the disturbances neutralization mode by the system for a number of tuning methods of PI-controller (Table 2.4).

Table 2.4 Quality indicators of automatic control for the disturbances neutralization mode

Method of tuning the PI-controller	The structure of the PI-controller							
	Classical				Modified			
	$\bar{e}_{DNM}$, rad/s	$\bar{u}_{DNM}$, V	$e_{max.DNM}$, %	$e_{min.\ DNM}$ %	$\bar{e}_{DNM}$, rad/s	$\bar{u}_{DNM}$, V	$e_{max.\ DNM}$, %	$e_{min.\ DNM}$, %
Ziegler-Nichols	7.22	8.76	51.42	-92.49	5.39	8.67	51.98	-24.77
Kappa-Tau	5.99	8.76	51.82	-84.11	7.29	8.61	52.22	-22.66
AMIGO	6.21	8.76	51.79	-81.62	6.75	8.62	51.11	-23.10
Chien-Hrones-Reswick	7.06	8.76	52.08	-89.34	5.81	8.65	51.45	-22.95
Cohen-Coon	7.50	8.76	51.49	-95.07	5.47	8.67	51.84	-23.07
Lambda	8.26	8.76	54.62	-95.08	4.56	8.69	50.97	-23.14
Skogestad (SIMC)	6.99	8.76	50.88	-90.70	5.37	8.67	51.97	-24.29

Comparative analysis of the data presented in Table 2.4 shows that the use of the modified structure of the PI-controller allowed reducing some undesirable

indicators of control. For example, the minimum relative errors for a PI-controller due to a modified structure decreased by 3.53-4.10 times compared with those obtained for the classical structure of the controller. The integral error estimate for some of the methods of setting the PI-controller has decreased, and for some, it has increased. However, the use of a modified structure does not significantly reduce unwanted indicators of $\bar{u}_{DNM}$ and $e_{\max.DNM}$.

Thus, in the framework of this study application of modified structure of the PI-controller with the purpose of neutralizing disturbances are reasonable only for such methods of tuning PI-controller: Ziegler-Nichols, Chien-Hrones-Reswick, Cohen-Coon, Lambda and Skogestad (SIMC) [1].

2.2 Applying of a method of equalities meeting in the automated direct current drive

In many practical cases, a process of automatic control is constrained by the different functions of the system's phase coordinates. For example, one of the possible constrain, that might be used to control the actuators of mobile robots, is the amount of energy consumed by the actuator during its start-up mode. It can be obtained as a definite integral of the nonlinear phase coordinate function of the system (power). One of the possible methods to take into account constrain is to inject an additional phase coordinate, the difference between the current amount of consumed energy and its set amount. Since the phase coordinates are different in physical content and magnitude, the next step is to normalize the components of the phase-vector. It is usually performed by dividing them by their set values (set-points). In this case, the phase coordinates are dimensionless.

For the considered case of the DC motor, which is as an actuator of the mechanism of a robot's movement, its mathematical model may be written as follows:

$$U = \dot{x}A_1 + \ddot{x}A_2 + \dddot{x}A_3, \tag{2.11}$$

where A_1, A_2, A_3 – coefficients, which may be expressed through the system's parameters.

For the system we have developed a controller, which minimized the following criterion:

$$CC = t_p \cdot \delta + \max(P) \to \min, \tag{2.12}$$

where δ – weight coefficient, which reflects the influence of settling time; P – the current power of the drive; t_p – settling time. Additionally, the automated system is constrained by the requirement of zero-overshoot.

The proposed model of the controller is as follows:

$$U = K_p \frac{v - \dot{x}}{v} + T_i^{-1} \int_0^t \frac{v - \dot{x}}{v} dt + K_{p.E} E_{sp}^{-1} \left(E_{sp} - \int_0^{t_p} IUdt \right) + \left(T_{i.E} E_{sp} \right)^{-1} \int_0^t (E_{sp} - \int_0^{t_p} IUdt) dt, \tag{2.13}$$

where K_p, T_i – proportional and integral gains of the controller by the relative error of the speed; $K_{p.E}$, $T_{i.E}$ – proportional and integral gains of the controller by the relative error of the consumed energy of the drive during its start-up; v – set-point of the speed; I – current strength; U – power supply voltage; E_{sp} – set-point of the consumed energy during start-up mode.

The controller (2.13) is a superposition of the PI-controllers, which act by deviations of the speed and the consumed energy.

In order to find optimal values of the gains K_p, T_i, $K_{p.E}$, $T_{i.E}$ ME-PSO [9] has been applied. Numerical values of the used parameters correspond to the DC drive П71, set-points are v=2.65 m/s and E_{sp}=11000 J.

As a result of the carried out calculation we have obtained the following values of the gains: K_p=0.3929; T_i=0.0042; $K_{p.E}$=0.3608; $T_{i.E}$=0.9360.

In order to estimate the results the plots have been built (Fig. 2.2) (set-points are denoted with dashed lines). It is clear, that the set-points are meet at the end of the start-up mode (Fig. 2.2) by the speed and by the consumed energy.

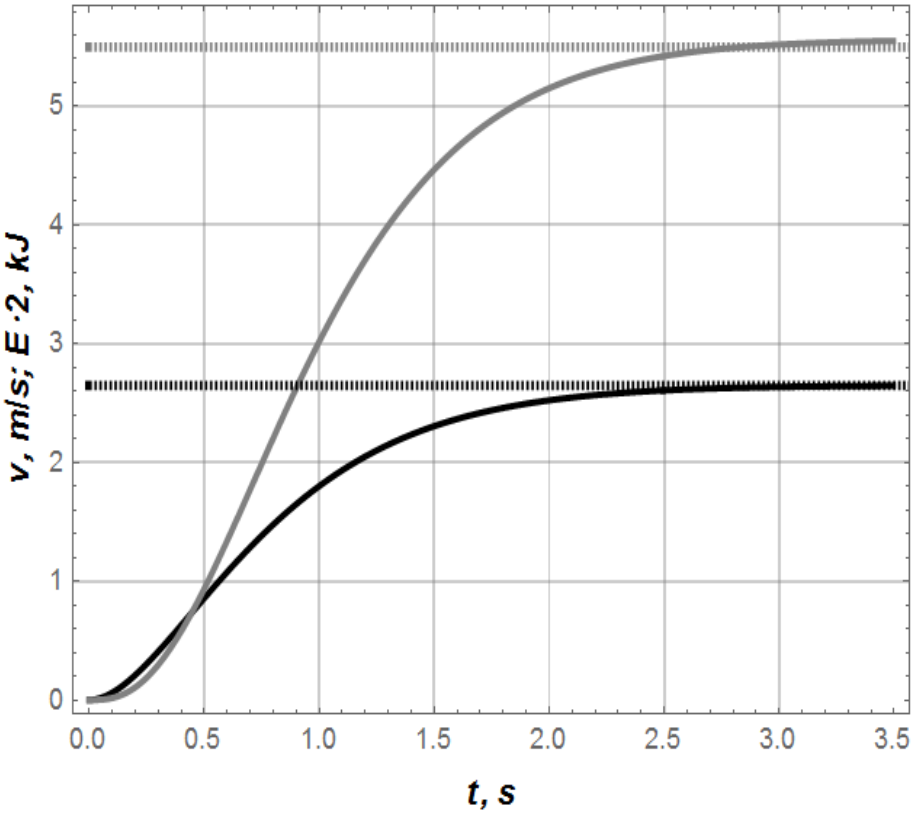

a)

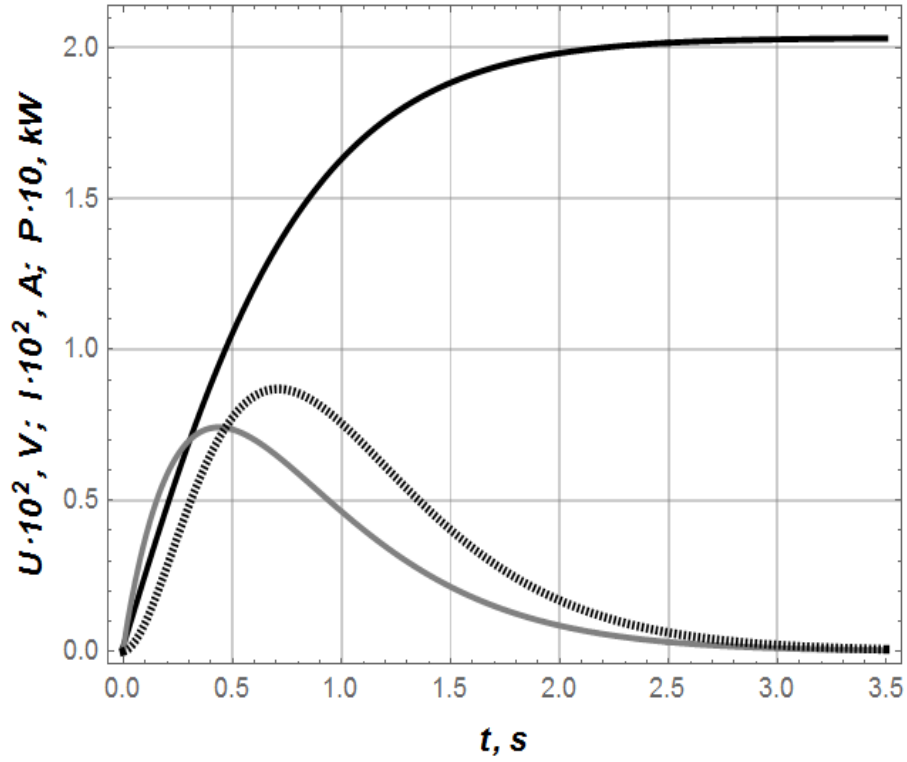

b)

Fig. 2.2 Plots of the dynamic and electric characteristics of the system during control: a) the speed of the robot platform (black line) and consumed energy (gray

line); b) power supply voltage (black line), current strength (gray line) and power of the drive (black dashed line)

One may observe from Fig. 2.2 (b), that the maximum value of the power is 8694 W. It means that the controlled process can be implemented by means of power electronics. The value of the maximum current does not overshoot 74.2 A. It supports the previous conclusion [10].

2.3 Artificial neural network in problems of controllers' development

One of the possible ways of approximation of some data sets is connected with the use of a trained artificial neural network (ANN). There is the universal approximation theorem [11], which states that a feed-forward ANN with a single hidden layer containing a finite number of neurons (nodes) can approximate continuous functions on compact subsets, under mild assumptions on the activation function. One of the first versions of the theorem was proved by George Cybenko [12] (as an activation function he applied sigmoid).

For instance, let consider a problem of automatic control: there is an unstable plant, which is described with the following transient function $G = \frac{1}{s^2 - 1}$ (it may be a one of representation of the mathematical model of an inverted pendulum); the cost function of the control is RMS of control (the control is the output of the considered ANN). The structure of the ANN concludes four layers of five nodes (neurons). The activation function of the nodes is sigmoid with a bias. The problem states that biases and weights should be found: their numerical values minimize the cost function.

In order to solve the stated problem, the ME-D-PSO method was applied. The results might be shown in a form of the 3D plot (fig. 2.3): as ANN has two inputs (controlled coordinate x and its first derivative with respect to time) and one output (control function).

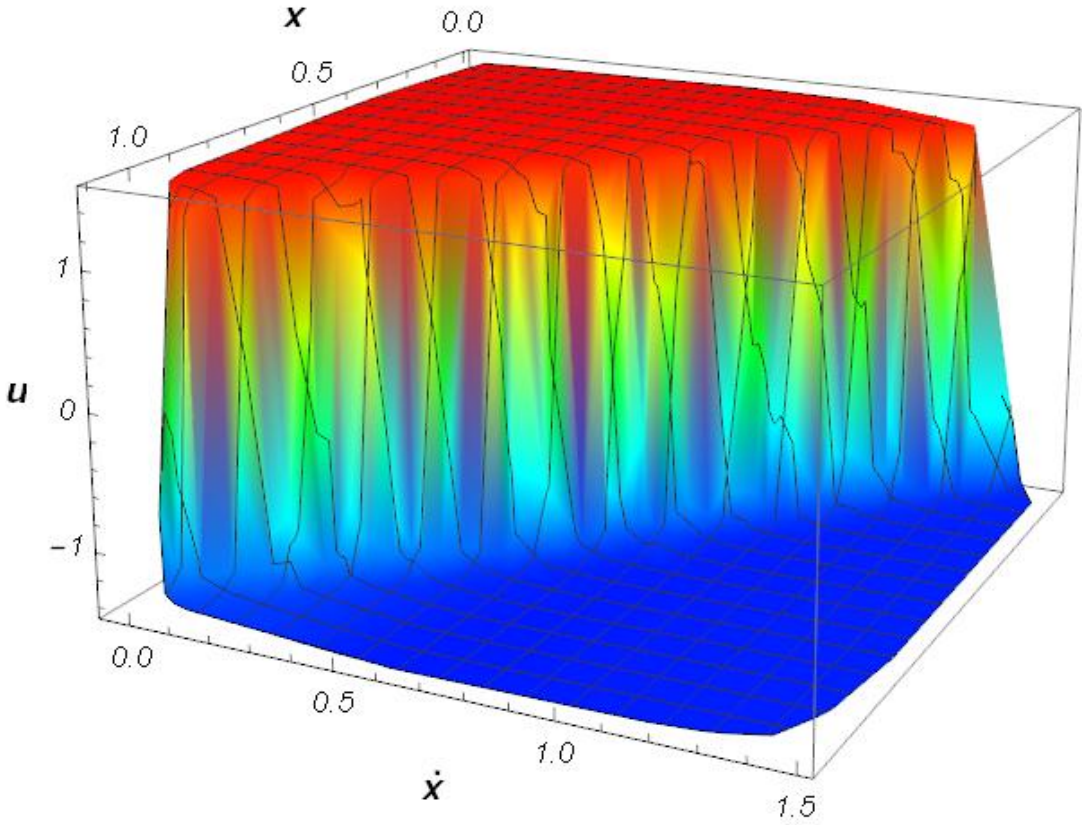

Fig. 2.3 3D-plot of the function of the trained ANN-controller

The plot on the fig. 2.3 clearly shows, that trained ANN-controller acts like a MISO function. It transforms the input vector into output control (scalar). Moreover, it is limited: lower and upper bounds do not violate values -1.5 and 1.5 respectively [13].

Conclusions to chapter 2

1. The work suggests a modification of the structure of the PI-controller, which consists of introducing a nonlinear functional dependence between the integral and the proportional component of the PI-controller. In this case, the modified structure of the PI-controller allows the use of standard methods for its tuning. The modified structure of the PI-controller improves the speed control parameters of the robot platform for set point processing modes (speed, overshoot, integral error estimation, and control) and neutralization of disturbances (the minimum relative error of control). This indicates the expediency of its use for plants of this type.
2. In the work, the modified structure of the controller has been proposed. It includes two parts, which act to reach two set-points. In the presented example of calculations, we have considered set-points of speed and the amount of energy consumed during the start-up of the direct current drive. The controller gains were found via the optimization technique. The tuned controller shows desired features.
3. Generally, ANN serves as the universal approximator of the optimal controller. Thus, the exploitation of ANN in the different systems of optimal control leads to quite good results. They are based on strong approximation features of ANN. It, in turn, may provide a good performance of the ANN-based controllers in terms of quality indicators (settling time, overshoot, integral criteria, etc.). This issue will be investigated in further studies.

References to chapter 2

1. Lysenko V., Bolbot I., Romasevych Yu., Loveykin V., Voytiuk V. Algorithms of robotic electrotechnical complex control in agricultural production (Book chapter). Control Systems: Theory and Applications. River Publishers. 2018, Ch. 11, pp. 271-289.
2. Ziegler J.G., Nichols N.B. Optimum Settings for Automatic Controllers. Transaction of the ASME. 1942, Vol. 64., pp. 759-768.
3. Åström K.J., Hägglund T. PID Controllers: Theory, Design and Tuning. Instrument Society of America' NC: Research Triangle Park. 2nd edition, 1995, p. 344.
4. Åström K.J., Hägglund T. Revisiting the Ziegler-Nichols step response method for PID control. Journal of Process Control. 2004, 14, pp. 635-650.
5. Chien K.L., Hrones J.A., Reswick J.B. On the automatic control of generalized passive systems. Transaction of the ASME. 1952, Vol. 74, No.2, pp. 175- 185.
6. Cohen G.H., Coon G.A. Theoretical Consideration of Retarded Control. Transaction of the ASME. 1953, Vol. 75, pp. 827-834.
7. Eriksson L. Control Design and Implementation of Networked Control Systems. Licentiate thesis' Department of Automation and Systems Technology. Helsinki University of Technology. 2008, p. 118.
8. Skogestad S. Simple analytic rules for model reduction and PID controller tuning'. J. Process Control. 2003, 13(4), pp. 291-309.
9. Romasevych Yu., Loveikin V. A Novel Multi-Epoch Particle Swarm Optimization Technique. Cybernetics and Information Technologies. 2018, 18(3), pp. 62-74.
10. Romasevych Y.O., Loveikin V.S., Liashko A.P. Applying of method of equalities meeting in the automated direct current drive. Proceedings of the IX International Scientific-Technical Conference „Problems of modern power

engineering and automation in the system nature management (theory, practice, history, education)". 2020, pp. 60-61.

11. Balázs Csanád Csáji Approximation with Artificial Neural Networks. Faculty of Sciences, Eötvös Loránd University, Hungary. 2001, p. 45.
12. Cybenko G. Approximations by superpositions of sigmoidal functions. Mathematics of Control, Signals, and Systems. 1989, 2(4), pp. 303-314. doi: 10.1007/BF02551274
13. Romasevych Y.O., Loveikin V.S. Artificial neural network as a universal approximator. Proceedings of the XV International Scientific-Practical Conference „Obuhova's Readings". 2020, pp. 45-46.

CHAPTER 3. SYNTHESIS OF FAST CONTROLLERS BASED ON FUZZY-LOGIC

3.1 Fuzzy-controllers' applications, their advantages and disadvantages

PID-controllers do not provide a high quality of control for nonlinear and/or complex plants, and in cases when information about plants is not enough. However, features of automatic controllers can be improved by using methods of fuzzy-logic. Note, when the information is sufficient for an accurate mathematical model of the plant, traditional (PID or PI) controller are better than fuzzy-controllers. It is caused by the fact that during the synthesis of the fuzzy-controllers the input data is not specified exactly, but approximately.

Fuzzy control [1] is mainly used:

1) when a plant is insufficiently identified, but there is an experience of its control;
2) in the non-linear systems with a complex identification;
3) when expert's knowledge should be used for the problem solution.

Examples of fuzzy-controllers' application are blast furnace or distillation column. Their mathematical models contain many empirical coefficients, which vary in wide ranges. The identification of the coefficients is quite a complex problem. At the same time, qualified operator controls the process quite well by using his or her experience.

In general, it is possible to indicate a reasonable area of fuzzy-controllers' application (Fig. 3.1). Fig. 3.1 shows, that fuzzy-controllers preferably used for plants of moderate or considerable complexity and there is non-full information about external influences. They take intermediate place between the classical approach on the synthesis of controllers and methods that are based on artificial neural networks.

Controllers based on fuzzy-logic are currently used in commercial systems for the control of: the movement of underground trains (Hitachi), photo and video camera with autofocus (Canon), air conditioners (Mitsubishi), washing machines

(Panasonic and Matshushita), automatic transmission of vehicles (Honda and Nissan), elevator movement (Toshiba) and other technical systems.

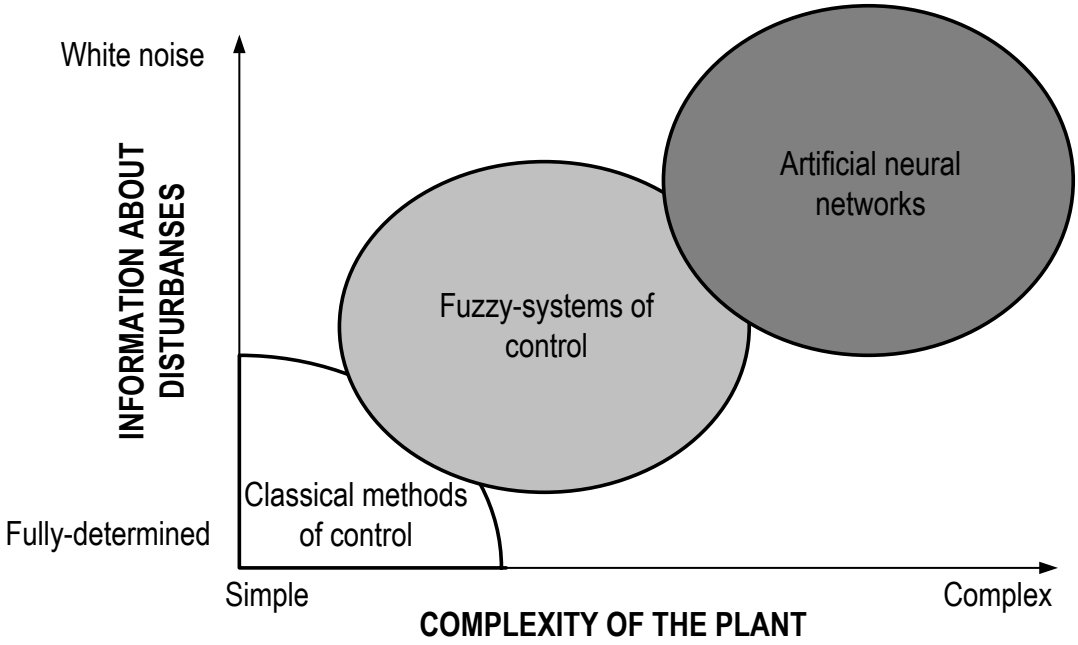

Fig. 3.1 Sets of reasonable applications in the synthesis of controllers

There are a large number of scientific publications on theoretical and applied problems of fuzzy control systems, including fuzzy-controllers. For example, on September 4, 2019, the Web of Science (Core Collection) scientific metric database contains 11,547 scientific papers on this topic. At of the same date, there are 16,870 works in the Scopus database (the request in both databases was performed on the topic of „fuzzy-controller"). This suggests a high degree of interest in the scientific community in the development and use of technologies based on fuzzy-logic.

These works present the results of the use of fuzzy-controllers for:

1) movement of the mobile robots [2-9] and groups of robots [10];
2) movement of robots' manipulators [11];
3) control of hydraulic servo-apparatus for the position of electro-hydraulic excavator [12];
4) control of manipulator movement by means of teleoperation system [13];

5) control of data transmission in networks (in particular, to improve the quality of video streaming [14] and for the transmission of voice messages through the Internet [15]);
6) control of parameters of technological processes of metallurgy (in particular, coiling entry temperature [16], finishing mill strip gage [17]);
7) control of linear ultrasonic motor of precise positioning in the production of nano- and microcomponents of semiconductors [18];
8) control the movement of the AC engines (particularly for synchronous engine with permanent magnet [19], for linear synchronous engines [20], asynchronous engines [21, 22]);
9) control the movement of the DC engines (particularly in the case of saturation and the influence of external perturbations [23], changes in angular velocity [24, 25]);
10) control of the cable tension of a lift [26];
11) control of electric car parameters (in particular, control of three power supplies of a hybrid electrical vehicle [27] and energy management in hybrid electrical vehicles [28]);
12) control of power systems (for example, to suppress unwanted frequency fluctuations [29, 30], control of electronic components in power systems [31], voltage control of synchronous generators [32]);
13) control of the active system of magnetic levitation [33];
14) control photovoltaic devices [34, 35];
15) control of aircraft (for example, for automatic landing systems [36], altitude and speed control of supersonic aircraft [37], altitude control of small aircraft [38] and, quadrocopters [39]).

Carrying the analysis of the presented works, we may define the advantages of fuzzy-controllers:

a. they allow to obtain the robustness even for nonlinear control systems;
b. their synthesis does not require a mathematical model of a plant;

c. they allow to design of a control system on the basis of linguistic (verbal) data, i.e. by using the experience of experts.

However, fuzzy-controllers have a few disadvantages:

a. the complexity of the synthesis of fuzzy-controllers (for example, in terms of developing a database of expert rules, setting the forms of membership functions, their number, and location, etc.);
b. impossibility of mathematical analysis of fuzzy-control systems with methods of the automatic control theory;
c. low accuracy of control;
d. increasing input variables (parameters that should be controlled) complicates calculations that fuzzy-controller executes in real time.

Practical experience in developing systems based on fuzzy-logic shows that the time and cost of their design is much less than by using traditional approaches. The developer of fuzzy-logic Lotfi Zadeh noted in this regard that „in almost every case you can build the same product without fuzzy-logic, but fuzzy is faster and cheaper" [40].

3.2 Method of synthesis of fast fuzzy-controllers

One of the disadvantages of automatic controllers, which are based on fuzzy-logic, is a long duration of operations (logical and arithmetic). To eliminate this disadvantage, it is necessary to use high-speed microcontrollers. However, the performance of fuzzy-controllers can be increased without their use.

This section describes an approach that allows one to obtain a fast fuzzy-based controller. In addition, its use in some cases allows to improve the quality of control by one or more qualitative indicators.

The essence of the proposed method is illustrated by using block-scheme, which is shown in Fig. 3.2.

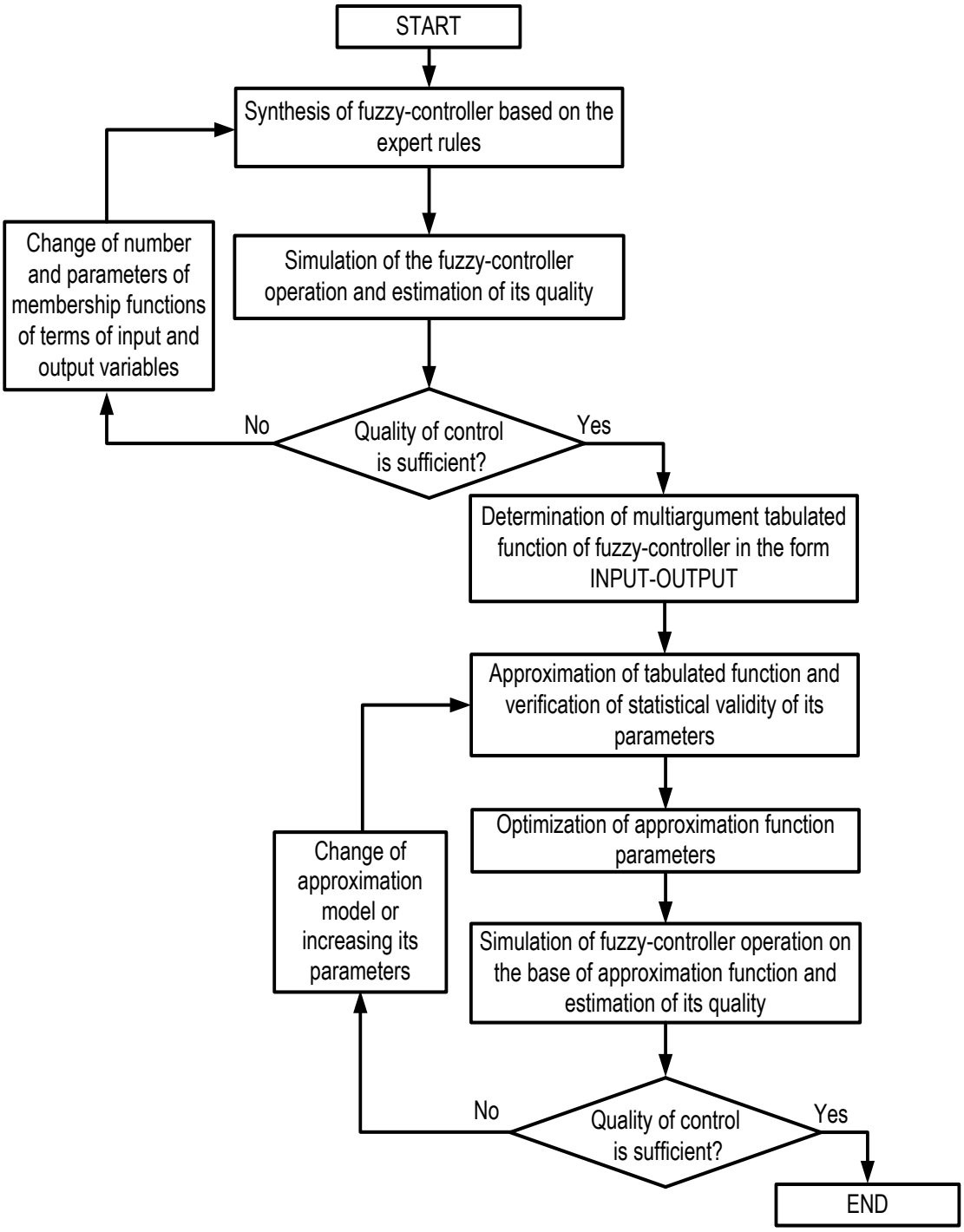

Fig. 3.2 Block-scheme of the method of synthesis of a fast fuzzy-controller

We will explain of the method, which is illustrated by the block-scheme (Fig. 3.2).

The first step in the method is the synthesis of a fuzzy-controller, which should be performed on the basis of expert knowledge (set of rules).

In the second stage, one should simulate the operation of the fuzzy-controller for the plant and modes of its operation. At this stage the quality of the controlled

process should be determined based on a list of indicators (for instance, *ITAE*, *IAE*, *ISE*, *ITSE*, settling time, overshoot, etc.). If the control quality is sufficient, then one may move to the next step, if not – then change the parameters of membership functions of the terms and/or the number of terms of input and output variables.

The next (third) stage consists on developing a multi-argument tabulated function of the fuzzy-controller in the INPUT-OUTPUT form (input and output in the general case are vectors). This calculation should be performed by controller feeding with sets of input variables and calculating its output values. Combinations of the input variables must correspond to the practical conditions of the control system. We can recommend two ways of constructing combinations of input variables, which we denote by x_i ($i \in \overline{(1,\ n)}$, here n is the number of input variables or dimension of the input vector). i-th input variable changes in the range $x_{i.\min} \ldots x_{i.\max}$.

The first way is as follows: one sets the sampling step for each of the components of the input vector (each input variable) Δx_i and performs a uniform search of all possible combinations of discrete values of the components of the input vector. In this case, the sample size INPUT-OUTPUT may be calculated with the next formula:

$$N = \prod_{i=1}^{n} \left(\frac{x_{i.\max} - x_{i.\min}}{\Delta x_i} + 1 \right). \qquad (3.1)$$

The second way of constructing the combinations of input variables x_i is in random choice of discrete values. In order to ensure sufficient uniformity of possible combinations of input variables, the sample size must be large enough. In general (for both ways), it depends on the dimension of the input vector of the fuzzy-controller and can include hundreds or thousands of „input-output" pairs.

Note that the third stage (construction of the tabulated function) is quite long and complex (in terms of the volume of calculations). This is due to the fact that the duration of access to the function of the fuzzy controller is relatively significant. To store the tabulated function of the fuzzy-controller, a PC must have the required amount of memory. Obviously, the memory of the microcontroller is not suitable for

this purpose, so these calculations must be performed by using specialized software on a PC. In the fourth stage, an approximation of the tabulated function is performed using one or more models (usually polynomial- or spline-based). At this stage, the parameters of the approximation models (for example, the coefficients of the polynomial) are also verified to approve their statistical validity. The standard approach for such calculations is the use of linear (or nonlinear) regression.

At the fifth stage, the optimization of the parameters of the approximation model is performed on the basis of numerical methods. The numerical values of the approximation model parameters that have been found in the previous stage (for example, the coefficients of the approximation polynomial) are the initial approximation to the optimal ones. They should be determined in the fifth stage during the iterative procedure of numerical optimization. In this case, the approximation model parameters are the arguments of the optimization problem, and the optimization criterion may be: *ITAE*, *IAE*, *ISE*, *ITSE*, settling time, overshoot, or other indicators. At the sixth stage, the quality of control should be determined according to a set of estimation indicators. It must be no worse than the original fuzzy-controller. If the quality of control is worse, one should move to the fourth stage and change approximation models (for example, replace the approximate polynomial by a spline function), or change the number of parameters (for example, increase the polynomial order).

3.3 Example of application of the method of synthesis of fast fuzzy-controllers and analysis of the control quality

3.3.1 Synthesis of the fuzzy-controller of a vehicle movement

In order to illustrate the developed method of synthesis of fast fuzzy-controllers, we will give an example of corresponding calculations. In order to explain the essence of the calculations, we choose the problem of the synthesis of a fast fuzzy-controller for a vehicle. Its mathematical model will be presented below.

Note that in the calculations we have used simple models and dependencies. This is due to the need to explain as clearly as possible (without insignificant details) the essence of the method.

The initial stage of the method is the synthesis of a fuzzy-controller of the vehicle movement. Let the vehicle movement is described by the following equation:

$$m\ddot{x} = u\left(e, \int_0^t e dt\right) - w, \tag{3.2}$$

where x – is the generalized coordinate of the vehicle; m – is the reduced mass of the vehicle; w – disturbances (resistance force acting on the vehicle) ; u – control, which is a function of the speed error e and the error integral $\int_0^t e dt$; e – is the current error of vehicle speed, which is determined as follows: $e=\dot{x}-v$ (v – is a speed setpoint). Thus, we consider the simplest case of a fuzzy-PI-controller.

Model (3.2) corresponds to a single-mass model of a vehicle that moves under the driving force, and which depends on u and the resistance forces. Model (3.2) in the first approximation may be used to describe the movement of a tractor during some technological operations, for instance, plowing.

The problem of fuzzy-controller synthesis is to stabilize the vehicle speed (in the ideal case it must equal to the setpoint v).

The initial stage of the synthesis is setting the terms for input and output variables. For this case, we have set three terms (*N*, *Z*, *B*) for each input variable, i.e. for the error and the error integral. For the output variable of the fuzzy-controller u we have set five terms (*NB*, *NS*, *Z*, *PS*, *PB*). Taking into account the simplicity and common use in the problems of synthesis of fuzzy-controllers of Λ- and Z-membership functions (Fig. 3.3), we will use them in the following calculations. Their simplicity does not require significant computing resources.

The subscripts in Fig. 3.3 correspond to the terms of the input and output variables.

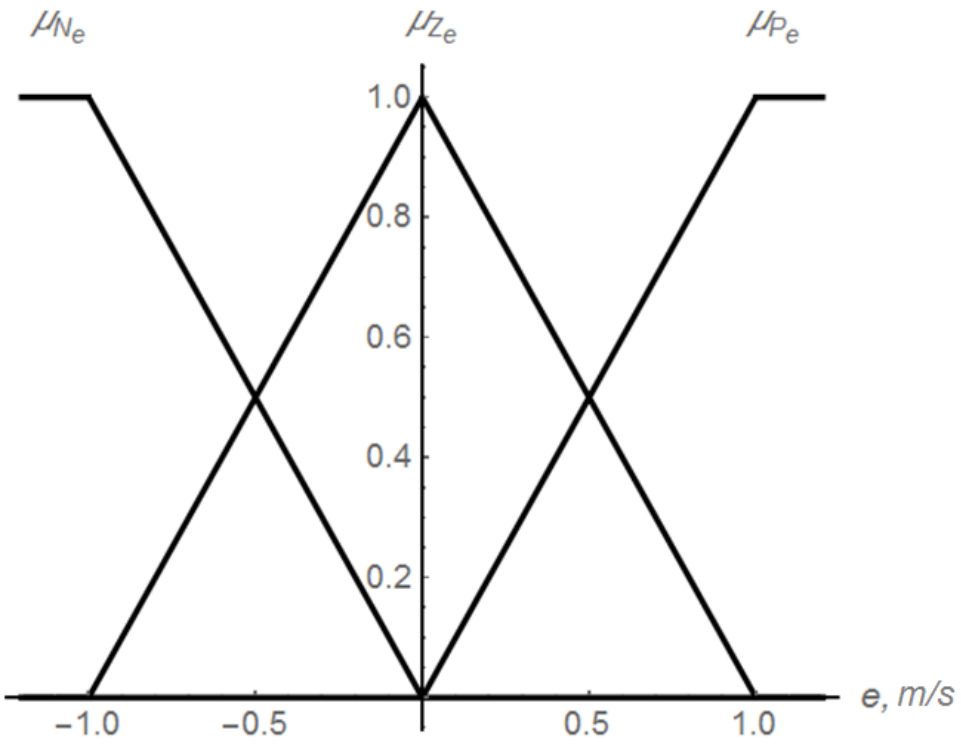
μ_{N_e}
μ_{Z_e}
μ_{P_e}
1.0
0.8
0.6
0.4
0.2
−1.0
−0.5
0.5
1.0
e, m/s

a)

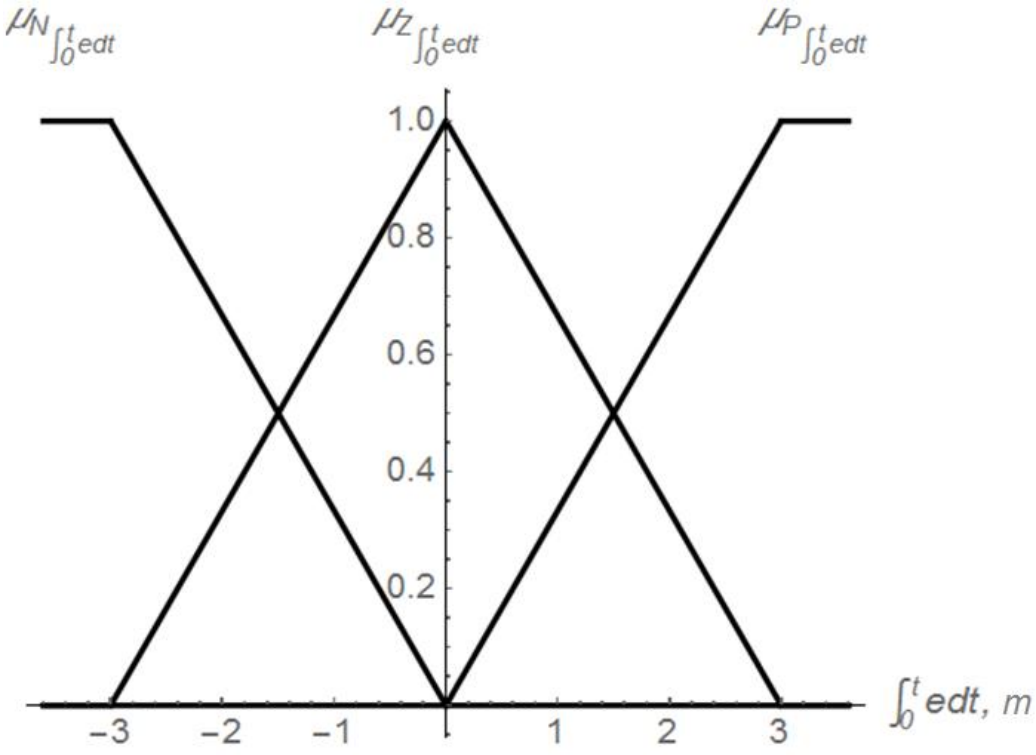
$\mu_{N_{\int_0^t edt}}$
$\mu_{Z_{\int_0^t edt}}$
$\mu_{P_{\int_0^t edt}}$
1.0
0.8
0.6
0.4
0.2
−3
−2
−1
1
2
3
$\int_0^t edt$, m

b)

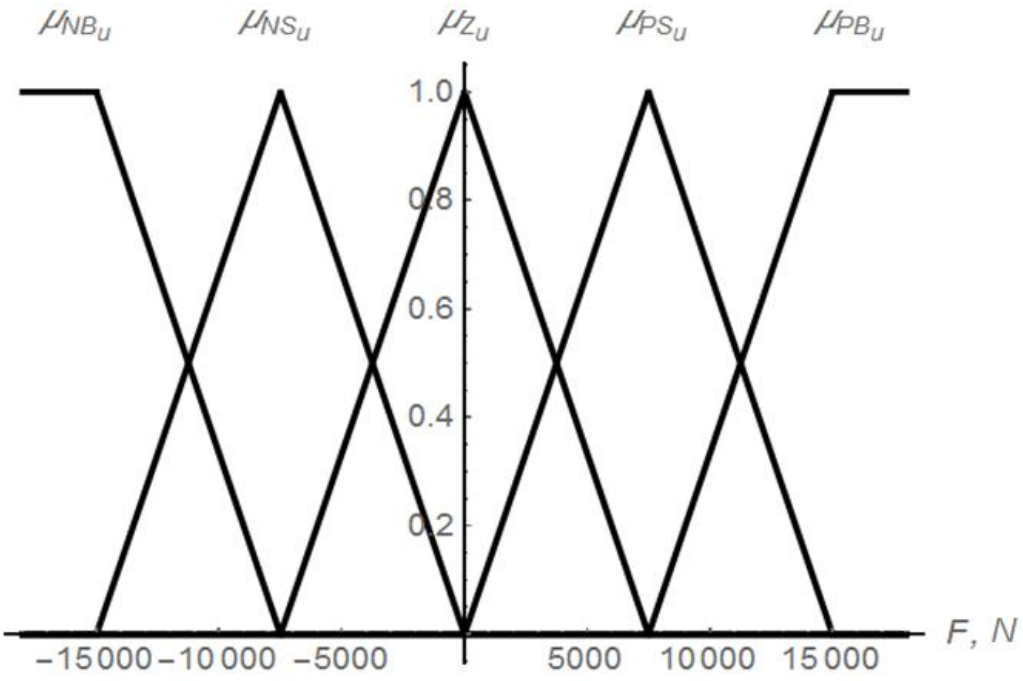

c)

Fig 3.3 Plots of the membership functions of the terms: a) error; b) integral of error; c) control (the output value of the fuzzy-controller)

The next step in the problem of fuzzy-controller synthesis is connected with development of a set of expert rules. Since the input values are only two, and the output is one, it is convenient to present the specified set of rules in the form of a table (Table 3.1).

Table 3.1 Set of expert rules for the synthesis of fuzzy-controller

$\int_0^t edt$ / e	$N_{\int_0^t edt}$	$Z_{\int_0^t edt}$	$P_{\int_0^t edt}$
N_e	PB_u	PS_u	Z_u
Z_e	PS_u	Z_u	NS_u
P_e	Z_u	NS_u	NB_u

The rules, which are given in the form of a table (Table 3.1) logically, follow from the practical experience of vehicle control. For example, when in the input of

the controller are variables that correspond to the terms N_e (significant negative speed error) and $N_{\int_0^t edt}$ (significant negative integral of the speed error), the output corresponds to the term PB_u (significant positive value of a control to eliminate the error and it's integral).

To implement the defuzzification stage, we use the Mamdani approach, i.e. the numerical value of the control u should be calculated as the center of a complex figure.

As a result, we obtain a function that implements the fuzzy-controller: its arguments are the error e and its integral $\int_0^t edt$, and the output is the control value u. Its plot is presented in Fig. 3.4.

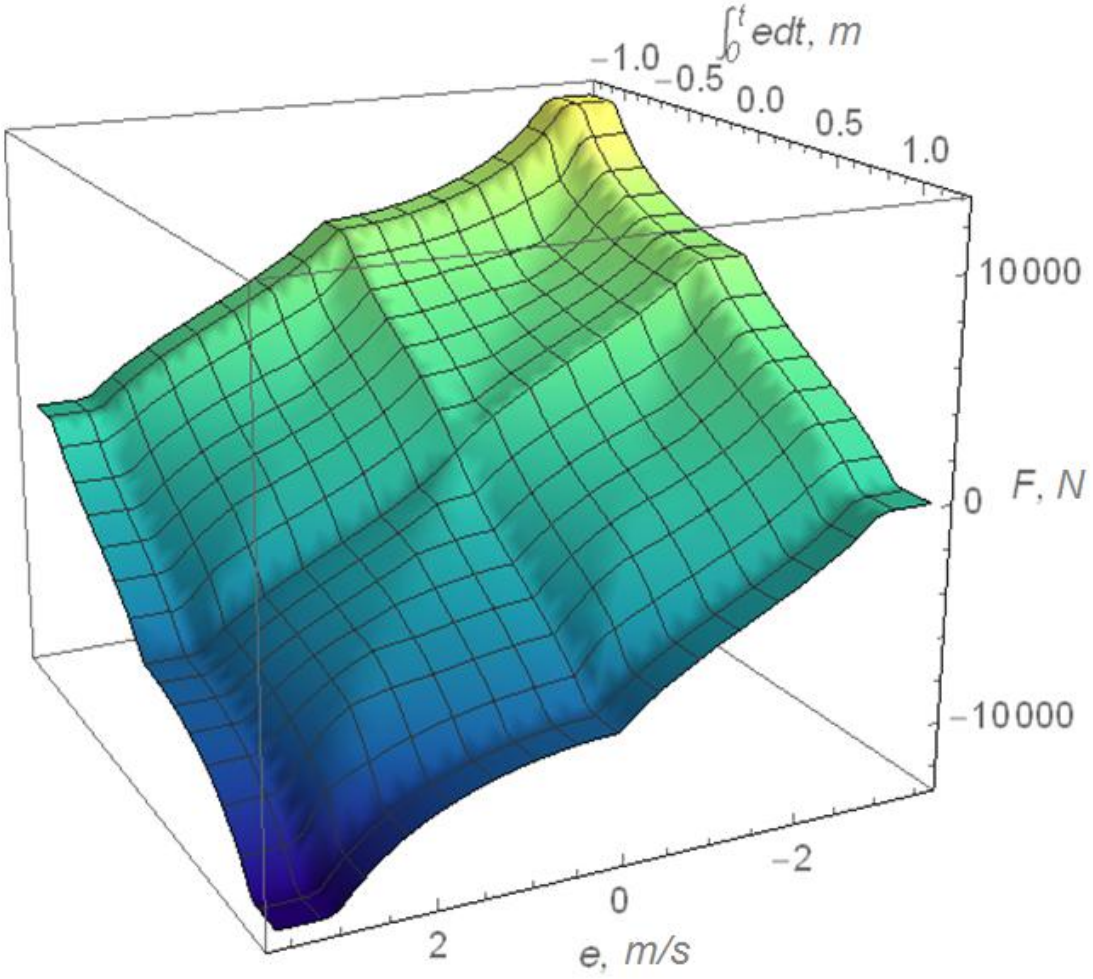

Fig. 3.4 Plot of output control u of the developed fuzzy-controller

The last stage of fuzzy-controller synthesis is connected with simulation its operation and evaluate the quality of control. In order to do this, we have built plots of functions that corresponds to the start of the vehicle (its mass m=5000 kg) from rest to the steady speed v=5 m/s under the action of external disturbances w, which is modeled with a random function, which varies from 0 to 3750 N.

In Fig. 3.5 the corresponding plots are presented. They show a significant speed overshoot and slow reaching the speed setpoint v.

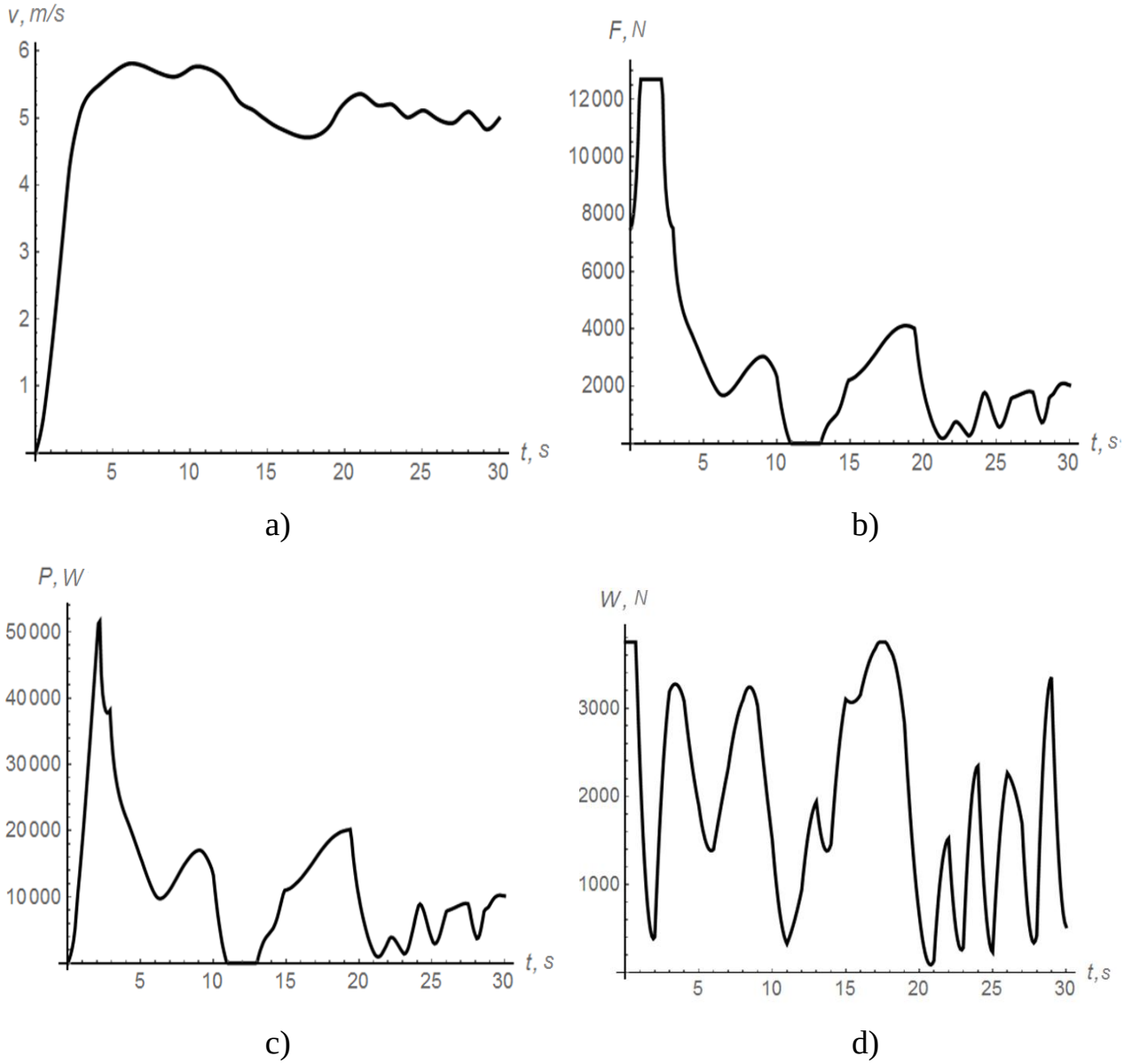

Fig 3.5 Plots of functions: a) the speed of the vehicle $\dot{x}$; b) driving force F ($F=mu$); c) power of the vehicle drive; d) external disturbances

To minimize the speed overshoot and other undesirable indicators (for example, a large peak power of the vehicle drive, which is equal to 51,591 kW) one should modify the expert rule-base and/or change the number and/or the shape of the membership functions of the input and output variables terms. However, these calculations are out of the frame of the study.

The plots, which are presented in Fig. 3.5, show an acceptable control quality around the speed setpoint. Thus, the fuzzy-controller of the vehicle is synthesized. In the further, we perform the synthesis of a fast controller, which has the desired properties of the developed fuzzy-controller, and is characterized by much better speed of operation.

3.3.2 Synthesis of the fast fuzzy-controller of a vehicle

The initial phase of the fast fuzzy-controller development requires the tabulated (discrete) function calculation. It corresponds to the function of the initial fuzzy-controller. In order to ensure sufficient uniformity of sampling of the function (Fig. 3.4), the sample size is assumed to be equal to 2000. The selection of the values of the input variables (error and error integral) is random.

The next step is connected with the approximation of the tabulated function with a polynomial. In calculations for this purpose the following dependence is used:

$$u_a = \sum_{i=1}^{n} A_i e^i + \sum_{i=1}^{n} B_i \left(\int_0^t e dt \right)^i, \; n = 3, \tag{3.3}$$

where A_i and B_i – polynomial coefficients (they are determined based on the minimization of the mean square error of the approximation); n is the order of the polynomial.

Model (3.6) does not contain the terms that reflect the product and degrees of error and the integral of the error. This restriction simplifies the calculations, which are intended only to illustrate the developed method. For the same purpose, the order of polynomial (3.3) has been taken to be equal to three.

Estimations of approximating function u_a coefficients, calculated using the least-squares method, are set at Table 3.2. All the calculations were performed for a confidence level 0.95. The study of the statistical significance of the coefficients was performed by using the Student's t-test.

Table 3.2 Parameters of the function u_a

Coefficient	Coefficient estimation	Statistical significance
A_1	-1656,06	significant
A_2	4,23241	insignificant
A_3	-34,192	significant
B_1	-4934,42	significant
B_2	-50,6152	insignificant
B_3	-932,561	significant

The refined model of the approximation function (polynomial u_a) does not include coefficients A_2 and B_2. The coefficients of the refined approximation function are given in Table 3.3. They all are statistically significant.

Table 3.3 Refined parameters of the function u_a

Coefficient	Coefficient estimation	Standard error
A_1	-1655,74	17,8533
A_3	-34,3038	3,02972
B_1	-4933,99	53,3455
B_3	-932,036	83,9493

The coefficient of determination of the refined approximation function equals to 0.985 which indicates accurate representation by the model (3.6) the tabulated function. In addition, the standard errors of the coefficients of the function u_a, are insignificant.

The next step of the calculations is providing the optimization of the parameters of the function u_a. In order to do this, the numerical values of the coefficients A_1, A_3, B_1, B_3, which are given in Table 3.3, were used. To determine the

optimal values of the coefficients, we have formed a MISO-function, which can be graphically represented as shown in Fig. 3.6.

Fig 3.6 Graphical representation of the MISO-function for optimization of the function u_a coefficients

In the body of the MISO-function the following operations are carried out: the numerical values of the coefficients A_1, A_3, B_1, B_3 should be substituted into expression (3.3), the numerical integration of equation (3.2) should be found, the value of the optimization criteria should be calculated. In this study, such a criterion is the IAE.

The ME-PSO [41] method was used for numerical optimization. At the initial iteration of the global best value refers to optimization criterion IAE, which was obtained by using numerical values of the coefficients A_1, A_3, B_1, B_3 (Table 3.3). Thus, the values of the coefficients obtained at the previous stage of synthesis of the fast fuzzy-controller may be considered as an initial approximation to their optimal values.

The search of the optimal values of the coefficients A_1, A_3 was performed within the specified limits, which were obtained by using the following dependencies:

$$\begin{cases} A_{i.\max} = A_i(1+\Delta A); \\ A_{i.\min} = A_i(1-\Delta A), \end{cases} \tag{3.4}$$

where $A_{i.\max}$ and $A_{i.\min}$ – the upper and lower limits of the search domain of the coefficient A_i respectively; ΔA – the relative „distance” of the limits of $A_{i.\max}$ and $A_{i.\min}$ to the current (taken as the first approximation) value of the coefficient A_i. Note that in expressions (3.4) symmetric boundaries of the domain of the coefficients are used.

In the general case, one of the limits may be at a bigger „distance" from the current value of the coefficient A_i (the value of the first approximation) than the other one.

Similar to (3.4) dependencies are valid for the coefficients B_i.

In this study, $\Delta A=\Delta B=0.5$. Such values ΔA and ΔB are grounded by the fact that in further calculations optimization algorithm ME-PSO [41] has been used. It has powerful search features that allow to determine the optimal coefficients A_1, A_3, B_1 and B_3.

When using this method, the following parameters are set: the number of iterations equals 20; the number of particles equals 20; the acceptable rate of the global best decreasing equals 0.005.

As a result of the ME-PSO application, the optimal values of the coefficients A_1, A_3, B_1 and B_3 were obtained. They are listed in Table 3.4.

In order to evaluate the efficiency of solving the problem, we have given a plot of the ME-PSO convergence to a minimum (Fig. 3.7).

Table 3.4 Optimal coefficients of the function u_a

Coefficients	Optimal values of coefficients
A_1	-2459,12
A_3	-1429,36
B_1	-807,834
B_3	-19,8497

As one can see from Fig. 3.7, the ME-PSO algorithm quickly convergences to the global minimum of the *IAE* criterion.

Therefore, it can be recommended for solving similar problems. Thus, the synthesis of the function u_a has been carried out. It may substitute the initial fuzzy-controller.

The advantages of the synthesized function u_a will be shown in the following investigations.

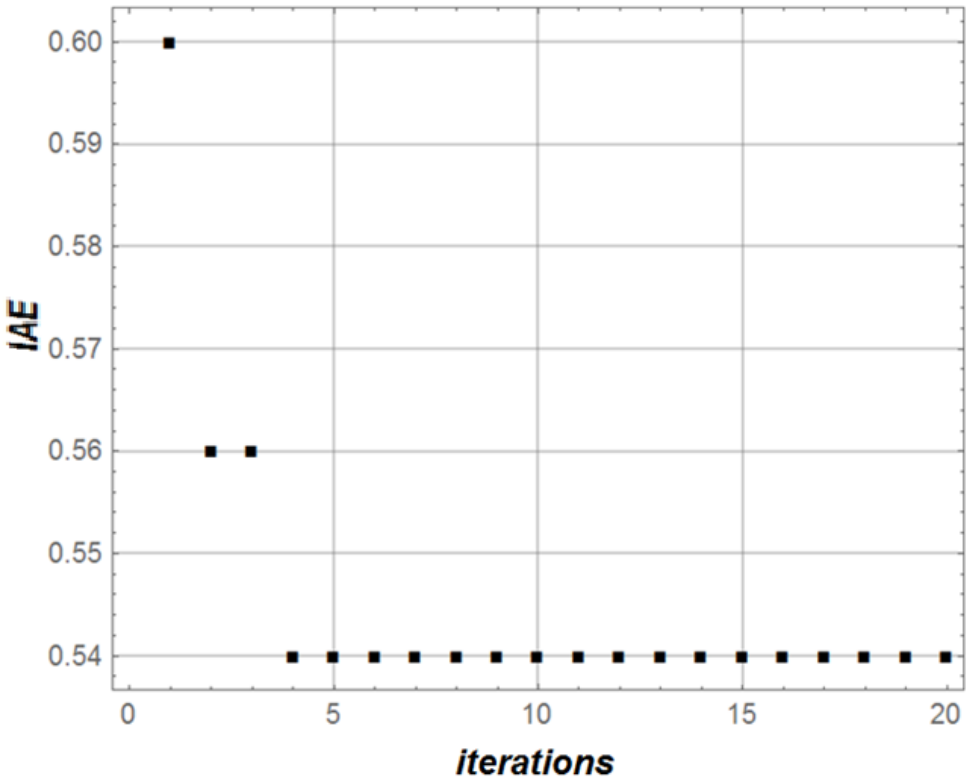

Fig 3.7 Plot of convergence of ME-PSO to the minimum of the *IAE* optimization criterion

3.3.3 Qualitative analysis of the fast fuzzy-controller operation

At the stage of evaluation of the fast fuzzy-controller operation, it is necessary to calculate the values of control quality indicators. On this basis, we may conduct a comparative analysis of the initial (original) and the fast fuzzy-controllers. The following indicators are: the value of the IAE criterion, of the average value of the control module ACM ($t_p^{-1}\int_0^{t_p}|u|dt$), the duration of control t_p ($t_p = t,\ when\ |\dot{x}(t)-v| \le 0{,}05v$), overshoot OS ($\frac{\max(\dot{x}-v)}{v}\cdot 100$). All the calculated numerical values of these indicators are given in Table 3.5.

As one may see from the data, that is given in Table. 3.5, the IAE and ACM of the fast controller are lower by 25.0% and 17.6%, respectively. Instead, the duration of control and overshoot deteriorated by 35.5% and 5.1%, respectively.

Table 3.5 Values of quality indicators of fuzzy-controllers' operation

fuzzy-controller	Values of the indicators			
	IAE	ACM	t_p, s	OS, %
initial	0,72	0,68	21,7	16,3
fast	0,54	0,56	29,4	21,4

Obviously, by rational selection of the optimization criterion one may obtain better indicators of the control quality. Let choose the following parameters of the IPTEC criterion ρ=2, ε=2 and v=2 to conduct the fast fuzzy-controller optimization. As a result of solving the optimization problem, we have obtained the following coefficients: A_1=-7301.66, A_3=-617.17, B_1=-876.63, B_3=-23.39. They correspond to the following indicators of quality of control: IAE=0.55, ACM=0.69, t_p=21.4 s, OS=16.7%. Comparing them with the values, which are given in Table. 3.5, we conclude that the optimization of the coefficients A_1, A_3, B_1, B_3 according to the IPTEC criterion with exponents ρ=2, ε=2 and v=2 allows to reduce the value of the IAE criterion. Other indicators of control quality are almost the same.

In order to illustrate the effect of improving the quality of control, we have presented plots (Fig. 3.8). In Fig. 3.8 gray plots correspond to the initial fuzzy-controller application and black ones – to the fast fuzzy-controller.

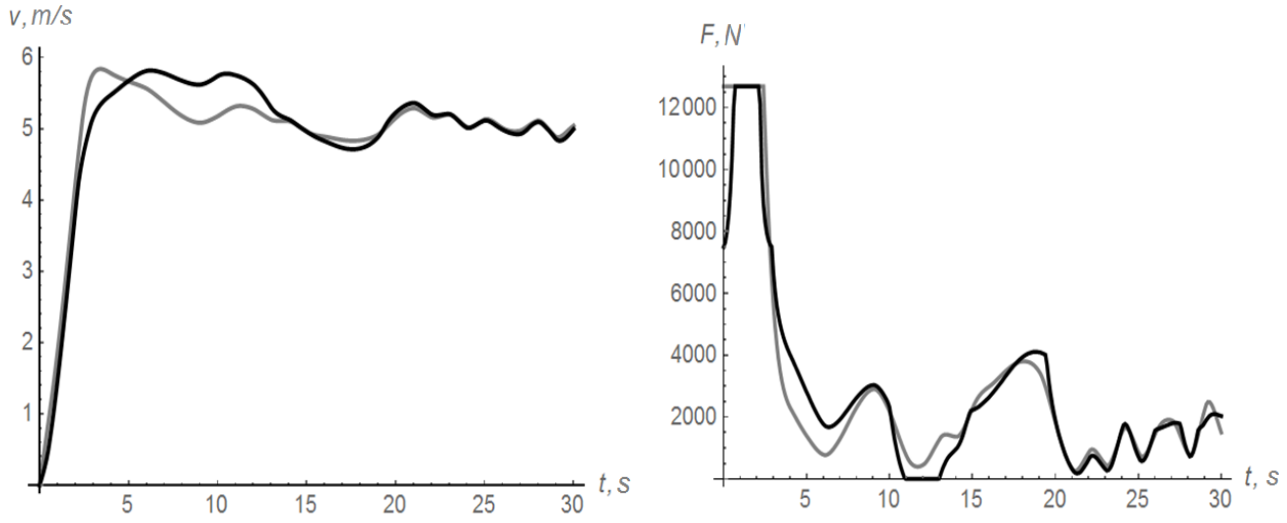

a) b)

Fig. 3.8 Plots of functions: a) the speed of the vehicle $\dot{x}$; b) driving force F ($F=mu$)

Analyzing the plots shown in Fig. 3.8, we have found that the reason for the decrease in the undesirable IAE criterion is connected with an increase of the intensity of control at the stage of the speed setpoint reaching.

In the next section we will show the main advantage of the synthesized fast controller – its high speed of operation.

3.3.4 Comparative analysis of the operation speed of the initial and fast fuzzy-controllers

One of the significant advantages of the synthesized fuzzy-controller is its fast operation. This is connected with the fact that to calculate the control vector it is only necessary to substitute the values of the input variables into a polynomial dependence (3.3). Such calculations are not a problem (in terms of speed of execution) for modern microcontroller devices. Therefore, the fast fuzzy-controller (optimized fuzzy-controller approximation function) does not require significant computing resources (access to the fast fuzzy-controller function is much faster).

On the other hand, a significant number of logical and arithmetic operations are performed to calculate the control of the output vector in the fuzzy-controller. This connected with a long duration of calculations and greater requirements for computing resources (e.g., the amount of RAM) to perform the calculations.

To assess the speed of access to the functions of the initial and fast fuzzy-controllers, we have conducted a comparative analysis. All the calculations have been performed on a PC, which has the following features: 3 GB of RAM, 1.9 GHz processor speed, AMD Turion 64 X2 processor.

In order to obtain statistically reliable data, we have calculated values of durations of access to the initial and fast fuzzy-controllers (all the calculations were performed at 2000 repeatability). The arguments of the functions were chosen randomly from the domain: for the error -1… 1 m/s, for the integral of the error -3… 3 m. Based on the obtained data, the statistical indicators were calculated. They have been given in Table 3.6.

Table 3.6 Statistical indicators of the duration of access to the functions of the initial and fast fuzzy-controllers

Statistical indicator	The value of the indicator for the fuzzy-controller	
	initial	fast
Maximum value, s	$1{,}62 \cdot 10^{-1}$	$4{,}33 \cdot 10^{-4}$
Minimum value, s	$7{,}88 \cdot 10^{-3}$	$1{,}37 \cdot 10^{-5}$
Average value, s	$1{,}34 \cdot 10^{-2}$	$1{,}57 \cdot 10^{-5}$
Median value, s	$9{,}00 \cdot 10^{-3}$	$1{,}42 \cdot 10^{-5}$
Coefficient of variation, %	107,7	119,5

Analysis of the data, given in Table. 3.6, shows that the duration of access to the both of functions varies widely (it is evidenced by significant coefficients of variation). Taking into consideration that fact we have conducted the calculations based on the median values. The median ratio of initial and fast fuzzy-controllers equals to $6{,}34 \cdot 10^{2}$. Thus, the average duration of access to the functions of initial and fast fuzzy-controller differs by two orders of magnitude. Such a significant reduction in access duration will have a positive effect on the ability to reduce the hardware requirements of fuzzy-controllers. The ratio of the maximum and minimum values of the durations of access to the functions of initial and fast fuzzy-controller are $3{,}74 \cdot 10^{3}$ and $5{,}75 \cdot 10^{2}$, respectively.

It should be noted that in the synthesis of the fast fuzzy-controller, a tabular function should be built. During this stage, one should have multiple access to the function of the initial fuzzy-controller. This, in turn, affects the duration of the stage. For more complex problems of synthesis of fast fuzzy-controllers the access duration is bigger. Thus, the duration of this stage is longer. However, the increase in the volume of calculations during the synthesis of the fast fuzzy-controller allows reducing their number during the operation of the controller [42].

Conclusions to chapter 3

1. A method for the synthesis of fast fuzzy-controllers has been developed. It consists in multi-stage procedure: synthesis of initial fuzzy-controller, calculation of tabulated function of initial fuzzy-controller, an approximation of the tabulated function, and optimization its parameters.
2. During optimization of the approximation function's parameters it is desirable to apply the *IPTEC* criterion with reasonably set parameters ρ, ε and v. Its application may increase the operation efficiency of the fast fuzzy-controller in terms of control quality indicators (overshoot, duration of control, integral indicators, etc.).
3. The duration of access to the function of the fast fuzzy-controller $6.34 \cdot 10^2$ times less, that to the function of the initial fuzzy-controller (by the median value). This allows increasing the speed of fuzzy-controller operation and makes the requirements to the hardware and software of the controller much softer.

References to chapter 3

1. Methods of robust, neuro-fuzzy and adaptive control: Handbook (edited by Egupov N.D., 2-nd edition). Moskow: Publisher MSTU named after Bauman. 2002, 744 p. (in Russian).
2. Hagras H. A. A Hierarchical Type-2 Fuzzy Logic Control Architecture for Autonomous Mobile Robots. IEEE Transactions on Fuzzy Systems. 2004, Vol. 12, pp. 524-539.
3. Biglarbegian M., Melek W., Mendel J. M. Design of Novel Interval Type-2 Fuzzy Controllers for Modular and Reconfigurable Robots: Theory and Experiments. IEEE Transactions on Industrial Electron. 2011, Vol. 58, pp. 1371-1384.
4. Liu Z., Zhang Y., Wang Y. A Type-2 Fuzzy Switching Control System for Biped Robots. IEEE Transactions on Systems, Man, and Cybernetics, Part C. 2007, Vol. 37, pp.1202-1213.
5. Juang C. F., Hsu C. H. Reinforcement Ant Optimized Fuzzy Controller for Mobile-RobotWall-Following Control. IEEE Transactions on Industrial Electronics. 2009, Vol. 56, pp. 3931-3940.
6. Kumbasar T., Hagras H. Big Bang–Big Crunch optimization based interval Type-2 fuzzy PID cascade controller design strategy. Information Sciences. 2014, Vol. 282, pp. 277-295.
7. Khanesar M. A., Kayacan E. Feedback error learning control of magnetic satellites using Type-2 fuzzy neural networks with elliptic membership functions. IEEE Transactions on Cybernetics. 2015, Vol. 45, pp. 858-868.
8. Astudillo L. and other. Intelligent Control of an Autonomous Mobile Robot using Type-2 Fuzzy Logic. Engineering Letters. 2006, Vol. 13, pp. 88-93.
9. Linda O., Manic M. Uncertainty-Robust Design of Interval Type-2 Fuzzy Logic Controller for Delta Parallel Robot. IEEE Transactions on Industrial Informatics. 2011, Vol. 7, pp. 661-670.

10. Allawi Z. T., Abdalla T. Y. A PSO-Optimized Type-2 Fuzzy Logic Controller for Navigation of Multiple Mobile Robots. In Proceedings of the IEEE International Conference on Methods and Models in Automation and Robotics (MMAR). Miedzyzdroje. Poland. 2-5 September 2014.
11. Chaoui H., Gueaieb W. Type-2 Fuzzy Logic Control of a Flexible-Joint Manipulator. Journal of Intelligent & Robotic Systems. 2008, Vol. 51, pp. 159-186.
12. Hassan M. Y., Kothapalli G. Interval Type-2 fuzzy position control of electro-hydraulic actuated robotic excavator. International Journal of Mining Science and Technology/ 2012, Vol. 22, pp. 437-445.
13. Ganjefar S., Solgi Y. A Lyapunov stable Type-2 fuzzy wavelet network controller design for a bilateral teleoperation system. Information Sciences. 2015, Vol. 311, pp. 1-17.
14. E. A. Jammeh and other. Interval Type-2 Fuzzy Logic Congestion Control for Video Streaming Across IP Networks. IEEE Transactions on Fuzzy Systems. 2009, Vol.17, pp. 1123-1149.
15. Jammeh E., Mkwawa I., Sun L., Ifeachor E. Type-2 fuzzy logic control of PQoS driven adaptive VoIP scheme. Electronics Letters. 2010, Vol. 46, pp. 137-138.
16. G. M. Méndez and other. Modelling and control of coiling entry temperature using interval Type-2 fuzzy logic systems. Ironmaking & Steelmaking. 2010, Vol. 37, pp. 126-134.
17. Méndez G.M., Castillo O., Colás R., Moreno H. Finishing mill strip gage setup and control by internal Type-1 non-singleton Type-2 fuzzy logic systems. Applied Soft Computing. 2014, Vol. 24, pp. 900-911.
18. Lin F. J., Shieh P. H., Hung Y. C. An intelligent control for linear ultrasonic motor using interval Type-2 fuzzy neural network. IET Electric Power Applications. 2008, Vol. 2, pp. 32-41.

19. Barkat S., Tlemçani A., Nouri H. Noninteracting Adaptive Control of PMSM Using Interval Type-2 Fuzzy Logic Systems. IEEE Trans. Fuzzy Syst. 2011, Vol. 19, pp. 925-936.
20. Chen C. S., Lin W. C. Self-adaptive interval Type-2 neural fuzzy network control for PMLSM drives. Expert Systems with Applications. 2011, Vol. 38, pp. 14679-14689.
21. Naik N. V., Singh S. P. Improved Torque and Flux Performance of Type-2 Fuzzy-based Direct Torque Control Induction Motor Using Space Vector Pulse-width Modulation. Electric Power Systems International Inc. 2014, Vol. 42, pp. 658-669.
22. Ramesh T., Panda A. K., Kumar S. S. Type-1 and Type-2 Fuzzy Logic and Sliding-Mode Based Speed Control of Direct Torque and Flux Control Induction Motor Drives–A Comparative Study. International Journal of Emerging Electric Power Systems. 2013, Vol. 14, pp. 385-400.
23. Yu W. S., Chen H. S. Interval Type-2 fuzzy adaptive tracking control design for PMDC motor with the sector dead-zones. Information Sciences. 2014, Vol. 288, pp. 108-134.
24. Maldonado Y., Castillo. O. Genetic Design of an Interval Type-2 Fuzzy Controller for Velocity Regulation in a DC motor. International Journal of Advanced Robotic Systems. 2012, Vol. 9, pp. 204-212.
25. Maldonado Y., Castillo O., Melin P. A multi-objective optimization of Type-2 fuzzy control speed in FPGAs. Applied Soft Computing. 2014, Vol. 24, pp. 1164-1174.
26. Wang T., Tong S. Direct inverse control of cable-driven parallel system based on Type-2 fuzzy systems. Information Sciences. 2015, Vol. 310, pp. 1-15.
27. Martínez J.S., John R.I., Hissel D., Péra M.C. A survey-based Type-2 fuzzy logic system for energy management in hybrid electrical vehicles. Information Sciences. 2012, Vol. 190, pp. 192-207.

28. Martínez J. S. and other. Experimental validation of a Type-2 fuzzy logic controller for energy management in hybrid electrical vehicles. Engineering Applications of Artificial Intelligence. 2013, Vol. 26, pp. 1772-1779.
29. Nechadi E., Harmas M. N., Hamzaoui A., Essounbouli N. Type-2 fuzzy based adaptive synergetic power system control. Electric Power Systems Research. 2012, Vol. 88, pp. 9-15.
30. Panda M. K., Pillai G., Kumar V. An interval Type-2 fuzzy logic controller for TCSC to improve the damping of power system oscillations. Front. Energy. 2013, Vol. 7, pp. 307-316.
31. Tripathy M., Mishra S. Interval Type-2-based thyristor controlled series capacitor to improve power system stability. IET Generation, Transmission & Distribution. 2011, Vol. 5, pp. 209-222.
32. Panda M. K., Pillai G. N., Kumar V. Design of an Interval Type-2 Fuzzy Logic Controller for Automatic Voltage Regulator System. Electric Power Systems International Inc. 2012, Vol. 40, pp. 219-235.
33. Sudha K.R., Santhi R.V. Robust decentralized load frequency control of interconnected power system with Generation Rate Constraint using Type-2 fuzzy approach. International Journal of Electrical Power & Energy Systems. 2011, Vol. 33, pp. 699-707.
34. Altin N. Interval Type-2 Fuzzy Logic Controller Based Maximum Power Point Tracking in Photovoltaic Systems. Advances in Electrical and Computer Engineering. 2013, Vol. 13, pp. 65-70.
35. Altin N. Single Phase Grid Interactive PV System With MPPT Capability Based on Type-2 Fuzzy Logic Systems. In Proceedings of the International Conference on Renewable Energy Research and Applications. Nagasaki. Japan. 11–14 November 2012.
36. Yang T. C., Juang J. G. Application of Adaptive Type-2 Fuzzy CMAC to Automatic Landing System. In Proceedings of the International Symposium on Computational Intelligence and Design. Hangzhou. China. 29-31 October 2010.

37. Yang F. and other. Direct adaptive Type-2 fuzzy neural network control for a generic hypersonic flight vehicle. Soft Computing. 2013, Vol. 17, pp. 2053-2064.
38. Chen X., Li D., Xu Z., Bai Y. Gain adaptive sliding mode controller based on interval type-II fuzzy neural network designed for attitude control for micro aircraft vehicle. International Journal of Intelligent Computing and Cybernetic. 2008, Vol. 7, pp. 209-226.
39. Chen X., Li D., Xu Z., Bai Y. Robust control of quadrotor MAV using self-organizing interval type-II fuzzy neural networks (SOIT-IIFNNs) controller. International Journal of Intelligent Computing and Cybernetic. 2011, Vol. 4, pp. 397-412.
40. Chaturvedi D. K. Soft Computing Techniques and its Applications in Electrical Engineering. Springer. 2008, 612 p.
41. Romasevych Yu., Loveikin V. A Novel Multi-Epoch Particle Swarm Optimization Technique. Cybernetics and Information Technologies. 2018, 18(3), pp. 62-74. DOI: 10.2478/cait-2018-0039
42. Romasevych Y.O., Loveikin V.S., Liashko A.P. The method of synthesis of fast fuzzy-controllers. Energetics and automatics. 2019, №5, pp. 5-21. (in Ukrainian)

CHAPTER 4. BIOTECHNICAL OBJECTS AND MODERN METHODS FOR FORECASTING THE NATURAL DISTURBANCES' IMPACT

4.1 Features of complex biotechnical objects and natural disturbances

The agricultural production in the world and Ukraine is filled with modern high-tech enterprises, the hallmark of which is the presence of a biological component. These companies are, first of all, poultry, greenhouses, mushroom production. The part of energy in production costs for these companies reach sometimes 70 % (greenhouses). Under the conditions of the high cost of energy and its actual deficits measures that reduce energy consumption are topical. Our analysis of international experience in the field of automation of control processes in agriculture showed that all of the existing control systems do not take into account possible future changes in the disturbances, in particular air temperature, on the technological object during the entire period of bioobject housing (growing), as well as the dynamics of bioobject states and perform exclusively stabilization mode for technological parameters, given the instantaneous values of the disturbances that is not always effective

With rampant increasing of energy prices is important to use control algorithms of electrotechnical complexes which accompany appropriate technology, taking into account the biological filling state and maximize production profit primarily by reducing energy costs. The intelligent control systems of electrotechnical objects are able to form such algorithms, which are used the theories of stochastic processes, neural networks, game theory and statistical decisions, etc.

Objects of agricultural production of industrial type are complex biotechnical systems, the efficiency of which is estimated by the ratio of energy consumption of production to the volumes, quality and timing of receipt of marketable products. Greenhouses, especially greenhouse combines, use significant volumes of energy resources and, given the high price of the latter, require the use of energy-efficient

consumption regimes. In the first place, this concerns the provision of appropriate microclimate parameters in greenhouses.

Improvement of greenhouse designs and improvement of microclimate control algorithms have been intensively developed in recent years, but mostly in the countries of northern and central Europe. Unfortunately, in Ukraine, planting of closed soil is significantly behind the best foreign samples. Often, outdated equipment and control systems for such equipment continue to function. In addition, foreign modern technologies of closed soil are often accompanied by the simplest stabilization algorithms that do not contribute to the saving of energy resources (noted significantly in Ukraine, since the energy content of buildings in closed-ground buildings is up to 50-70%).

The evolution of control systems of electrotechnical complex for technological objects (Fig. 4.1) started with systems that form the stabilization algorithms (phase I). But even now, despite sophisticated technological equipment available both in poultry and for greenhouse continue to use simple control algorithms of electrotechnical complexes - stabilizing algorithms. At the same time international and national experience has shown that their application can be justified only to some extent, under conditions of low energy prices. In this case, by technological standards and controls stabilized without taking into account the character of natural disturbances and states of biological objects, which allows in certain seasons to maximize their productivity. But even in these cases often actuators capacity is not enough for the viability of biological filling in optimal in terms of its performance conditions.

In the 90's of the previous century, when energy costs began to rise, offered as a separate development, the use of algorithms that minimize energy use for individual processes (Stage II) [10]. Later, given the properties of objects change their dynamic parameters were tested adaptive systems (Stage III) capable of in service take into account these circumstances, realizing optimum process control algorithms [5]. But systematically tailored to suit biological content, the analysis of natural disturbances, state of the market value on energy production and quality to ensure maximum profit

production can only intelligent control system (Stage IV) [1]. As shown in the figure, their advantage is obvious and provided a significant decrease in the energy component in the production costs structure.

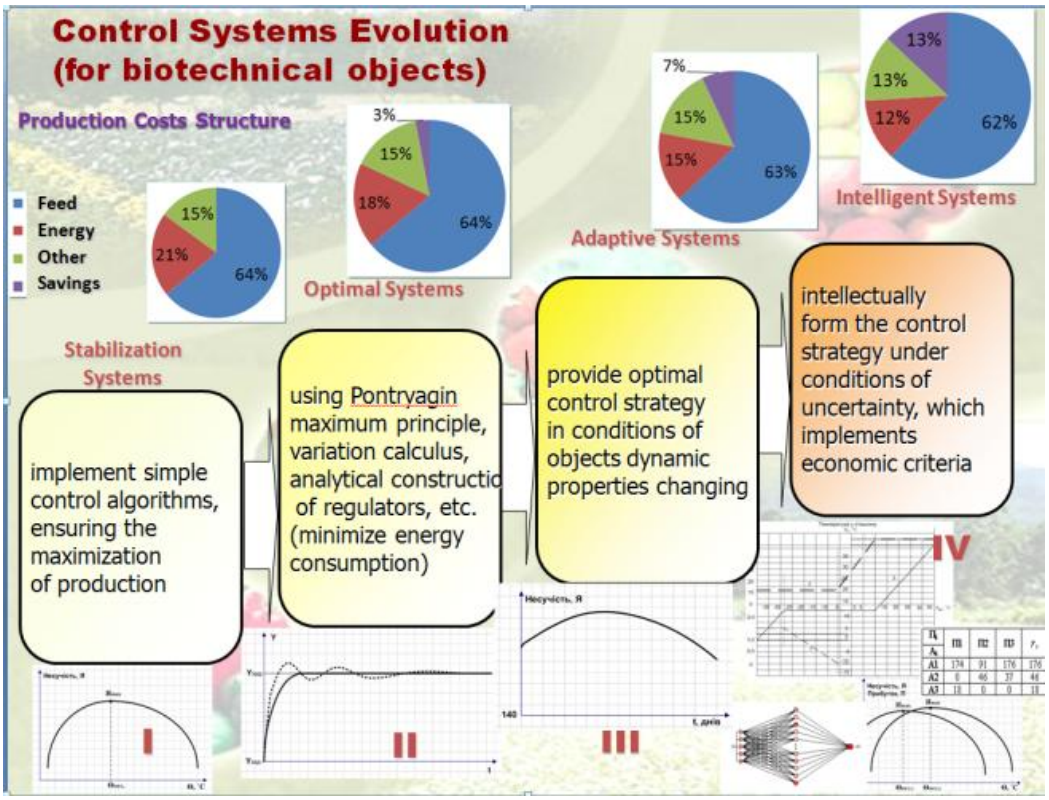

Fig. 4.1 Control Systems Evolution

Biotechnological objects primarily include poultry farms and greenhouses. Both areas except technology and process equipment (technical facility) have biological filling (chicken, plants). Each of these biotechnical objects characterized by significant energy consumption. So for poultry in the cost structure of production, the share of energy up to 20 %, and for greenhouse plants - up to 70 % [2].

With rampant increasing of energy prices is important to use control algorithms of electrotechnical complexes which accompany appropriate technology, taking into account the biological filling state and maximize production profit primarily by reducing energy costs. The intelligent control systems of electrotechnical objects are able to form such algorithms, which are used the theories of stochastic processes, neural networks, game theory and statistical decisions, etc. [8].

Promising measures to improve the situation in the field of greenhouse production of plant products is to improve the design of greenhouses, optimize the processes of growing plants by introducing intelligent computer integrated control systems that can ensure the implementation of the economic criterion of production efficiency - the maximum profit of production.

According to preliminary research reducing of energy consumption through the development and implementation of intelligent control systems using the latest methods and means of automation, able to predefine control action based on disturbances forecasting, technological requirements and biological object characteristics.

Review of the functioning of the process facilities along with the peculiarities of the dynamics of natural disturbances and living organisms' states and the rational use of energy resources will increase profits from production. Experimental studies depending on the main quality parameters of biological objects from change of microclimate and establish the most productive growing conditions have provided the mathematical model of states of plants that were later used in the formation of management strategies.

Neural network forecasting of external disturbances can increase system performance up to 20 % and can increase technological efficiency up to 13 %. Also, additional energy savings can provide phytomonitoring of plants. Phytomonitoring can be implemented using modern robotic technical systems to ensure reliability and efficiency of a given measurement.

Despite on modern technological equipment available in poultry houses and greenhouses simple control algorithms of electrotechnical complexes are implemented. This is usually the stabilization algorithms proposed for maintenance of process parameters to maximize performance of poultry and plants (defined by scientific researches). These algorithms are not energy efficient because of a biological component states, its performance and character of natural disturbances are not taking into account [5]. In addition, often, as illustrated by the poultry house,

typical actuators capacity is not enough to hold biological object (hens) at a temperature that ensures its maximum performance (Fig. 4.2).

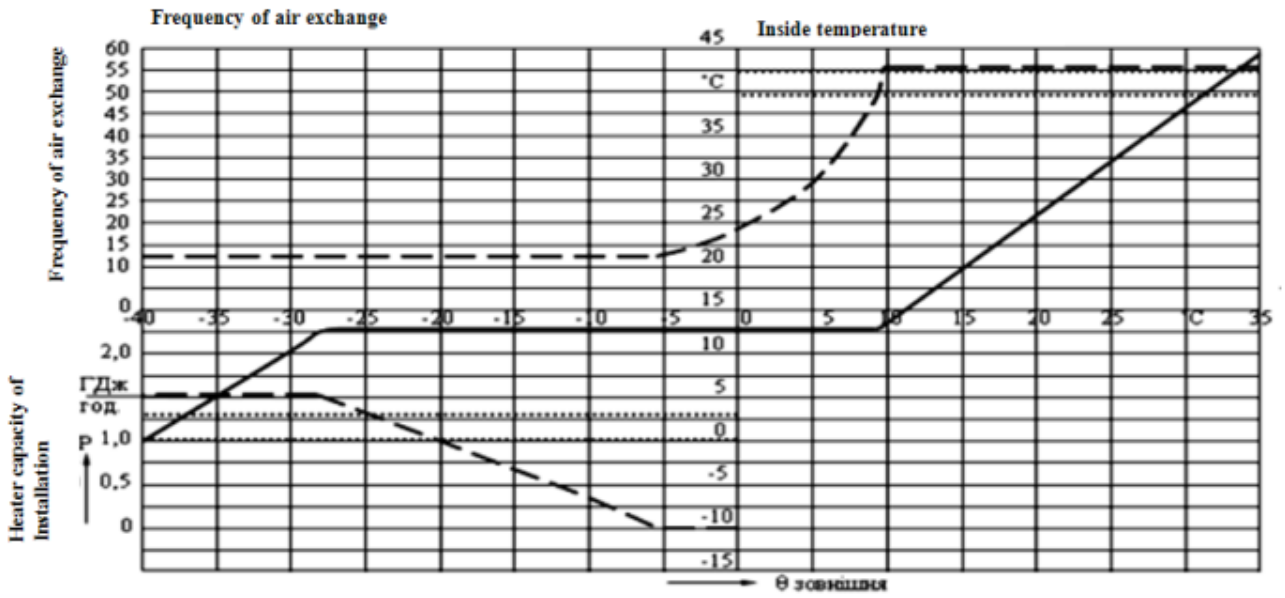

Fig.4.2 Static characteristic of typical poultry house

A generalized analysis of the technological, zootechnical, cultivation and organizational processes which occur in greenhouses and poultry houses has been carried out in order to define the peculiar features of biotechnical facilities. As a result of the analysis of these processes, it has been established that greenhouses and poultry houses are complex systems and their study and research requires a systematic analytical approach [7].

Thus, poultry which are used for industrial production are homothermic organisms maintaining body temperature at a constant level as their characteristic feature. The thermoregulatory effect which is built on the cybernetic principle of feedback control includes the activity of a number of body systems which are aimed at increasing the heat production and limiting the heat loss when cooling the body as well as limiting the heat production and increasing the heat loss when the body is heated. By the critical point we mean the ambient temperature at which the lowest level of metabolism in the body takes place while the mechanism of heat loss is largely considered discontinued. However, experiments prove that there is a seasonal

change of the critical point [8] as well as its change depending on the behaviour of the biological object.

The crops which are grown in a greenhouse are living organisms. The plant in the greenhouse is affected by a complex set of factors which can be conveniently classified into four groups: biotic (depend on the plant only), abiotic (do not depend on the plant), geographic and anthropogenic (driven by the human activity).

The formation of chlorophyll occurs in the plant cells when influenced by the sunlight. During the process of photosynthesis (assimilation), chlorophyll absorbs carbon which in turn enters into a biochemical reaction under the action of light which results in the formation of such organic compounds as starch, sugar, proteins, fats, organic acids, etc. The plants simultaneously emit oxygen.

Respiration (dissimilation) which involves the constant absorption of oxygen and emition of carbon is another process peculiar to plants. The relationship between the photosynthesis and respiration changes during the day. At the daytime, the absorption of carbon is about 10 times faster than the decomposition of the organic substances during respiration. Photosynthesis consumes approximately 2 to 5 per cent of all the incoming solar energy. This energy is mainly spent on moisture evaporation and heat exchange between the air and the soil. The temperature which affects the plant in the greenhouse is considered to be an abiotic factor. We distinguish between the soil and the air temperatures. The thermal regime of the plants is formed under the influence of the radiation balance, the heat exchange with the environment and the evaporation of moisture by the plants. The temperature, as well as light, effect the biochemical processes in the cells. The temperature influences the processes of photosynthesis and respiration in a different way. However, at temperatures below 10˚C both processes halt. The temperature which provides maximum photosynthesis can vary depending on the species of the plant. It constitutes from 26 to 30 ˚C for tomatoes. However, for most plants the process of photosynthesis halts at the temperatures below 10 ˚C and above 50 ˚C [6, 7].

Respiratory processes inside the plants also depend on the temperature. The temperature which maximizes this process constitutes from 36 to 40˚C for most

plants. The increase in the organic mass depends on the interaction of photosynthesis and respiration. Since both processes depend on the external factors the accumulation of the organic substance can be considered to be the difference between the amount of the substance which was formed from the photosynthesis and the substance which was decomposed during respiration (Fig.4.3).

To ensure maximum productivity in the plant growing it is necessary to carry out the control actions which make it possible to maintain the microclimate, moisture and nutrient properties of the soil at the levels which would maximize the organic substance growth at any time during their development while taking into consideration the physiological characteristics of the plants [4].

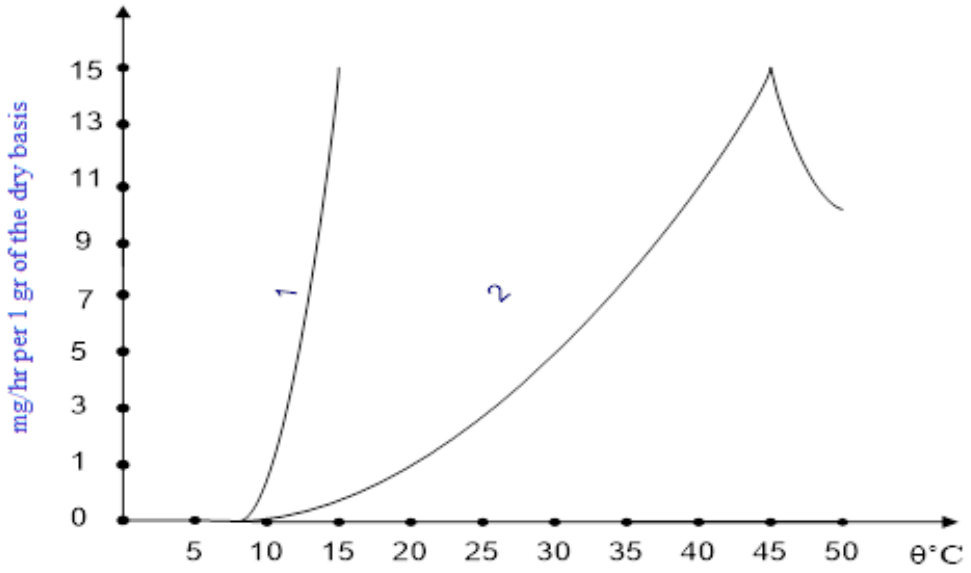

Fig. 4.3 The dependence of assimilation (1) and dissimilation (2) on the temperature

Ensuring the above-mentioned conditions of the plant development requires significant investment into the construction of the facilities and the technological equipment as well as significant energy expenditures which are necessary to maintain the specified parameters. Such control systems do not use an efficiency indicator which would maximize the difference between the profits from the products grown and the costs of growing them.

The assessment criteria for the production of the crop products in the greenhouses can be as follows: the accuracy of the growing conditions maintenance which preclude the biological object from dying regardless of the changes in the external disturbances or provide the lowest percentage of losses within the individual least durable representatives; the quality indicators of the received products; the highest productivity of the biological object during its management; the minimum costs spent on physical, energy and labor resources for the management of a biological object.

Plants states are influenced by solar radiation. Thus, there is a need for analysis and forecasting of outside air temperature and solar radiation intensity for using the forecast results in the formation of electrotechnical complex control strategies with the aim to reduce energy costs in the production of agricultural products.

The solution of this problem is possible in two variants: the identification based on the theory of random processes images (areas) of natural disturbances that characterize the implementation of temperature; neural networks.

4.2 Analytical review of time series forecasting methods and substantiation of neural network structure

According to estimates of foreign and domestic researchers of time series (TS) forecasting, there are already more than 100 forecasting methods. The number of basic forecasting methods, which in some variations are repeated in other methods, is much smaller. Many of these "methods" refer rather to individual techniques or procedures of forecasting, others represent a set of individual techniques that differ from the basic or from each other in the number of specific techniques and the sequence of their application [15].

A large number of classification schemes of time series prediction methods are known, but most of them are either unacceptable or have insufficient cognitive value. The main error of the existing classification schemes is the violation of the principles of classification. Among the main such principles are [17, 19]:

- sufficient coverage completeness of prognostic methods,
- unity of classification feature at each level of distribution,
- openness of classification.

Of course, different classification schemes designed for a specific purpose or task have a right to exist.

Each level of detail is determined by its classification feature:

- formalization degree,
- general principle of action,
- way of prognostic information obtaining.

According to the formalization degree, all forecasting methods are divided into intuitive and formalized [20].

Intuitive forecasting of TS is used when the object of forecasting is either too simple or so complex that it is almost impossible to analytically take into account the influence of many factors [21]. In these cases, resort to expert questioning. The obtained individual and collective expert assessments are used as final forecasts or as initial data in complex forecasting systems. Accordingly, intuitive methods are divided into: the method of individual expert assessments and the method of collective expert assessments. The first includes such methods as interviews, scripts and analytical notes.

The most common is the class of formalized methods which is divided into subclasses:

– extrapolation methods (the method of least squares, exponential smoothing, probabilistic modeling);

– system-structured methods (morphological analysis, functional-hierarchical modeling, matrix method, network modeling, method of structural analogy, method of graphs and tree of goals, prognostic scenario);

– mathematical methods (correlation and regression analysis, the method of group consideration of arguments, factor analysis, pattern recognition, variation methods, spectral analysis, Markov networks, mathematical logic);

– associative methods (methods of imitation modeling, methods of theory of pattern recognition, neural network forecasting, logical-historical methods)

– methods of anticipatory information (analysis of packet information, analysis of information flow).

When choosing the methods of forecasting the TS, an important indicator is the depth of the forecast. It is necessary not only to know the absolute value of this indicator, but also to relate it to the duration of the evolutionary cycle of the object of forecasting.

For this purpose it is possible to use the dimensionless indicator of depth (range) of forecasting offered by V. Bilokon

$$(\tau)\tau = \Delta t / t, \qquad (4.1)$$

where Δt is the absolute lead time; τ is the value of the evolutionary cycle of the prediction object.

Formalized forecasting methods are effective if the value of the depth of anticipating falls within the evolutionary cycle ($\tau << 1$).

At the time of occurrence within the forecast period of the "jump" in the development of the object of forecasting ($T \approx 1$) it is necessary to use intuitive methods both to anticipate the force of the "jump" and to valuation the time of its execution, or the theory of catastrophes. In this case, formalized methods are used to assess the evolutionary areas of development before and after the jump.

If in the forecast period several evolutionary cycles of development of the forecasting object ($T >> 1$) are concluded, then during the elaborating of forecasting systems intuitive methods become more important.

Methods of collective expert assessments can already be attributed to complex forecasting systems (usually incomplete), as the latter combine methods of individual expert assessments and statistical methods of processing these assessments. But since statistical methods are used in auxiliary procedures for the production of forecasting information, collective expert assessments should be attributed to singular forecasting

methods. The group of individual expert assessments can include (the principle of classification - a method of obtaining prognostic information) the following methods: the method of "interview", analytical reports, script writing.

The group of collective expert evaluations includes questionnaires, methods of "commissions", "brainstorming" (collective generation of ideas).

The class of formalized methods, depending on the general principles of action can be divided into groups of extrapolation, system-structural, associative methods and methods of anticipatory information [23].

The group of methods of predictive extrapolation can include the methods of least squares, exponential smoothing, probabilistic modeling and adaptive smoothing. The group of system-structural methods includes methods of functional-hierarchical modeling, morphological analysis, network modeling, structural analogy.

Associative methods can be divided into methods of simulation and historical-logical analysis.

The group of methods of anticipatory information can include methods of analysis of flows of publication and packages of information.

As a time series for which we will develop an accordant mathematical apparatus, we will take the ambient temperature. Temperature forecasting which based on the theory of statistical solutions, in production conditions demonstrates acceptable sensitivity and adequacy [2].

At the same time, it is obviously that an additional significant input parameter of the intelligent control system of an industrial facility will only increase the efficiency of its operation. As an input value, you can use the predicted value of temperature, if the forecast is based on the theory of analysis of the partial discharges [12].

Among similar researches the project of the distributed calculations for forecasting of changes of a climate of the Earth for the next 50 years is allocated - "Climate Prediction", which involves scientists from the Universities of Oxford and Reading, the Meteorological Center of Great Britain, Rutherford-Appleton Laboratory and the software company Tessella Support Services. However for the

task of energy-efficient management of industrial poultry house as a biological object such long-term predictions are not required. It is enough to get an adequate forecast for a few hours ahead [22].

In comparison with classical methods of analysis of time series NN have certain advantages [13]:

1. Constant optimization of own structure for the purpose of a prognostic error minimization in real time.

2. Higher potential opportunities in the analysis of complex dynamic systems and patterns.

3. Ability to successfully solve problems based on incomplete, distorted and internally contradictory input information.

4.3 Synthesis and study of neural network structures forecasting temperature time series

The Statistica Neural Networks software [24] package was used to synthesize and study the corresponding NNs. Criterion - minimization of NN error. In the context of our task, its advantage over similar developments is the realization of a functional unit for optimizing the architecture of neuromodels, which uses linear approaches and a method of imitation "annealing" based on the Gibbs probability distribution [14]:

$$P(\overline{x^*} \to \overline{x_{i+1}} \Big| \overline{x_i}) = \begin{cases} 1, F(\overline{x^*}) - F(\overline{x_i}) < 0 \\ \exp(-\dfrac{F(\overline{x^*}) - F(\overline{x_i})}{Q_i}), \; F(\overline{x^*}) - F(\overline{x_i}) \geq 0 \end{cases} \qquad (4.2)$$

where Qi> 0 - elements of an arbitrarily descending to zero sequence.

For the time temperature range we will take the statistical data for September 2006. Discrete data acquisition - 3 hours. The length of the time series is 243 elements.

To improve the quality of NN operation, we will perform preliminary normalization of input data according to the linear dependence (range: [0, 1]):

$$x_н = \frac{x_i - x_{\min}}{x_{\max} - x_{\min}} \qquad (4.3)$$

where x_i is the real value of the time series element; x_{min} - time series element that has a minimum value; x_{max} is the element of the time series that has the maximum value.

We activate the network constructor with the task to issue 5 NN with the best modeling indicators. At the same time, we set the forecast one step forward with the length of the time window equal to five.

For efficient modeling in the Statistica Neural Networks package, the input data is automatically divided into three blocks: training, control, test. The presence of three blocks is not mandatory, but the test block improves the quality of further work, because it allows you to make sure that there is no "retraining" (overfitting) of the network. To increase visibility forecasting do not set the last 8 elements (24 hours) of the temperature time series

As a result of solving the optimization problem, the best NNs were selected (Figs. 4.4, 4.5): radial-basic function (errors: training– 2,617 ^{0}C, control– 2,617 ^{0}C, test – 2,06 ^{0}C), linear with two neurons in the input layer (errors: training – 0,103 ^{0}C, control – 0,086 ^{0}C, test – 0,097 ^{0}C), linear with three neurons in the input layer (errors: training – 0,103 ^{0}C, control – 0,086 ^{0}C, test – 0,096 ^{0}C), multilayer perceptron with five neurons in the hidden layer (errors: training – 0,077 ^{0}C, control – 0,068 ^{0}C, test – 0,074 ^{0}C), multilayer perceptron with two neurons in the hidden layer (errors: training – 0,073 ^{0}C, control – 0,065 ^{0}C, test – 0,07 ^{0}C).

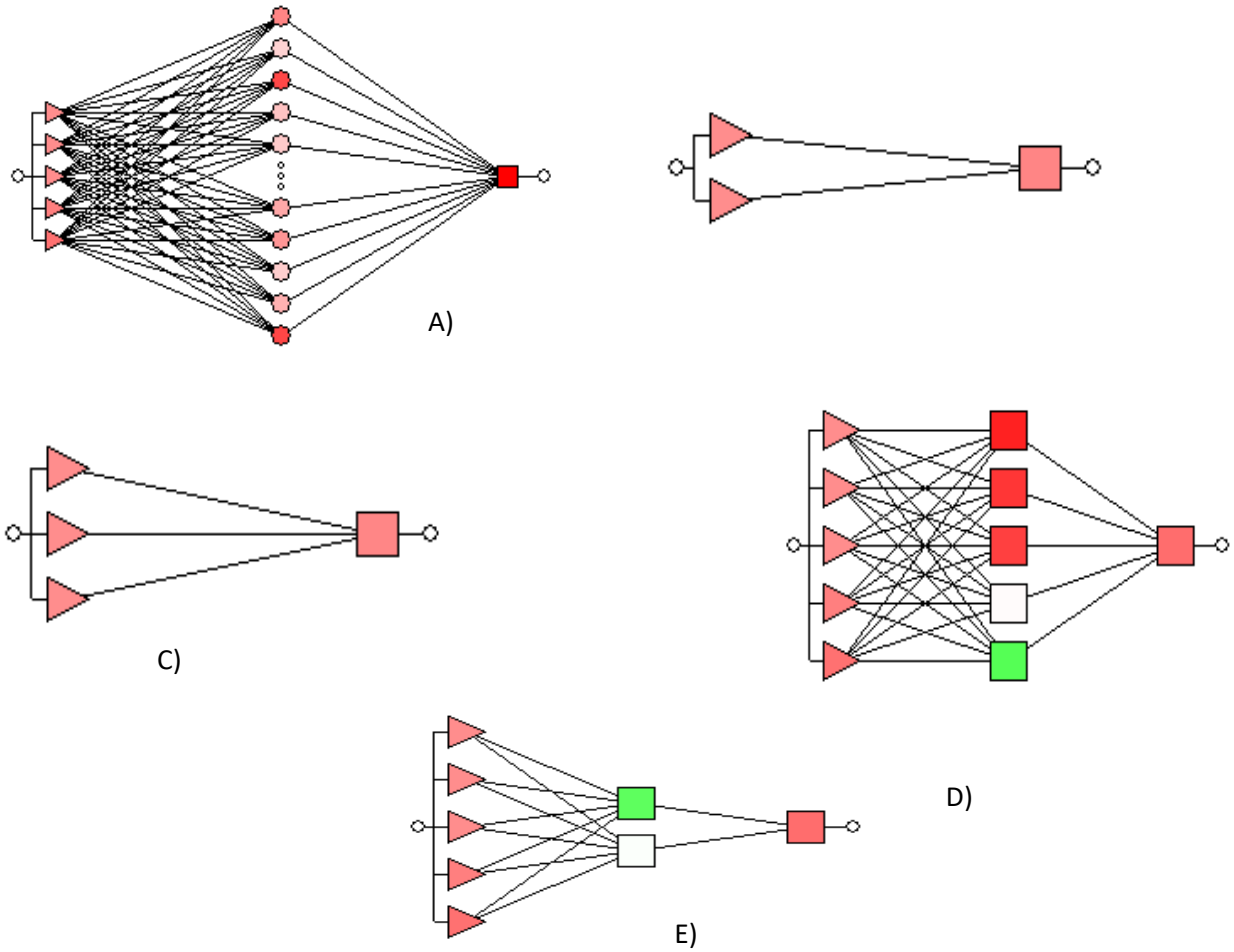

Fig. 4.4 Optimal architectures of NN prediction of temperature time series: A - radial-basis function (RBF), B - linear with two neurons in the input layer (Linear 1), C - linear with three neurons in the input layer (Linear 2), D - multilayer perceptron with five neurons in the hidden layer (MLP 1), E - multilayer perceptron with two neurons in the hidden layer (MLP 2)

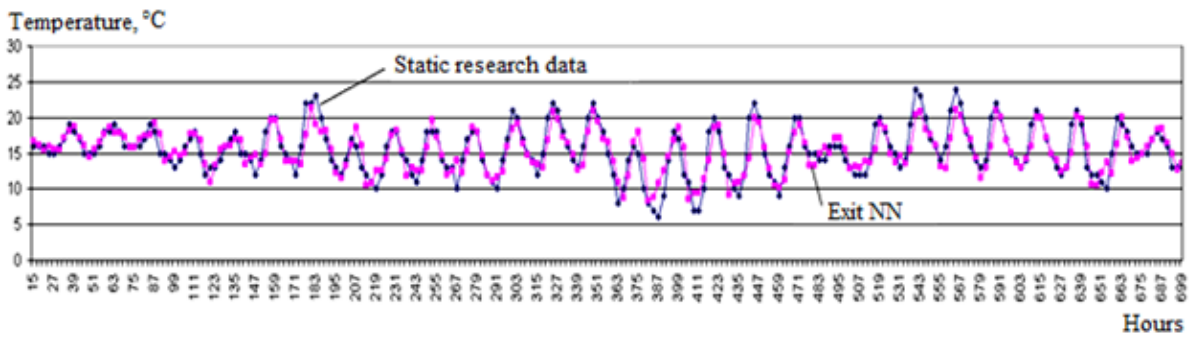

A)

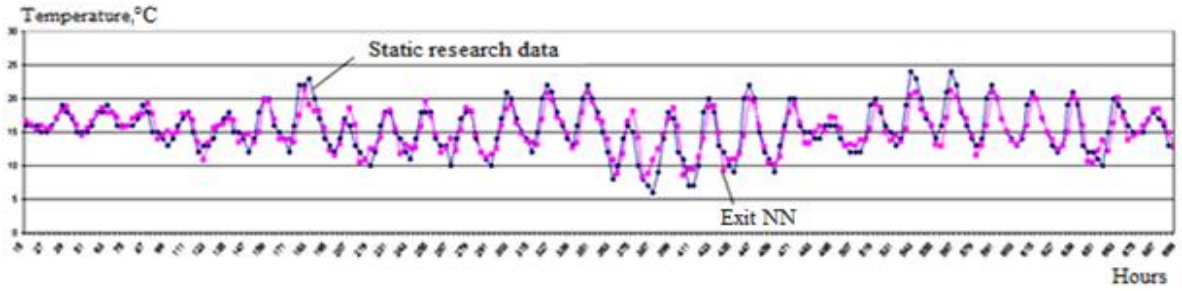

B)

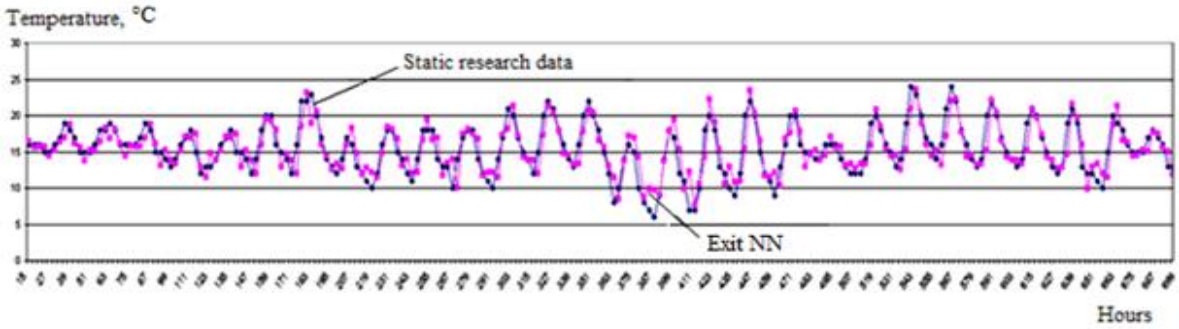

C)

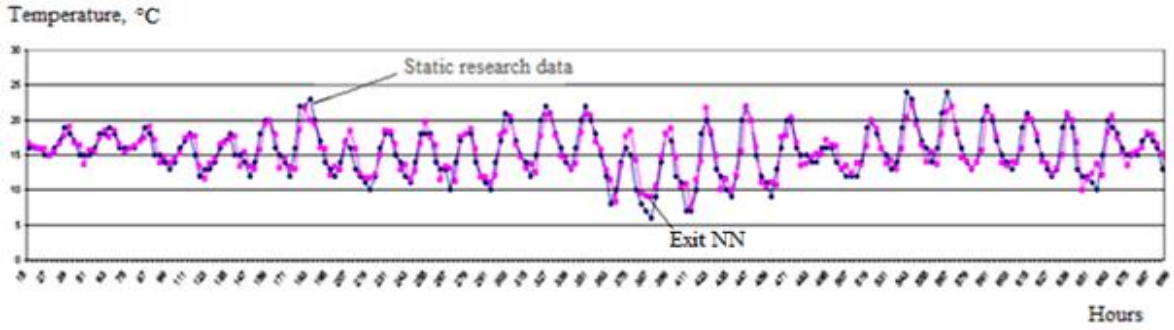

D)

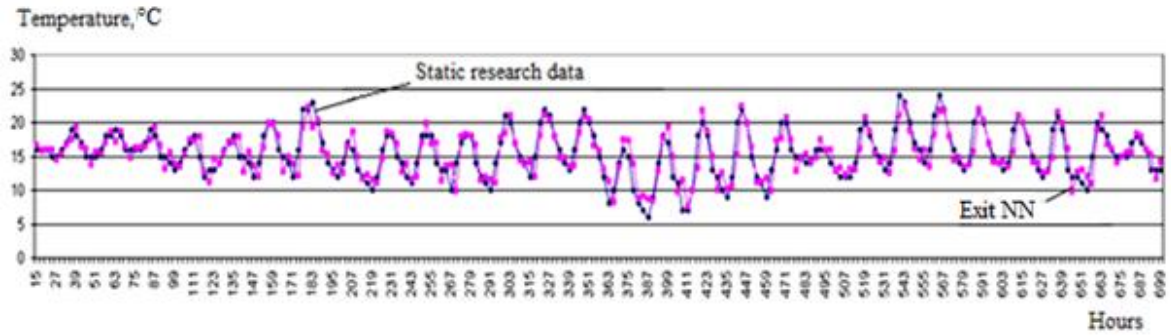

E)

Fig. 4.5 Graphs of educational forecasting of temperature time series of NN: A - radial-basis function (RBF), B - linear with two neurons in the input layer (Linear 1), C - linear with three neurons in the input layer (Linear 2), D - multilayer perceptron

with five neurons in the hidden layer (MLP 1), E - multilayer perceptron with two neurons in the hidden layer (MLP 2)

Despite the relatively poor quality of training (build) NN radial-basis function will also be used for further research, because given the internal functional features, during the validation (validation) it can potentially demonstrate the required quality. The next step in the analysis of time series of ambient temperature will be to obtain the appropriate predictions, which will go beyond the training sample.

For this, we implement a projection of the time series for each of the networks, setting the depth of the forecast by 8 elements forward (Fig. 4.6).

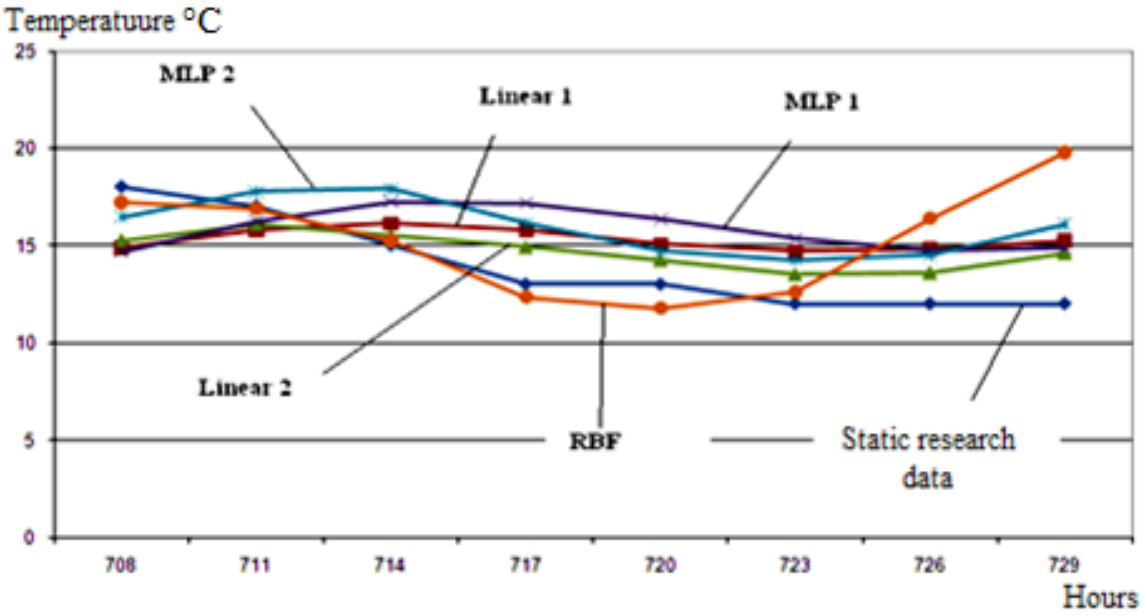

Fig. 4.6 Neural network projections of time series of ambient temperature

During the forecast for the day ahead, in general (Fig. 4.6) sufficient accuracy of the forecast is observed (root mean square error – 1,789107–3,220811 ^{0}C). The best predictive properties were demonstrated by the Linear 2 network - 1,789107 ^{0}C (Table 4.1), which is explained by a certain linearity of temperature change in this time interval.

Table 4.1 RMS temperature prediction errors for projection depths of 8 time series elements

RBF, ^{0}C	Linear 1, ^{0}C	Linear 2, ^{0}C	MLP 1, ^{0}C	MLP 2, ^{0}C
3,220811	2,503599	1,789107	3,007316	2,555901

The projection graph also shows (Fig. 4.6) that the maximum accuracy occurs at a projection depth of 6 elements - 18 hours (Table 4.2). Especially for NN RBF (root mean square error – 0,6055 ^{0}C). This is due to the logistic function of activating the output layer of the network, which "cuts" the original values, not allowing extrapolation, because this type of function takes as an argument the distance between the input vector and some predefined center of activationaly function.

The value of this function is higher, when closer to the center of the input vector:

$$y = \exp(-\frac{(S-R)^2}{2\sigma^2}), \tag{4.4}$$

where $S = //X - C//$ – the distance between the center C and the vector of input signals X; σ – parameter determines the rate of decline of the function during the distance of the vector from the center; R – parameter that determines the shift of the activationaly function along the abscissa.

Table 4.2 RMS errors of temperature prediction for the depth of projection of 6 elements of the time series

RBF, ^{0}C	Linear 1, ^{0}C	Linear 2, ^{0}C	MLP 1, ^{0}C	MLP 2, ^{0}C
0,6055	1,992287	1,419686	2,657	1,912155

Analyzing the projections of temperature time series (Fig. 4.6), it should also be noted that NN during the general trend of decreasing temperature (708–717 hours), relatively correctly predicted its stabilization at 717–720 hours and increase at 723 hours.

4.4 Synthesis and study of time series projections of solar radiation based on neural networks

After obtaining experimental data on the intensity of solar radiation conducted approbation researches concerning forecasting of its values. For this purpose, we used the data of a passive experiment at PJSC "Agrocombinat Teplichny" for November 11, 2019.

The following NNs have been selected as the best as a result of solving the optimization task (Table 4.3): the multilayer perceptron MLP 2-7-1 (with the training effectiveness of 97.64%), the multilayer perceptron MLP 2-9-1 (with the training effectiveness of 97.58%), the multilayer perceptron MLP 2-9-1 (with the training effectiveness of 97.64%), the multilayer perceptron MLP 2-9-1 (with the training effectiveness of 99.74%), and the multilayer perceptron MLP 2-4-1 (with the training effectiveness of 97.61%).

The training parameters of the synthesized NNs based on the results of solving the optimization task are given in the table below.

Table 4.3 The results of solving the optimization task of the neural networks synthesis.

Totals of the models				
No.	Architecture	Training effectiveness	Performance control	Performance test
1	Linear	0.224338	0.224689	0.220108
2	MLP 2-9-1	0.227858	0.228170	0.223156
3	MLP 2-9-1	0.226913	0.227158	0.222548
4	RBF 2-9-1	0.227793	0.228498	0.228306
5	RBF 2-4-1	0.221512	0.225771	0.225956

The best results were demonstrated by the NM of the radial-basis function, which took place in the case of the temperature time series with five inputs and two

hidden layers (the second - 173 neurons) (Fig. 4.8, 4.9): learning error - 0.009317 W/m^2, control error - 0,008983 W/m^2, test error - 0,008991 W/m^2.

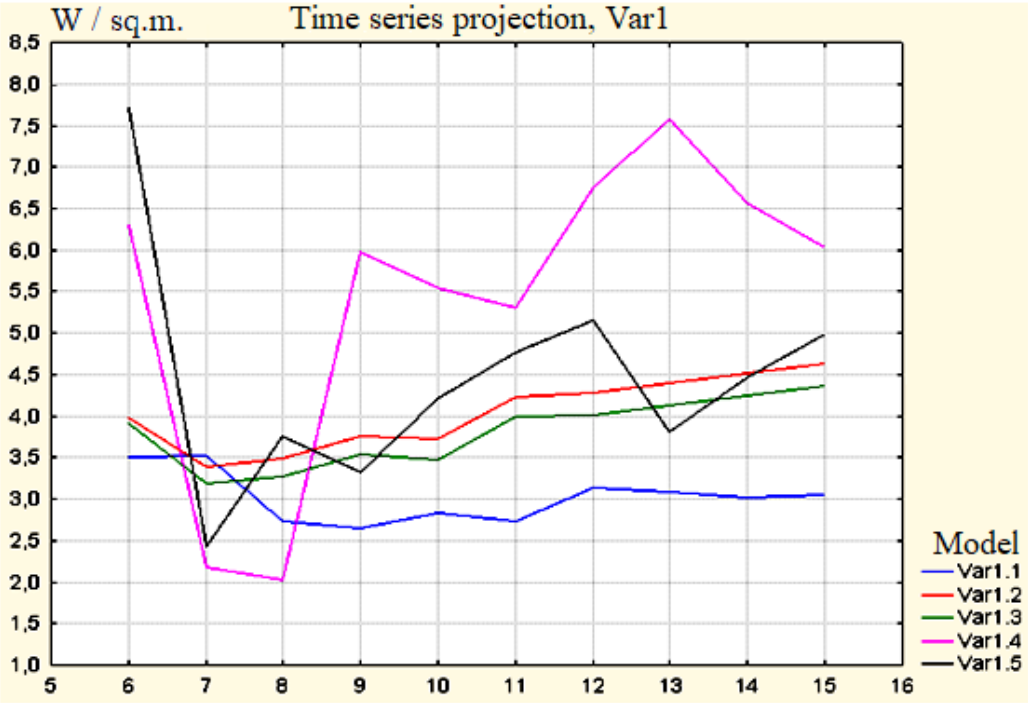

Fig. 4.8 Neural network projections of the time series of solar radiation

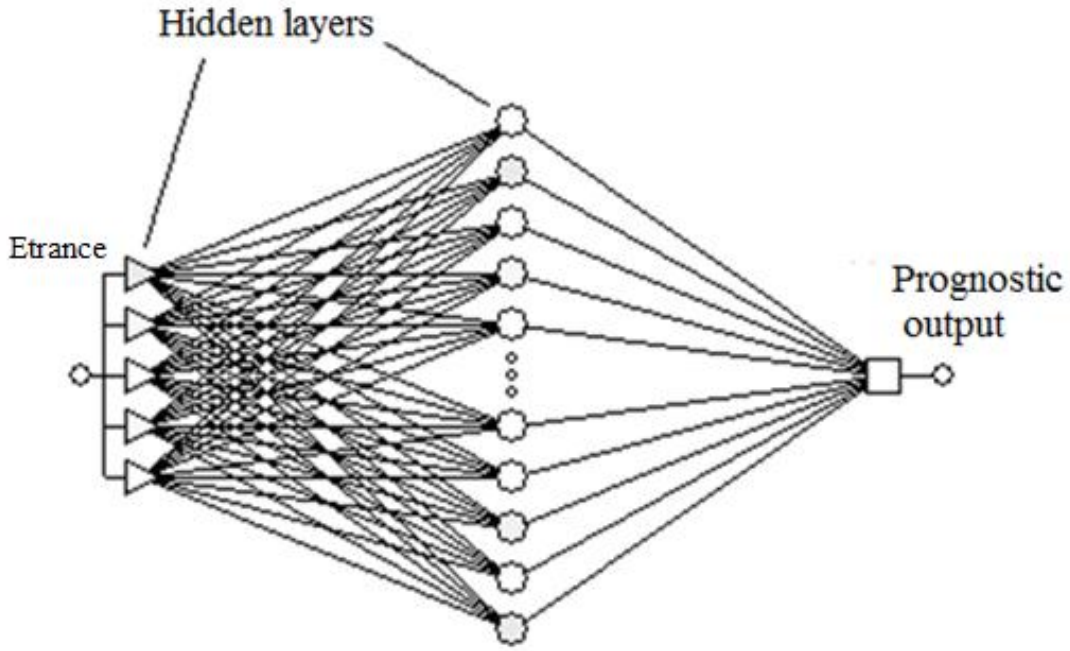

Fig. 4.9 Architecture of optimal NN of the radial-basis function

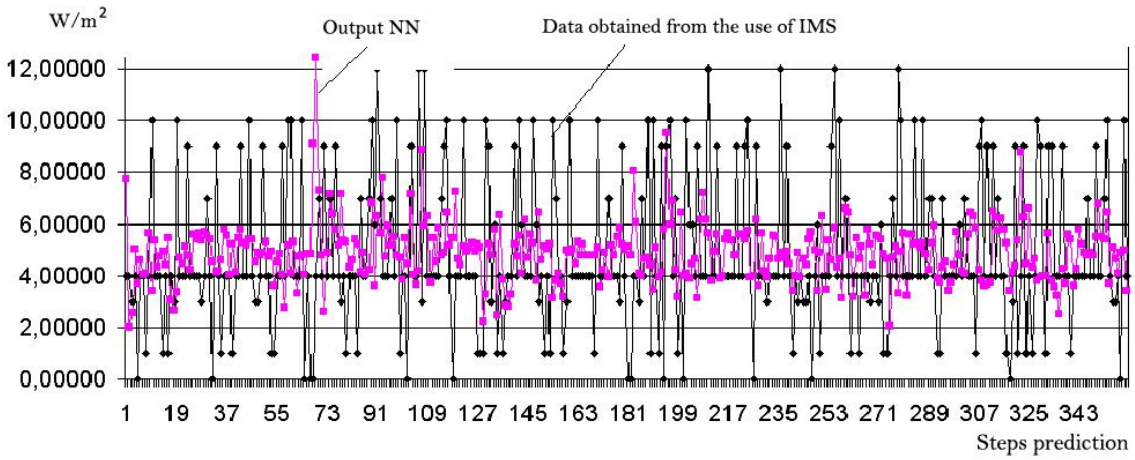

Fig. 4.10 Comparison of NN output and experimental data (time interval - 30 min)

Analysis of the functioning of NN shows that this quality of its work even in the case of effective training without "overfitting", does not meet the technological requirements, so for further research it is necessary to apply the filtering of the input signal.

Conclusions to chapter 4

1. The research results of intelligent control systems of electrical complexes for biotechnological objects are given in this chapter. The study of developed control system shows ability of improving the system performance by 20 % over and reducing of natural gas consumption for heating by 13 % compared with control system that is based on the stabilization algorithm of technological parameters.
2. The use of the method of neural network prediction of external natural disturbances on a biotechnical object is theoretically substantiated. External natural disturbances in the form of air temperature and intensity of solar radiation are presented as time series.
3. Preliminary analysis of the quality of disturbance prediction by different types of neural networks showed that multi-layer perseptron networks with two neurons in the hidden layer for temperature and with three neurons for solar radiation intensity have the best accuracy.
4. The prediction of solar radiation intensity does not meet the technological requirements. It is advisable to use mathematical filtering of the information channel using the transformation.

References to chapter 4

1. Lysenko V., Dudnyk A. “Optimal control: status and prospects in the Greenhouse industry”. Scientific Herald of National University of Life and Environmental Sciences of Ukraine, vol. 166, pp. 104 – 113, 2011.
2. Lysenko V., Shtepa V., Zayets N., Dudnyk A. “Neural network forecasting of outside temperature time series”, Biological Resources and Nature Management, vol. 3 - 4, pp. 102 – 108, 2011.
3. Shurub Yu.V., Dudnyk A.O., Lavinskiy D.S. Optimization of regulators of frequency controlled induction electric drives under the stochastic loadings // Technical electrodynamics, 2016, no.4, pp. 53-55.
4. Dudnyk A. “Automated Control System In Greenhouse With Neural Network Predictions Of External Disturbances”. Energetika ta avtomatika, vol. 1, pp. 37-44.
5. Lysenko V., Dudnyk A. “Automation of biotechnological objects”. Proceedings of the XIIIth International Conference “TCSET’2016. Modern Problems of Radio Engineering, Telecommunications and Computer Science”, IEEE Xplore (Electronic ISBN: 978-6-1760-7807-4), pp. 44-47.
6. Chang Yang Development of an automation system for greenhouse seedling production management using radio-frequency-identification and local remote sensing techniques / Chang Yang,Kuang-Wen Hsieh Chao-Yin Tsai, Yu-I. Huang, Yu-Liang Chen, Suming Chen // Engineering in Agriculture, Environment and Food. – 2014. – Volume 7, Issue 1, Pages 52-58.
7. Uday A. Greenhouse Automation System / Uday A. Waykole,. Dhiraj G. Agrawal // 1st International Conference on Recent Trends in Engineering & Technology, Mar-2012. – Special Issue of International Journal of electronics, Communication & Soft Computing Science & Engineering, ISSN: 2277-9477.
8. Lysenko V., Shtepa V., Dudnik A. (2011). Probability (Bayes) neural network of grading temperature modes. News of agrarian sciences, 4, 53-56. (in Ukrainian).

9. Dudnyk, Alla. (2015). Information providing and software of control system in greenhouse with neural network predictions of external disturbances. Scientific Herald of National University of Life and Environmental Sciences of Ukraine. Series: Engineering and Energy AIC 224, 46-50.
10. Lysenko V., Reshetyuk V., Shtepa V. & Dudnik A. (2013). Greenhouse Environment Control System with Neural Network Predictions of External Disturbances. Contemporary aspects of production engineering: XXII International student's scientific conference, 40–52.
11. Huang, N. E., Hu, K., Yang, A. C., Chang, H. C., Jia, D., Liang, W. K., Meijer, J. H. (2016). On Holo-Hilbert spectral analysis: a full informational spectral representation for nonlinear and non-stationary data. Phil. Trans. R. Soc. A, 374(2065), 20150206.
12. Arbib M. 2003. The handbook of brain theory and neural networks. London: MIT Press. 1309 p.
13. Sajmon Hajkin. 2006. Neyronnyye seti: polnyy kurs. [Neural networks: full course]. Moscow, Vilyams, 1104 p. (in Russian).
14. Hawkins, Jeff. 2004. On Intelligence (1st ed.). Times Books. p. 272. ISBN 978-0805074567.
15. Kibzun A. 2002. Teorija Veroiatnostei I Matematicheskaia Statistika. [Theory of Probability and Mathematical Statistics]. Moskva: FIZMATLIT. p. 224. (in Russian).
16. Kruglov, V.V. and V.V. Borisov. Iskusstvennyye neyronnyye seti. Teoriya i praktika. [Artificial Neural Networks. Theory and practice]. 2001. Moscow, Goryachaya liniya - Telekom, 382 p. (in Russian).
17. Russell S. and Norvig P. 2010. Artificial Intelligence. Upper Saddle River: Prentice-Hall.
18. Ripley Brian D. 2007. Pattern Recognition and Neural Networks. Cambridge University Press. ISBN 978-0-521-71770-0.

19. Luger, George & Stubblefield, William. 2004. Artificial Intelligence: Structures and Strategies for Complex Problem Solving (5th ed.), The Benjamin/Cummings Publishing Company, Inc., c. 720, ISBN 0-8053-4780-1
20. Osowski, S. and Rudinskij, I. 2004. Nejronnye Seti Dlâ Obrabotki Informacii. Moskva: Finansy i Statistika. (in Russian).
21. Schmidhuber, J. 2015. Deep Learning in Neural Networks: An Overview. Neural Networks. 61: 85–117.
22. Aksenov, S.V and Novoseltsev, V.B. 2006. Organizatsiya i ispol’zovaniye neyronnykh setey (metody i tekhnologii) [Organization and use of neural networks (methods and technologies)]. Tomsk, NTL. 128 p. (in Russian).
23. Simon H. 2008. Neural Networks. New Delhi: Prentice-Hall of India.
24. Neural networks. StatSoft. Electronic textbook on statistics. Available at: http://www.statsoft.ru/home/textbook/modules/stneunet.html.

CHAPTER 5. NOISE FILTRATION IN NATURAL DISTURBANCES ASSESSMENT AND SYNTHESIS OF INTELLIGENT CONTROL SYSTEMS

5.1 Theoretical substantiation of the use of the Gilbert-Huang transformation for noise filtering

According to preliminary research reducing of energy consumption through the development and implementation of intelligent control systems using the latest methods and means of automation, able to predefine control action based on disturbances forecasting, technological requirements and biological object characteristics [29, 30].

Neural network forecasting of external disturbances can increase system performance up to 20 % and can increase technological efficiency up to 13 %. Also, additional energy savings can provide phytomonitoring of plants. Phytomonitoring can be implemented using modern robotic technical systems to ensure reliability and efficiency of a given measurement.

Review of the functioning of the process facilities along with the peculiarities of the dynamics of natural disturbances and living organisms' states and the rational use of energy resources will increase profits from production. Experimental studies depending on the main quality parameters of biological objects from change of microclimate and establish the most productive growing conditions have provided the mathematical model of states of plants that were later used in the formation of management strategies [7, 12, 29].

The method of neural network prediction of natural external disturbances in biotechnical object has been developed. Networks type – multilayer perceptron with in hidden layers, have high predictive ability for temperature time series and solar radiation intensity. Genetic algorithm is a method that could be used for optimizing neural networks settings.

These factors affect differently depending on the altitude of a satellite orbit. Accordingly, different methods for protection of systems of technical vision should

be developed. And ability to predict a negative factor will significantly increase the level of protection.

For effective study of solar radiation and forecasting possible disturbances the Information Measurement System (IMS) was developed (Fig. 5.1).

As mathematical approach for the prediction the Neural Networks (NN) to temperature time series were applied [37]. However, received prediction results did not have needed accuracy (Fig. 5.2). The best results were achieved with NN Radial Basis Function (RBF) having five inputs and two hidden layers (teaching error – 0,009317 W/m^2, control error – 0,008983 W/m^2, test error – 0,008991 W/m^2).

Fig. 5.1 Information Measurement System of solar radiation intensity

Noise in information signal can be associated with influence of next natural factors: intensity of sunlight on the IMS sensor; location latitude and longitude; distance from the Sun to the Earth; height of clouds and type of clouds; absolute humidity; the horizontal and vertical components of wind's velocity; size and concentration of aerosol; centers of condensation in clouds; size of cloud droplets; altitudes of upper and lower boundaries of clouds; rainfall intensity and so on [34].

That why development of mathematical filters is needed to achieve required precision of prediction.

Traditional methods of data analysis are applicable for the linear and stationary signals and systems. At the same time, it is obvious that time series of solar radiation is nonlinear and non-stationary [30]. Therefore, the precondition for adequate data representation is a formation of adaptive basis, which will functionally depend on the content of a signal (but not pre-selected and constant, as in classical approaches).

Hilbert-Huang Transform (HHT) meets these requirements, which is the based

on the Empirical Mode Decomposition (EMD) method for time-frequency analysis of nonlinear and non-stationary processes and also for Hilbert Spectral Analysis (HSA) [31]. HHT allows a time-frequency analysis of data (signals), which does not require a priori given functional basis of transformation. The basis functions are obtained directly from the data by "empirical modes" screening functions. Instant frequency is calculated from the derivatives of phase' functions by Hilbert transform of the basis functions. The result is represented in the time-frequency space.

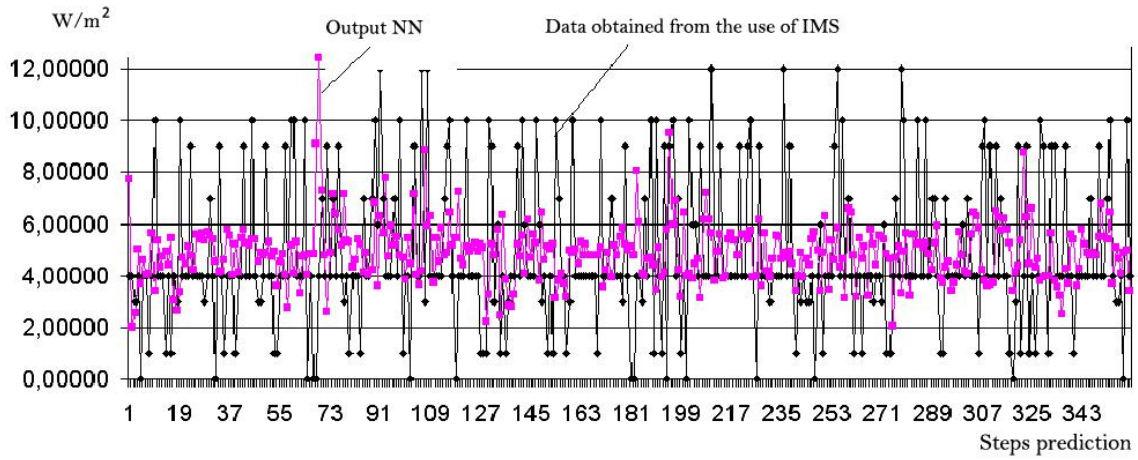

Fig. 5.2 Comparing the output NN radial basis function and experimental data (time interval is 30 minutes, discretization is 5 seconds)

Note, that only in the recent decades, researchers begun to develop methods for analyses of nonlinear, but stationary and deterministic, and linear, but non-stationary systems (this is wavelet analysis, distribution of Wigner-Ville, etc.). Most of the physical systems and processes are nonlinear and non-stationary. In this case data analysis will use certain simplifications, which allows transformation of a priori given basis into easier for analysis metric space.

This research focuses on the development of the method for NN-based prediction of intensity of solar radiation, which is one of the most negative factors in electronic components of systems of technical vision [36].

Generally, EMD method is based on the assumption that any data set contains various modes of oscillatory processes [32]. Each of these modes can be represented by the Inner Mode Function (IMF) with the following restrictions: the number of

extremes and number of zero crossings of the function must be equal (or differ by no more than one unit); in any part of the function an average value of envelope curves, defined by local extremes, must be 0.

IMF are oscillation modes that instead of constant amplitude and frequency can have variable amplitude and frequency as a function of time.

The essence of EMD is sequential iteration to find the functions of empirical modes $c_j(t)$ and the remainder $r_j(t) = r_j\text{-}1(t)\text{-}c_j(t)$, where j = 1, 2, 3, …, n with $r_0 = y(t)$. The decomposition to represent the signal in a sum of modal functions and remainder [33]:

$$x(t) = \sum_{j=1}^{n} cj(t) + rn(t), \quad (5.1)$$

where n – is computation parameter, number of empirical modes.

Existing studies [27] have demonstrated that although an appropriate adaptive basis is not defined analytically, but meets the requirements of the traditional bases: completeness, convergence, orthogonality and uniqueness.

EMD gives clear algorithm of iterative calculation, which creates preconditions for its effective implementation in intelligent control systems:

1) identification of local extrema of signals and grouping them into arrays of vectors of coordinates and corresponding amplitude values;

2) calculating the upper and lower envelopes of the signal y(k) by selected maxima and minima;

3) calculation of the mean function $m_1(k)$ and the first approximation to the first function IMF mode:

$$h_1(k) = y(k) - m_1(k) \quad (5.2)$$

4) repeating steps 1-3, substituting function $h_1(k)$ into y(k), and finding the second approximation to the first IMF mode – the function $h_2(k)$:

$$h_2(k) = h_1(k) - m_2(k) \quad (5.3)$$

Similarly, subsequent approximations to the first function of IMF mode is calculated. The criterion to stop calculation can be normalized square difference between two successive operations of approximation:

$$\delta = \frac{\sum_k \left(h_{i-1}(k) - h_i(k)\right)^2}{\sum_k \left(h_i(k)\right)^2} \quad (5.4)$$

Last value $h_i(k)$ is taken as the high-frequency function of mode $c_1(k) = h_i(k)$ of IMF family, which is a part of the output signal. This allows us to remove $c_1(k)$ from the signal, keeping low-frequency components:

$$r_1(k) = y(k) - c_1(k) \quad (5.5)$$

Function $r_1(k)$ is processed as new data, similar with the method to find second mode IMF function– $c_2(k)$:

$$r_2(k) = r_1(k) - c_2(k) \quad (5.6)$$

Thus, the decomposition of signal is achieved in n-modes empirical approximation in the sum with reminder $r_n(k)$ (5.1). The stop criterion for decomposition of the signal is a maximum 'straightening' of remainder, i.e. turning it into a trend signal accordingly to the interval. In practice, the process can be completed by the following criteria: reminder $r_n(k)$ becomes a monotonic function without extremes; reminders $r_n(k)$ are relatively minor by value or by power comparatively to signal; predefined relative square error of reconstruction of the signal (4) without reminder $r_n(k)$ is achieved.

5.2 Filtration of the solar radiation intensity signal by means of the Gilbert-Huang transformation

The time interval of 6 hours was used for research (data obtained by IMS), which is technically justified for further predictions. This time period was extended to the end portions of 1% (43 points) to eliminate conversion errors on finite intervals processed array data analyzed. Also carried out its alignment relative to the arithmetic average of - 133.807 W/m^2.

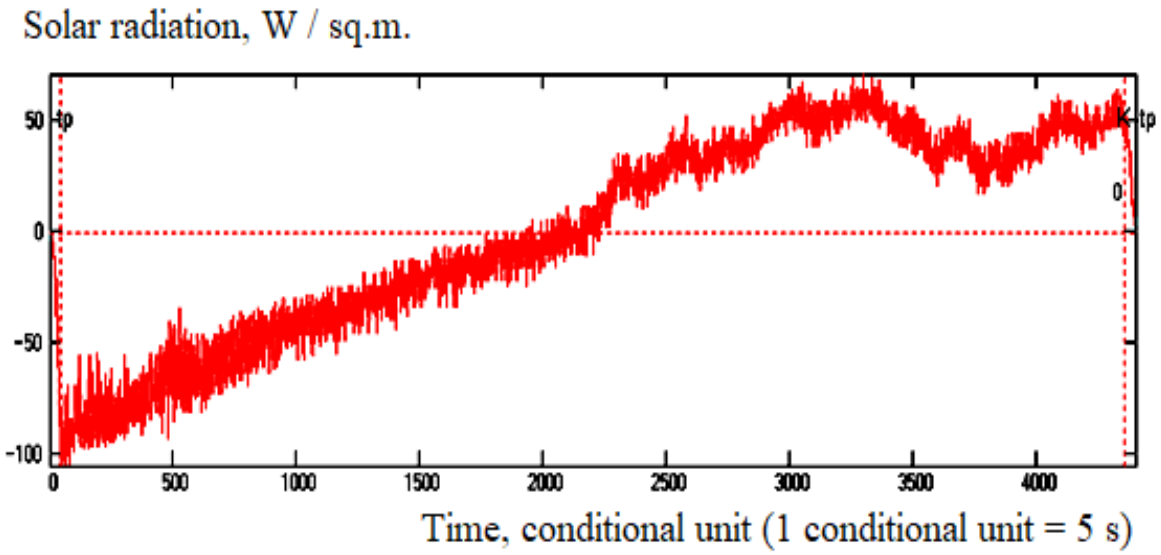

Fig. 5.3 Normalized and extended time series of solar radiation

For establish the cutting limit, the filtered signal and the angle of divergence with the input signal were calculated.

This angle is maximal for the first window and gradually decreases with increasing signal shift window spectrum, but this decrease is uneven and slows down in the boundary of the information part due to the stability of statistical noises and weak dependence on filter boundaries and widths of their transition zones.

The deceleration can be recorded at the local minimum of the derivative change of the divergence angle. Thus, we set the cutting limit - 65 C.U. (Fig. 5.4); the upper limit of complete suppression of high-frequency components for all filters is the same.

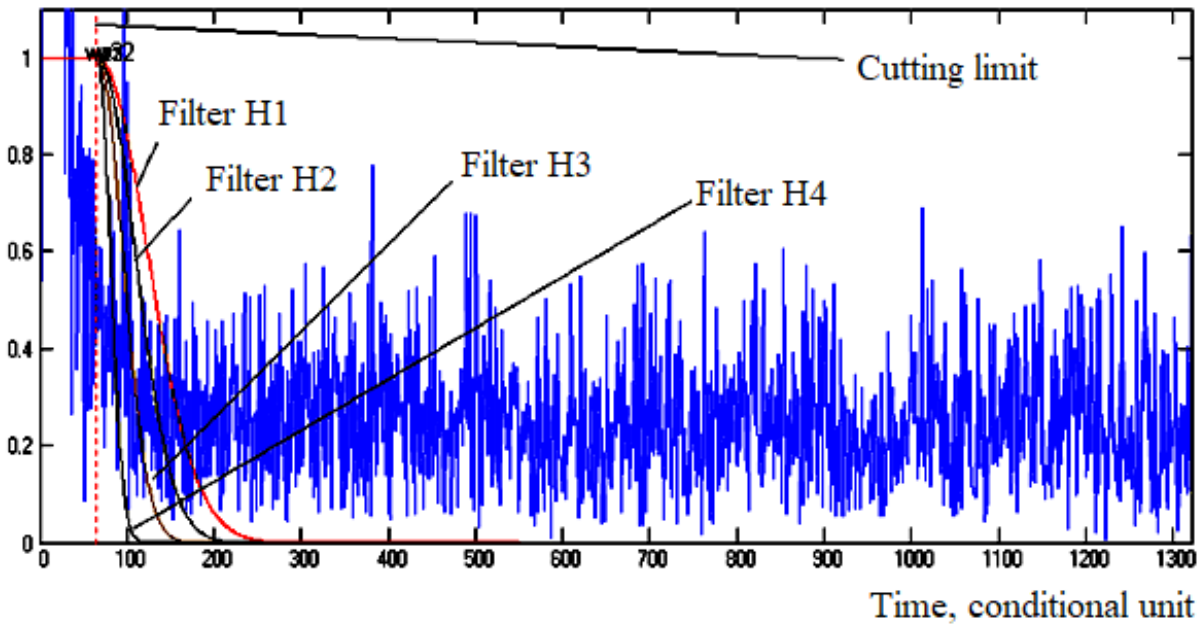

Fig. 5.4 Solar radiation time series spectrum module with corresponding filter settings

Also we accepted that cleaning from the noise of the time series of solar radiation will require four times the elimination of noise, i.e. the formation of IMF-1 = IMF-1a + IMF-1b + IMF-1c + IMF-1d (Fig. 5.5).

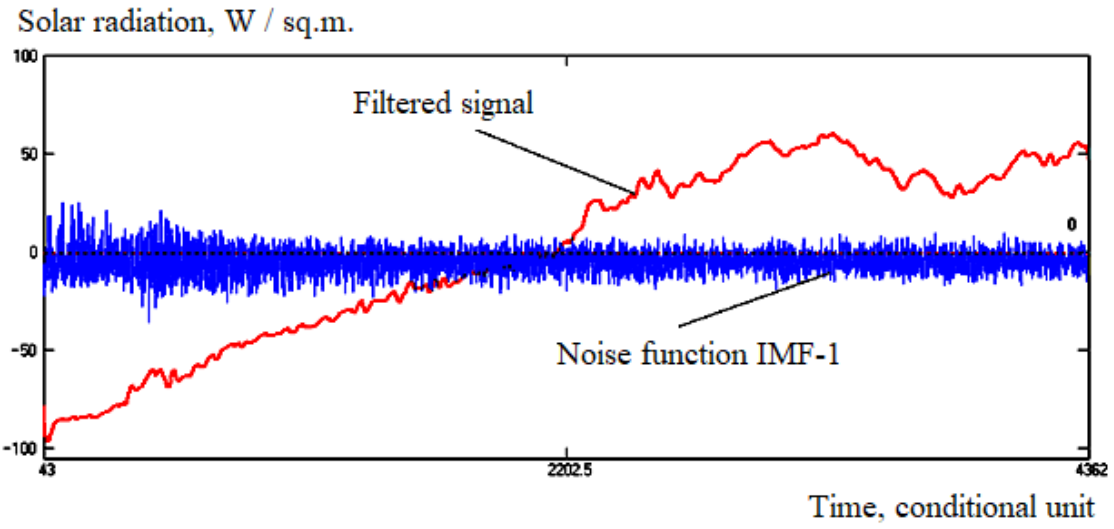

Fig. 5.5 The results of solar radiation time series filtering

After denorming the filtered signal, we visually analyzed the results of using the Hilbert-Huang transform and established the number of detected noise components in the input signal - 23.762% (Fig. 5.6) [11].

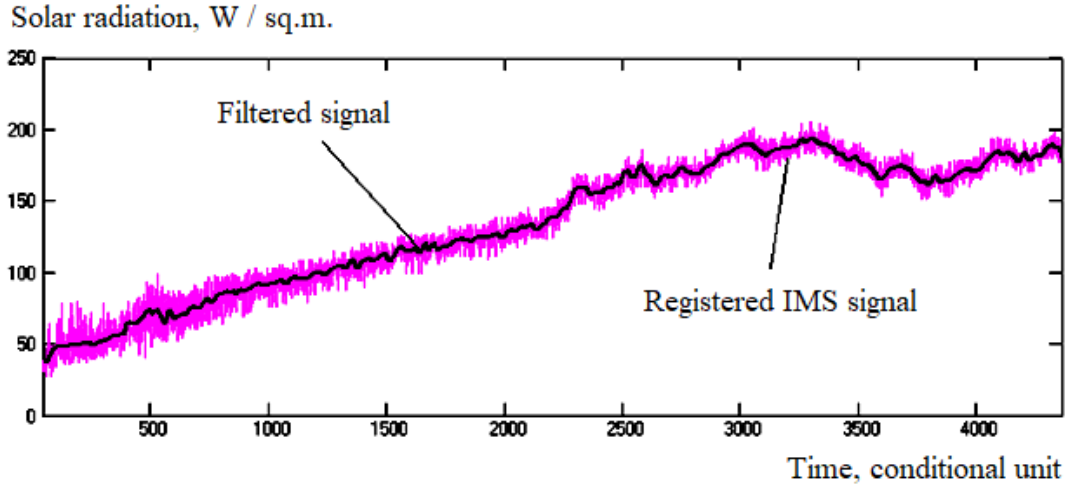

Fig. 5.6 Overlay input and filtered signals of time series of solar radiation

Therefore, the purified EMD signal is characterized by technologically sufficient resolution, so the filtered signals obtained on the basis of the Hilbert-Huang transformation can be used to build appropriate prognostic models.

After using of mathematical filter for solar radiation intensity predictors precision significantly increased, enabling further research of these neural networks and to search for optimization techniques that minimize their work error.

5.3 Synthesis of an intelligent control system with temperature forecasting in a poultry farm

The characteristics of the change in the natural disturbances in the poultry house depend on the climatic zone where the production is located [1, 3]. The annual time-series of fluctuations Θ1, Θ2, …, Θn of the air temperature, which were observed in the specified area, have been built on the basis of the data obtained from the Hydrometeorological Center of Ukraine (HMCU). These samples represent a non-stationary random process and determining its statistical characteristics is a very complicated stochastic problem which is almost impossible to solve. However, the

analysis of change in the individual sections of annual samples (of the time-series) has proved that they can be forecasted due to the fact that they are the samples of either stationary random processes or stationary processes with additive deterministic components, that is to say, quasi-stationary processes. Each of the annual samples can be presented in the form of 45-70 stationary or quasi-stationary sections as mentioned above. 569 sections have been allocated during the period of 10 years. A cluster analysis of these time-series segments has been performed in order to classify these facilities by their characteristic features and to forecast their further appearance [5].

The task of the algorithm for pattern recognition of areas with temperature disturbances is to sequentially redefine the deterministic and statistical characteristics of temperature changes outside the technological facility where the biological component part is being managed [10].

The initial characteristics of these changes are determined on the basis of the HMCU forecast which forecasts the possible temperature fluctuations during the night hours ($\Theta_{n.h.}$ and $\Theta_{n.l.}$) and during the day hours ($\Theta_{d.h.}$ and $\Theta_{d.l.}$). Due to this information, the approximate (forecasted) values of the mathematical expectation $m_{\Theta_П}$ and the amplitude of fluctuations $A_{\Theta_П}$ in the temperature changes of the following day are calculated.

$$m_{\Theta} = \frac{\Theta_{n.h} + \Theta_{d.h.}}{4} + \frac{\Theta_{d.l.} + \Theta_{n.l.}}{4}. \tag{5.7}$$

$$A_{\Theta} = \frac{\Theta_{d.l.} - \Theta_{n.l.}}{4} + \frac{\Theta_{d.h.} - \Theta_{n.h.}}{4}. \tag{5.8}$$

Thereupon, a comparison of the forecasted mathematical expectation m_{Θ} to the mathematical expectation of the current day temperature changes m_{Θ} is carried out. If $(m_{\Theta} - 1) \le m_{\Theta} \le (m_{\Theta} + 1)$, then the temperature section still coincides with the image defined for the previous day. If the forecasted values m_{Θ} deviate by more than 1 ºC, it is assumed that the temperature image is expected to change.

The image recognition algorithm is based on comparing the degree of proximity L of the object (the sections of the air temperature change) ω to any of the

classes Ω_q, where $q=\overline{1,m}$. 5 classes have been previously identified in our system, [9], therefore m=5. The root mean square distance (expressed in ºC) between the object ω and the set of objects ω_{q1}, ω_{q2}, ..., ω_{qk}, which belong to the Ω_q class (k stands for the number of images (objects) of the Ω_q class) has been imputed as the degree of proximity:

$$L(\omega,\Omega_q)=\sqrt{k_q^{-1}\sum_{k=1}^{k_q} d^2(\omega,\omega_{qk})}. \tag{5.9}$$

The decision to assign object ω to the Ω_q class is made if

$$L(\omega,\Omega_q)=\boldsymbol{min}\, L(\omega,\Omega_i), \tag{5.10}$$

where $i=\overline{1,m}$.

Thus, when a new image appears it is determined to which class it belongs in the first place. It was proposed to use an intelligent pattern recognition system based on probabilistic neural networks to solve this task, proceeding from the necessity for an adequate analysis of the start of the change of one image to another and taking into consideration the functional peculiarities of the systems based on the methods of mathematical statistics.

The Bayesian formula is one of the main in the Elementary Probability Theory, which allows us to determine the probability of a certain event (hypothesis) in the presence of circumstantial confirmations (data) only [22-25] which may contain inaccuracies, which is exceptionally important for solving our task. The Bayesian formula record is as follows:

$$P(A|B)=\frac{P(A|B)P(A)}{P(B)}, \tag{5.11}$$

where *P(A)* stands for the aprior probability of the hypothesis *A*; *P(A|B)* stands for the probability of the hypothesis *A* in case of occurrence of the event *B* (the aposterior probability); *P (B|A)* stands for the probability of occurrence of the event *B* in case of trueness of the hypothesis *A*; *P(B)* stands for the probability of occurrence of the event *B*.

An important corollary of the Bayesian formula is the formula for the total probability of an event, which depends on several incompatible hypotheses (and on them only):

$$P(B) = \sum_{i=1}^{N} P(A_i) P(B|A_i), \tag{5.12}$$

where N stands for the number of hypotheses.

Taking into consideration (5.11), we conclude that the probability of occurrence of the event B depends on a number of hypotheses A_i, if the degrees of reliability of these hypotheses are known (for example, experimental data on the external air temperature).

The Bayesian network built on these theoretical principles is a probabilistic model which represents a set of variables and their probabilistic dependence relationships. Formally, a Bayesian network is a directed acyclic graph with variables being its nodes while the ribs encode the conditional dependences between the variables. The nodes can represent variables of any type and can be weighted parameters, hidden variables or hypotheses. If the rib connects the node A to node B, then A is named the father of B, and B is called the descendant of A. The set of ancestor nodes of the node X_i is denoted as parents (X_i). Then, the common distribution of values in the nodes can be conveniently recorded as a result of local distributions:

$$P(X_1,...,X_n) = \prod_{i=1}^{n} P(X_i | parents(X_i)) \tag{5.13}$$

where n stands for the number of local distributions.

Probabilistic neural networks (PNN) are a special case of Bayesian networks, a type of neural networks which are effectively used to solve the classification tasks in which the probability density of belonging to classes is estimated with the help of the kernel approximation. When solving the classification tasks, the network outputs can be advantageously interpreted as probability estimates of whether an element belongs to a certain class. In fact, the network trains itself to estimate the probability density function.

A total of 132 temperature images with the corresponding numerical values of the input parameters have been generated [37].

During the synthesis of the PNN-classifier of the temperature images the following were used as input values (Table 5.1):

- the mathematical expectation (m_0);
- the amplitude of temperature fluctuations (A);
- the minimum standard deviation (σ_{min});
- the maximum standard deviation (σ_{max}).

The uncertainty losses are never significant enough according to the HMCU, given that the parameters of the images of temperature disturbances become more reliable after 20 hours of observations.

Table 5.1 The variation range of the input values

m_0, ºC	A, ºC	min, ºC	max, ºC
-24 – +18	0 – 10	0,5 – 2,5	3 – 5

The network output is the number of the class (image) to which the resulting set of the input values belongs.

The neural network layer of addition is to have one element for each element from the training data set - 132. All the elements of this layer are connected only to the elements of the layer of samples which belong to the corresponding image.

The activity of the sample layer element is equal to:

$$O_j = \exp\left(\frac{-\sum(w_{ij} - x_i)^2}{\sigma^2}\right), \qquad (5.14)$$

where w stands for the value of the weighting numbers.

The weighting values of the relationships leading from the elements of the sample layer to the elements of the addition layer are equal to 1.

The addition layer element simply summarizes the output values of the sample layer elements. This sum estimates the value of the probability distribution density function for the set of instances of the corresponding image. The output elements are threshold discriminators which indicate the element of the addition layer with the

maximum value of activation (that is to say, they indicate one of the 132 temperature images).

A network of this kind does not require the training which is required for the perceptron-type networks, radial-basis function, etc., since all the parameters of the PNN network, such as the number of elements and values of weights are determined directly by the training data.

The procedure of using the PNN network is relatively simple: once a network is built, an unknown instance can be led to the network input and the output layer can indicate the image to which the sample most likely belongs resulting from a direct passage through the network. 20 possible sets of input parameters belonging to different classes have been created to examine the quality of classification.

The probabilistic neural network has correctly classified all the sets with a clear advantage at the output of the addition layer of the probability distribution density of the corresponding winning images (Fig. 5.7).

Within the scope of the task, we are interested not so much in the discrete classification of images but in the value of the output of the addition layer which calculates the probability distribution density for the set of instances of the corresponding image. That is to say, we can monitor the dynamics of changes in the temperature images at the output of this layer.

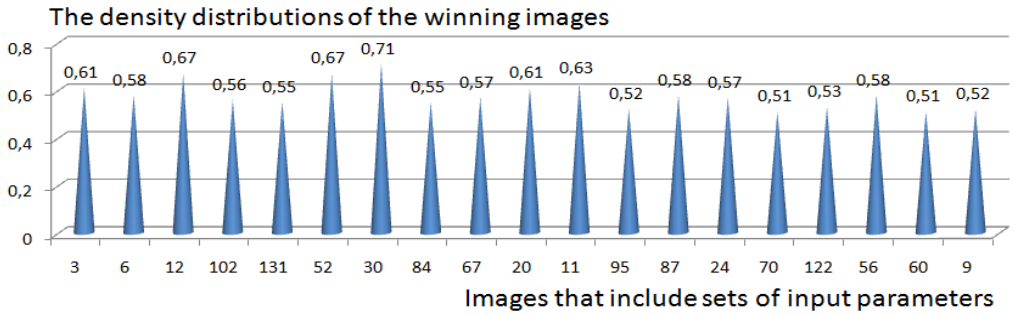

Fig. 5.7 The probability density distribution of the winning images during the research conduct

An experimental sample of the intelligent control system was installed in the poultry house No 4 at the State Enterprise “Training and Research Poultry Breeding Plant named after Frunze”, its functional diagram is presented in Fig. 5.8.

In the figure, V stands for the reconstruction of the control device action; U stands for the decision of the control strategy; f stands for the image type and its parameters; Q_n stands for the temperature forecast; θ_z stands for the ambient temperature; U_v stands for the ventilation control; U_n stands for the heating control; q stands for the air flow; Q stands for the flow of the heated air; θ_z stands for the given temperature; θ stands for the temperature which was measured in the poultry house; Δ stands for the temperature deviation (Patent No. 44637 UA, IPC G05B 13/00 (2009).

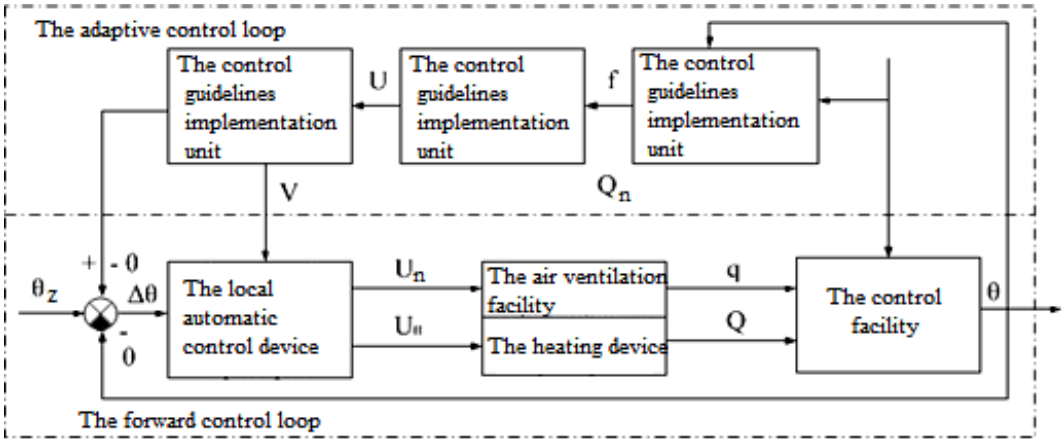

Fig. 5.8 The functional diagram of the intelligent control system of the poultry house temperature

The architecture of the computer-integrated control system is built in such a way so as to ensure the maximum reliability of its operation. The industrial controller possesses adequate resources (modules, an expansion base) to connect a large number of sensors and uses open protocols, that is to say, enables control by means of actuators in accordance with different control principles.

5.4 Synthesis of an intelligent control system with the external natural disturbances forecasting in a greenhouse

Appropriate technological conditions for plant growth and development are created in under cover structures. The ambient temperature and solar radiation are the main natural disturbances which affect the vegetation of plants in the greenhouse.

Therefore, the development of an intelligent system which can make it possible to predict these natural disturbances is an urgent task.

We use the software package Statistica Neural Networks and the multilayer perceptron which is traditional for solving the tasks on time-series forecasting [10] for the synthesis and investigation of the corresponding NNs, the criterion being the minimization of the NN error [19]. In the context of our task, its advantage over the similar items under development lies in the implementation of a functional block for optimizing the architecture of the neuromodels which uses linear approaches and a simulated annealing method on the basis of the Gibbs probability distribution:

$$P(\overline{x^*} \to \overline{x_{i+1}} | \overline{x_i}) = \begin{cases} 1, F(\overline{x^*}) - F(\overline{x_i}) < 0 \\ \exp(-\dfrac{F(\overline{x^*}) - F(\overline{x_i})}{Q_i}), \quad F(\overline{x^*}) - F(\overline{x_i}) \geq 0 \end{cases} \tag{5.15}$$

where $Qi > 0$ are the elements of an arbitrarily descending to zero sequence.

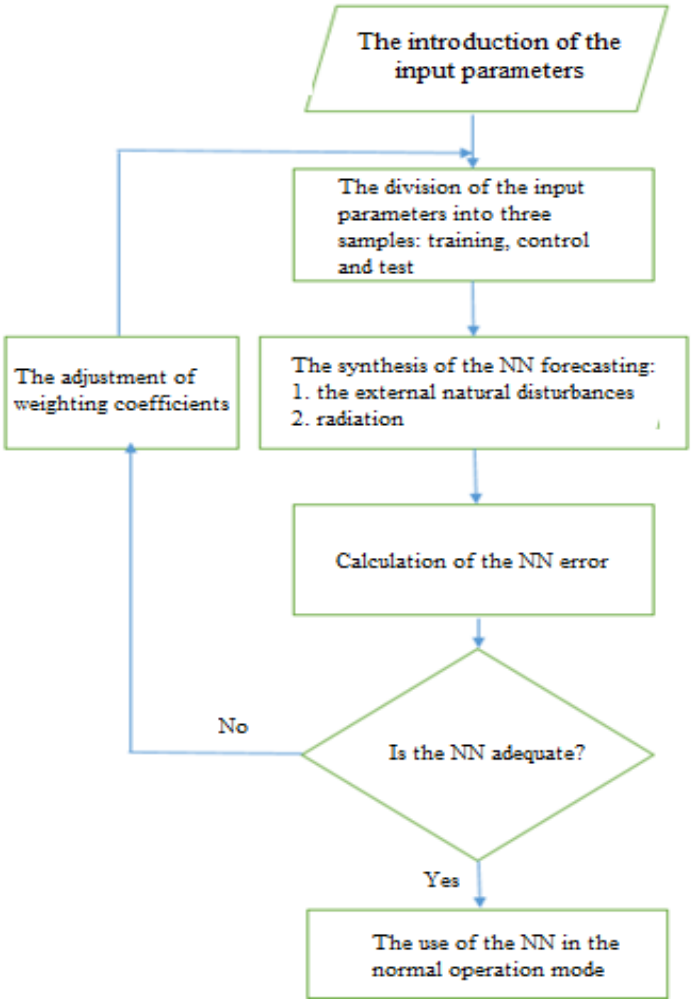

Fig. 5.9 The NN synthesis algorithm for the forecasting of the external natural disturbances and radiation

In the context of the proposed sequence (Fig. 5.9) the input data is automatically divided into three blocks: training, control and test for the effective modelling in the Statistica Neural Networks package. The presence of the three blocks is not obligatory, whereas the test block improves the quality of the further work since it ensures that there is no overfitting of the network.

The values of the day and time of the forecasting are used as the input data, that is to say, there are two input variables (Var1 stands for the day, Var2 stands for the time) and one output variable (Var4 stands for the ambient temperature).

Table 5.2 The results of solving the optimization task of the neural networks synthesis

Totals of the models								
No	Architecture	Training effectiveness	Performance control	Performance test	Training algorithm	Error function	Hidden neurons activity function	Output neurons activity function
1	MLP 2-8-1	0.893260	0.892000	0.894734	BFGS 118	Quadratic sum	hyperbolic	exponent
2	MLP 2-8-1	0.997834	0.994275	0.987809	BFGS 259	Quadratic sum	hyperbolic	hyperbolic
3	MLP 2-7-1	0.889667	0.888883	0.891928	BFGS 113	Quadratic sum	hyperbolic	identity
4	MLP 2-3-1	0.877182	0.864570	0.872726	BFGS 112	Quadratic sum	logistic	identity
5	MLP 2-3-1	0.877309	0.865464	0.874213	BFGS 93	Quadratic sum	logistic	hyperbolic

The following NNs have been selected as the best as a result of solving the optimization task (Table 5.2): the multilayer perceptron MLP 2-8-1 (with the training effectiveness of 89.3 %), the multilayer perceptron MLP 2-8-1 (with the training effectiveness of 99.7 %), the multilayer perceptron MLP 2-7-1 (with the training effectiveness of 88.9 %), the multilayer perceptron MLP 2-3-1 (with the training effectiveness of 87.7 %), the multilayer perceptron MLP 2-3-1 (with the training effectiveness of 87.7 %).

The best result was demonstrated by the MLP 2-8-1 network, which provided the effectiveness of 99.7 %in all the samples, that is to say, it presented the forecast with the maximum accuracy.

To verify the correctness of the time-series construction for the forecasting of the ambient temperature and radiation, it is necessary to determine the adequacy of choice for the input variables: the day and time in increments of 1 hour.

In order to find these mathematical, functional or structural dependence relationships between two or more variables (in accordance with the accumulated experimental data) the methods of correlation analysis are of great use, which indicates the absence or presence of a connection between the variables with a certain predetermined confidence probability.

The linear correlation coefficient is widely used for the quantity evaluation of the density of the network connections (Table 5.3). If the values of the variables X and Y are given, then it is calculated by the following formula:

$$r_{XY} = r_{YX} = \frac{\overline{XY} - \overline{X} \cdot \overline{Y}}{\sigma_X \cdot \sigma_Y} \tag{5.16}$$

If $|r|<0.30$, then the connection between the features is weak; $0.30 \leq |r| \leq 0.70$ stands for the moderate connection; $|r|>0.70$ stands for the strong or dense connection. When $|r|=1$, then the connection is functional. If $|r| \approx 0$, then there is no linear connection between X and Y. However, the nonlinear interaction is possible and it requires additional verification.

Table 5.3 The values of correlation coefficients between the input and target variables

	Correlation coefficients		
	- 10.500000 Training	- 10.500000 Test	- 10.500000 Test
MLP 2-8-1	0.893260	0.892000	0.894734
MLP 2-8-1	0.907834	0.904275	0.907809
MLP 2-7-1	0.889667	0.888883	0.891928
MLP 2-3-1	0.877182	0.864570	0.872726
MLP 2-3-1	0.877309	0.865464	0.874213

All the correlation coefficients are greater than 0.7, which indicates the adequacy of the input parameters choice.

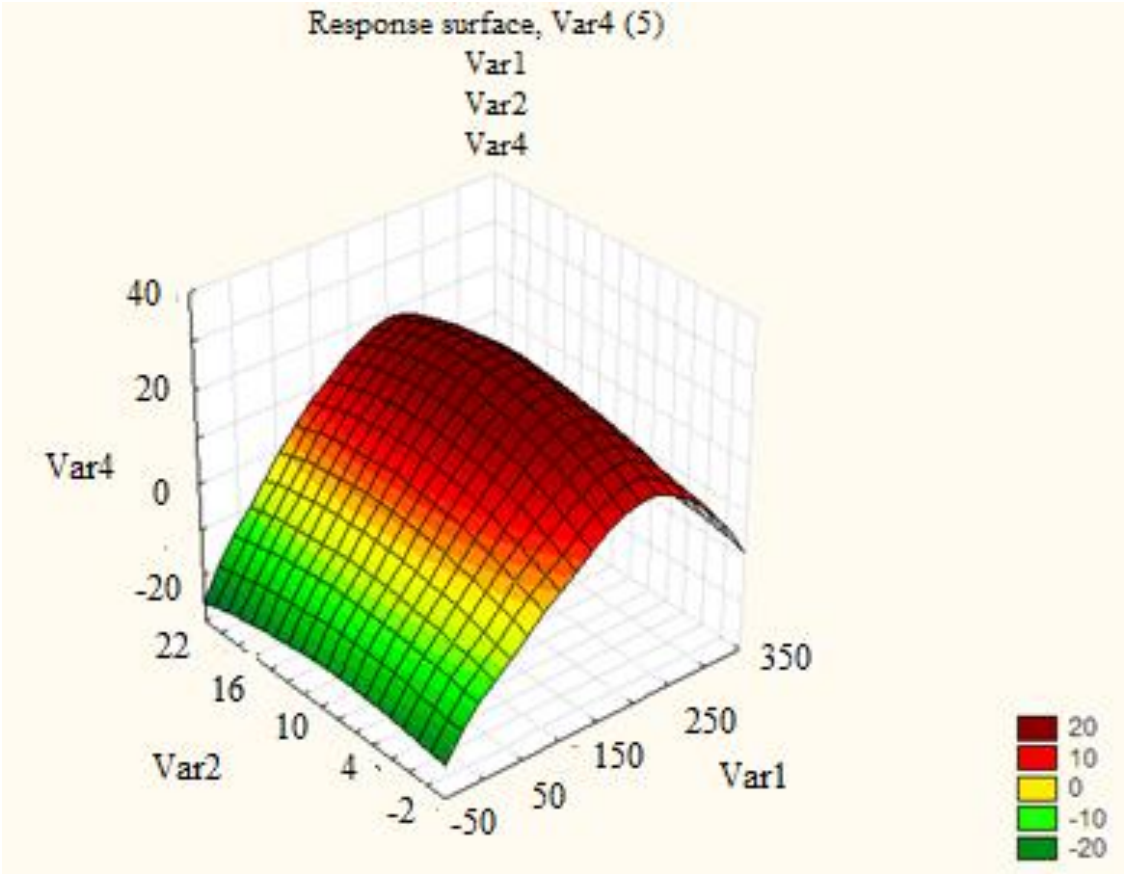

Fig. 5.10 The response surface between the input and output variables

Despite the relatively low training quality of some NNs, we are going to use them for further research, since during the forecasting (validation) they can potentially demonstrate the required quality while taking into consideration the internal functional peculiarities.

The next step in the analysis of the time-series of the ambient temperature is obtaining the appropriate predictions which are to go beyond the training sample.

To accomplish this, we implement a projection of the time-series for each of the networks, setting the depth of the forecast at 8 steps forward (Fig. 5.11).

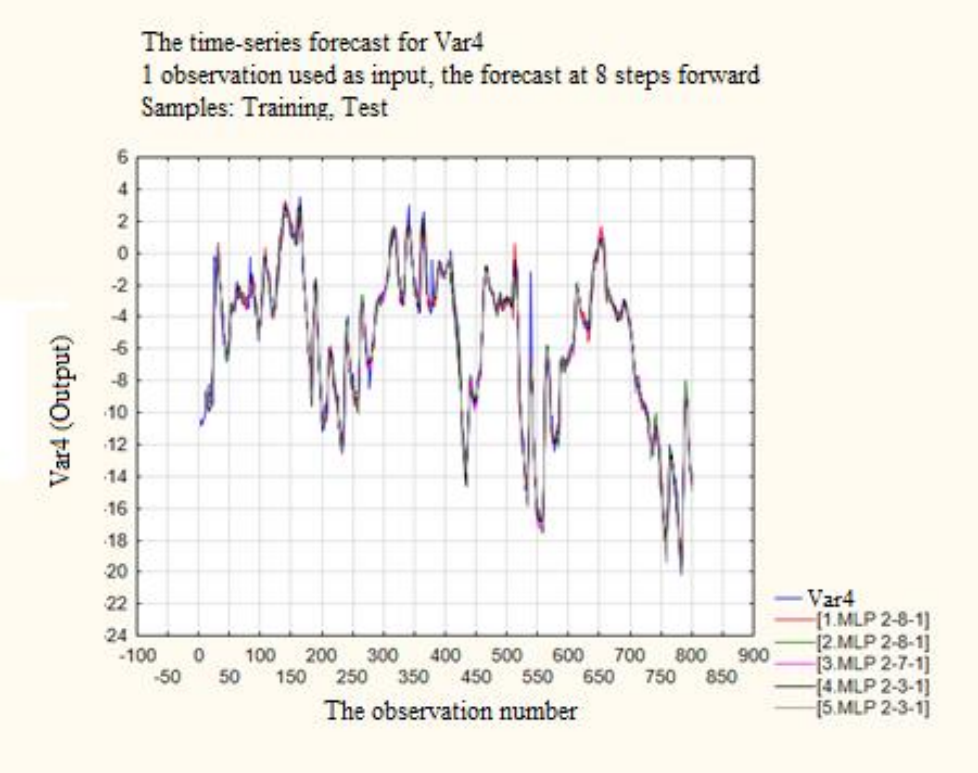

Fig. 5.11 Neural network projections of the time-series of the ambient temperature

During the forecasting at 8 hours forward, the generally sufficient accuracy of the forecast is observed (the mean square error being 1.19–3.43 ºC).

The values of the day and time forecasting are used as input data, that is to say, there are two input variables (Var1 stands for day, Var2 stands for the time) and one output variable (Var4 stands for radiation).

The following NNs have been selected as the best as a result of solving the optimization task (Table 5.4): the multilayer perceptron MLP 2-7-1 (with the training effectiveness of 97.6 %), the multilayer perceptron MLP 2-9-1 (with the training effectiveness of 97.5 %), the multilayer perceptron MLP 2 -9-1 (with the training effectiveness of 97.6 %), the multilayer perceptron MLP 2-9-1 (with the training effectiveness of 99.7 %), the multilayer perceptron MLP 2-4-1 (with the training effectiveness of 97.6 %).

The training parameters of the synthesized neural networks based on the results of solving the optimization task are given in the table below:

Table 5.4 The results of solving the optimization task of the neural networks synthesis

Totals of the models								
No	Architecture	Training effectiveness	Performance control	Performance test	Training algorithm	Error function	Hidden neurons activity function	Output neurons activity function
1	MLP 2-7-1	0.976400	0.975040	0.976665	BFGS 224	Quadratic sum	hyperbolic	logistic
2	MLP 2-9-1	0.975863	0.974947	0.977057	BFGS 252	Quadratic sum	hyperbolic	identity
3	MLP 2-9-1	0.976452	0.974613	0.977243	BFGS 494	Quadratic sum	hyperbolic	exponent
4	MLP 2-9-1	0.997452	0.996349	0.997915	BFGS 133	Quadratic sum	hyperbolic	exponent
5	MLP 2-4-1	0.976123	0.975051	0.976370	BFGS 177	Quadratic sum	hyperbolic	logistic

Although all the synthesized networks possess a fairly high training effectiveness, the best result has been demonstrated by the MLP 2-9-1 network, which demonstrated the effectiveness in all the samples of 99.7 %, and secured the maximum forecast accuracy.

In order to verify the correctness of the construction of the time-series for radiation, it is also necessary to determine the adequacy of the input variables choice: the day and time in increments of 1 hour. A linear correlation coefficient has been used for the quantity evaluation of the density of the network connections (Table 5.5).

Table 5.5 The values of the correlation coefficients between the input and target variables

	Correlation coefficients		
	value Training	value Test	value Test
1	2	3	4
MLP 2-7-1	0.976400	0.975040	0.976665

Table 5.5 continuation

1	2	3	4
MLP 2-9-1	0.975863	0.974947	0.977057
MLP 2-9-1	0.976452	0.974613	0.977243
MLP 2-9-1	0.977452	0.976349	0.977915
MLP 2-4-1	0.976123	0.975051	0.976370

All the correlation coefficients are greater than 0.7, which indicates the adequacy of the input parameters choice.

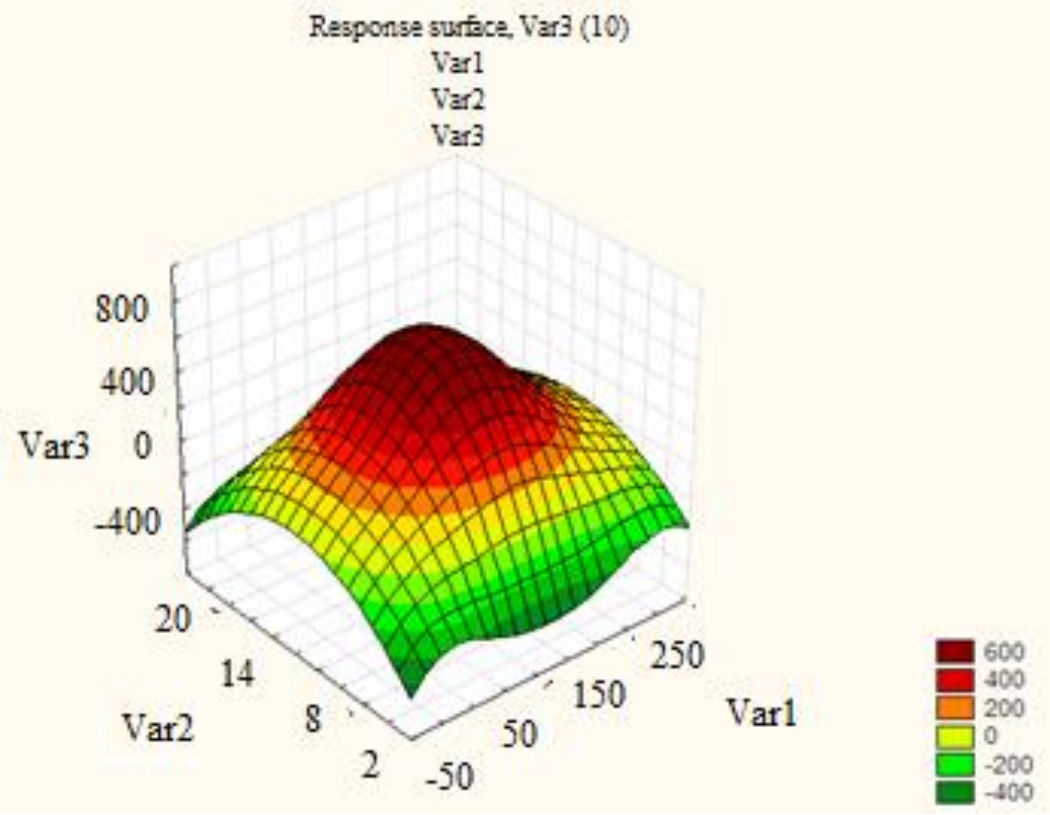

Fig. 5.12 The response surface between the input and output variables

The next step in the analysis of radiation time-series is to obtain the appropriate predictions which are to go beyond the training sample. In order to do this, we implement the projection of the time-series for each of the networks, setting the depth of the forecast at 8 steps forward (Fig. 5.13).

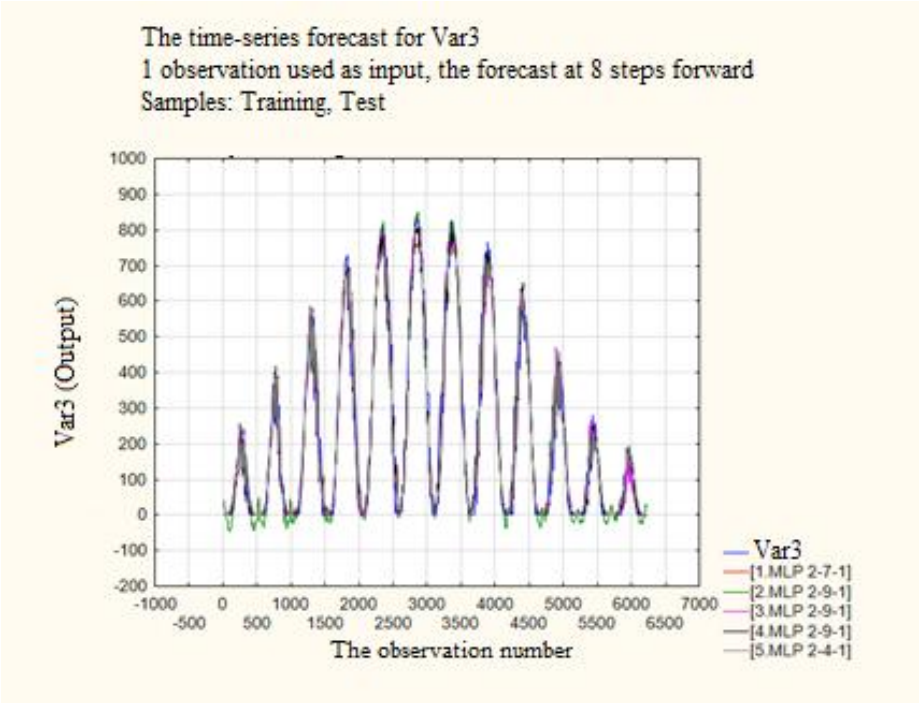

Fig. 5.13 The neural network projections of the radiation time-series

During the forecasting at 8 hours forward, generally sufficient accuracy of the forecast is observed (the mean square error being 1.76 % − 5.3 %). Thus, the use of the intelligent systems based on neural networks to forecast radiation by means of analyzing and processing the time-series data is accurate enough to be used in the control system.

Conclusions to chapter 5

1. The intelligent temperature control system of the poultry house has been developed and implemented and it provides an opportunity to forecast, on the basis of the NN classifier of temperature images, the change in the ambient temperature outside the technological facility where the biological component part is managed.
2. The intelligent system based on NNs has been created to forecast the external forecasting and radiation. The best result of forecasting the ambient temperature has been demonstrated by the MLP 2-8-1 network, which ensured the effectiveness of 99.7% in all the samples. The best result in forecasting solar radiation has been demonstrated by the MLP 2-9-1 network, which provided the effectiveness of 99.74% in all the samples. The developed intelligent system provides means for the maximum accuracy of forecasting the external natural disturbances and radiation which is taken into consideration while molding the control strategy for natural disturbances.
3. The intelligent temperature control system in the greenhouse based on the analysis and forecasting of the temperature and solar radiation has been developed in order to use the forecast results in the formation of control strategies for the greenhouse complexes for the purpose of reducing the energy costs in agricultural production.
4. The intelligent control algorithms for biotechnical facilities are to be created and scientifically substantiated with regard to the findings of the study and being determined with consideration of the forecasted changes in the external natural disturbances and the information on the quality of the biological component part. This would enable minimizing the cost of resources and ensure the maximum profit of the enterprise.

References to chapter 5

1. Besulin, V. I. 2003. Ptakhivnytstvo i tekhnolohiya vyrobnytstva yayets′ ta m'yasa ptytsi [Poultry farming and production technology of eggs and poultry meat]. Bila Tserkva State Agrarian University. 447 p. (in Ukrainian).
2. Magdelaine Pascale.2010. Future prospects for the European egg industry. World Poultry. Vol. 25 No 11:14-16.
3. Ivanov, K.P. 1990. The bioenergetic mechanisms of homeothermy [O bioénergeticheskikh mekhanizmakh gomoĭotermii.] Zhurnal obshchei biologii. Vol. 51, Issue 1:36-53.
4. Yaroshenko, F.O. 2004. Ptakhivnytstvo Ukrayiny: problemy i perspektyvy rozvytku [Poultry farming of Ukraine: state, problems and prospects of development]. Agrarna nauka. 504 p. (in Ukrainian).
5. Jan Hulzebosch. 2006. Wide range of housing options for layers. World Poultry. Vol. 22 No 6:20-22.
6. Gorobets, V.G., V.I. Trokhaniak, I.L. Rogovskii, T.I. Lendiel, A.O. Dudnyk, and M.Y. Masiuk. 2018. The numerical simulation of hydrodynamics and mass transfer processes for ventilating system effective location. INMATEH - Agricultural Engineering. Vol. 56, Issue 3:185-192.
7. Saleeva, I.P., A.V. Sklyar, T.E. Marinchenko, M.V. Postnova, A.V. Ivanov, and A.I. Tikhomirov. 2019. Proceedings of International Scientific and Technical Conference Smart Energy Systems, Article number 05070.
8. Gorobets, V.G., V.I. Trokhaniak, I.O. Antypov, and Y.O. Bohdan. 2018. The numerical simulation of heat and mass transfer processes in tunneling air ventilation system in poultry houses. INMATEH - Agricultural Engineering. Vol.55, Issue 2:87-96
9. Dudnyk, A., M. Hachkovska, N. Zaiets, T. Lendiel, and I. Yakymenko. 2019. Managing a greenhouse complex using the synergetic approach and neural networks. Eastern-European Journal of Enterprise Technologies. Vol. 4, Issue 2-100:72-78.

10. Lysenko, V. P. 2014. Artificial intelligence systems: fuzzy logic, neural networks, fuzzy neural networks, genetic algorithm. NULES of Ukraine. 341 p. (in Ukrainian).
11. Lysenko, V. and Dudnyk, A. 2016. Automation of biotechnological objects, Proceedings of International Conference on Modern Problems of Radio Engineering, Telecommunications, and Computer Science, pp. 44-46.
12. Platz, S., E. Heyn, F. Hergt, B. Weigl, and M. Erhard. 2009. Berliner und Munchener Tierarztliche Wochenschrift. Vol. 122, Issue 7-8:235-240.
13. Arbib M. 2003. The handbook of brain theory and neural networks. London: MIT Press. 1309 p.
14. Sajmon Hajkin. 2006. Neyronnyye seti: polnyy kurs. [Neural networks: full course]. Moscow, Vilyams, 1104 p. (in Russian).
15. Hawkins, Jeff. 2004. On Intelligence (1st ed.). Times Books. p. 272. ISBN 978-0805074567.
16. Kibzun A. 2002. Teorija Veroiatnostei I Matematicheskaia Statistika. [Theory of Probability and Mathematical Statistics]. Moskva: FIZMATLIT. p. 224. (in Russian).
17. Kruglov, V.V. and V.V. Borisov. Iskusstvennyye neyronnyye seti. Teoriya i praktika. [Artificial Neural Networks. Theory and practice]. 2001. Moscow, Goryachaya liniya - Telekom, 382 p. (in Russian).
18. Russell S. and Norvig P. 2010. Artificial Intelligence. Upper Saddle River: Prentice-Hall.
19. Ripley Brian D. 2007. Pattern Recognition and Neural Networks. Cambridge University Press. ISBN 978-0-521-71770-0.
20. Luger, George & Stubblefield, William. 2004. Artificial Intelligence: Structures and Strategies for Complex Problem Solving (5th ed.), The Benjamin/Cummings Publishing Company, Inc., c. 720, ISBN 0-8053-4780-1
21. Osowski, S. and Rudinskij, I. 2004. Nejronnye Seti Dlâ Obrabotki Informacii. Moskva: Finansy i Statistika. (in Russian).

22. Schmidhuber, J. 2015. Deep Learning in Neural Networks: An Overview. Neural Networks. 61: 85–117.
23. Aksenov, S.V and Novoseltsev, V.B. 2006. Organizatsiya i ispol'zovaniye neyronnykh setey (metody i tekhnologii) [Organization and use of neural networks (methods and technologies)]. Tomsk, NTL. 128 p. (in Russian).
24. Simon H. 2008. Neural Networks. New Delhi: Prentice-Hall of India.
25. Neural networks. StatSoft. Electronic textbook on statistics. Available at: http://www.statsoft.ru/home/textbook/modules/stneunet.html
26. Kuntsevich, V.M., Gubarev, V.F., Kondratenko, Y.P., Lebedev, D.V., Lysenko, V.P. (Eds). 2018. Control Systems: Theory and Applications. Series in Automation, Control and Robotics, River Publishers, Gistrup, Delft.
27. Kondratenko, Y. P., Chikrii, A. A., Gubarev, V. F., Kacprzyk, J. (Eds). 2019. Advanced Control Techniques in Complex Engineering Systems: Theory and Applications. Dedicated to Professor Vsevolod M. Kuntsevich. Studies in Systems, Decision and Control, Vol. 203. Cham: Springer Nature Switzerland AG.
28. J. Kacprzyk, et al. A Status Quo Biased Multistage Decision Model for Regional Agricultural Socioeconomic Planning Under Fuzzy Information. In: Kondratenko, Y.P., Chikrii, A.A., Gubarev, V.F., Kacprzyk, J. (Eds). 2019. Advanced Control Techniques in Complex Engineering Systems: Theory and Applications. Dedicated to Prof. V.M.Kuntsevich. Studies in Systems, Decision and Control, Vol. 203. Cham: Springer Nature Switzerland AG, pp. 201-226.
29. Schrader D. H., Mc Nelis D. D. Microwave Irradiation of Plant Roots in soil. - J. of Microwave Power. 1975. - vol. -10, № 1. - p. 77 - 91.
30. Thornley J.H.M., Hurd R.G. An Analysis of the Growth of Young Tomato Plants in Water Culture at Different Light Integrals and C02 Concentrations \\ Annals of Botany \ – Vol.38, Issue 2 – pp. 389-400 - 1979.
31. Huang N. E. Shen Z., Long S. R., Wu M. C., Shih H. H., Zheng Q., Yen N.-C., Tung C. C., and Liu H. H. The empirical mode decomposition and the Hilbert

spectrum for nonlinear and non-stationary time series analysis. Proceedings of R. Soc. London, Ser. A, 454, pp. 903-995, 1998.

32. The Hilbert-Huang transform and its applications / editors, Norden E. Huang, Samuel S.P. Shen. - World Scientific Publishing Co. Pte. Ltd. 5 Toh Tuck Link, Singapore 596224.
33. The empirical mode decomposition and the Hilbert spectrum for nonlinear and nonstationary time series analysis / Huang N. E., Shen Z., Long S. R., Wu M. L. [and others]. — Proc. R. Soc. London, 1998. — Vol. 454. — P. 903—995.
34. Kirill Ya. Kondratyev, Lev S. Ivlev, Vladimir F. Krapivin and Costas A. Varostos, Atmospheric Aerosol Properties: Formation, Processes and Impacts, Springer Praxis Books, 2006.
35. Applied Time Series Analysis: Basic techniques. Robert K. Otnes, Loren Enochson, Loren D. Enochson. Wiley, 1978 – 449 p.
36. Dudnyk A. O. Empirical mode decomposition of noise reduction of information channels of control systems of biotechnical objects / A.Dudnyk, V. Lysenko, V.Shtepa //Proceedings of the conference. 2012. – P. 8–9.
37. Lysenko V., Shtepa V., Dudnik A. (2011). Probability (Bayes) neural network of grading temperature modes. News of agrarian sciences, 4, 53-56. (in Ukrainian).

CHAPTER 6. SYNTHESIS OF CONTROL SYSTEMS WITH SYNERGETIC APPROACH AND NEURAL NETWORKS

6.1 Synthesis of effective management strategies using synergetic approach

A distinctive feature in managing current neural networks is the presence of an appropriate set of direct and inverse relationships. Intelligent management of a greenhouse complex must take into consideration that the application of intelligent control systems is based on the principles listed below, as confirmed by studies that addressed the neuro-fuzzy systems to control energy consumption at greenhouses and biotechnological facilities [1, 2]:

- the presence of a close informational interaction between control systems and actual external environment and the use of specially organized information communication channels;
- principal openness of the systems in order to enhance intelligence and improve their own performance;
- the existence of mechanisms to predict the external world and their own performance across the dynamic world of innovation;
- building a management system in the form of a multilevel hierarchical structure in accordance with the rule: improving intelligence while reducing requirements to accuracy as the rank of the hierarchy increases;
- maintaining operation at a disruption in communication or at a loss of controlling influence from the higher levels of hierarchy of the governing structure.

By accounting for these principles, the systems of this kind could be synthesized by achieving the combination of processes of self-organization and management, namely, through using, in order to synthesize intelligent control systems, the synergistic approach.

Such an approach is most similar to the applied theory of management that implies a transition from the initial task, including managing the object of control and

an external force. The next stage forms an expanded statement of the task such that external forces become internal interactions within a general (closed) system. To do this, external influences are represented as partial solutions to some additional differential equations that describe an information model, thereby exercising their "immersion" into the general structure of the extended system [3].

In this case, an important issue for the synthesized control system is the robustness of its functioning. This is defined in part by the principle of preserving the operation at a loss of communication. A given task could be solved as a result of separating the internal processes of functioning of a greenhouse complex, which could be achieved by using a neural network technology. This indicates the relevance of our research aimed at intelligent management of a greenhouse complex using the synergistic approach and artificial neural networks.

Paper [4] proposed a synergistic approach to managing complex technological facilities, to defining and describing the areas to attract the attractor as the centers that form dissipative space-time structures. The reported research results allow the estimation of performance of a complex system from the point of view of self-organization for the case of chaotic influences, both external and internal. However, the issue on the synergistic control over complex systems remains to be resolved, namely managing a greenhouse complex. The reason for this may be that special attention should be given not to the force of action on the system but rather to considering the accuracy and character of information support to decision making [1, 5]. It is the accuracy of information support for decision-making that defines an efficient organizational and technical structure.

Synthesis of effective management strategies to control non-linear systems was examined by using the methods pacification [5], backstepping [6, 7], robust [8, 9] and synergistic control [5, 10]. Among them, the most promising for complex greenhouse facilities are the methods of synergistic control, discussed in papers [10-12]. From the point of view of unresolved issues within the framework of the current study, these papers described the algorithm of adaptive control over nonlinear systems, the application of an integrated synergistic approach to complex non-linear objects, as

well as successful implementation of the proposed solutions. All this gives grounds to assert that it is expedient to apply a given approach, which makes it possible to consider the physical and chemical features of technological processes, to reflect the phenomena of natural self-organization. Application of a set of the synergistic approach and artificial neural networks provides for resource-saving modes of operation. These operation modes are characterized by resistance against external perturbations, structural and parametric changes; in addition they make it possible to organize an efficient search for target states under different conditions. The resource-saving modes of operation are distinguished by the necessary flexibility at modifying goals and task variation; they have high reliability and ability to avoid emergencies [5, 13].

Still unresolved are issues on optimal planning and synergistic control over multi-parametric objects that have the input, output, and disturbing coordinates.

Paper [10] describes modern approaches to methods for managing an object based on the synergistic approach. If control is carried out by changing parameters of the order, the result of such actions would be the instability, symmetry disruption, as well as break in the boundaries of a complex nonlinear system. Consequently, there could be several possible scenarios of system performance after a phase transition. For the case of control by modifying the initial conditions there is a possibility for the system to develop in multiple directions, including a chaotic performance. The difficulty of such an approach is that it is not always possible to change the initial conditions. Sometimes the regulation is strict. Each of these methods is used when it is impossible to apply another. Thus, if there is a prospect, given a set of characteristics and parameters for the system, to define the set of parameters of order, and there is no any possibility to change input conditions, then control is executed by changing the parameters of order. If the set of parameters is too large, or one cannot define them through complex inter-relationships within the system, it is necessary to use control by modifying the initial conditions.

Moreover, study [2] has been shown that these methods produce satisfactory results for the models of actual systems subject to idealization. All this gives grounds

to assert that it is expedient to study new approaches to the management of complex non-linear technological systems such as a greenhouse complex. This part of the task could be solved by combining the proposed synergistic approach and artificial neural networks. The task is based on the synthesis of a neural network controller based on a dynamic controller with the synergetic control law (in parallel with a sequential consideration of invariant multi-images of control over values for temperature and humidity of the internal air at a greenhouse) and could be solved by training an artificial neural network of the preset configuration.

The aim of this study is the synthesis of an intelligent control system for a greenhouse complex using the synergistic approach and artificial neural networks. The proposed approach would provide the necessary possibilities for practical research and for applying the results in order to predict subsequent performance of an object and, in the future, in order to devise effective resource-saving control strategies for a greenhouse complex.

To accomplish the aim, the following tasks have been set:

- to construct control laws that would ensure optimal control over operational modes of a greenhouse;
- to synthesize a neural network controller for a greenhouse complex;
- to synergistically synthesize a greenhouse complex controller.

Mathematical model (6.1), (6.2) describes changes in the temperature and humidity of inside air in a greenhouse [14]

$$\begin{aligned} \frac{dT_{ins}(t)}{dt} &= \frac{1}{\rho C_a V_t}[Q_h(t) + S_a(t) - \lambda Q_f(t)] - (\frac{v_\upsilon(t)}{V_t} + \frac{k_{t.gr.}}{\rho C_a V_t})[T_{ins}(t) - T_{out}(t)], \\ \frac{d\varphi_{ins}(t)}{dt} &= \frac{1}{V_r} Q_f(t) + \frac{1}{V_r} E[S_a(t), \varphi_{ins}(t)] - \frac{v_\upsilon(t)}{V_r}[\varphi_{ins}(t) - \varphi_{out}(t)] \end{aligned} \quad (6.1)$$

$$E[S_a(t), \varphi_{ins}(t)] = \alpha \frac{S_\alpha(t)}{\lambda} - \beta \varphi_{ins}(t)] \quad (6.2)$$

where T_{ins}, T_{out} is the air temperature inside and outside a greenhouse, respectively, (°C);

φ_{ins}, φ_{out} is the relative air humidity inside and outside a greenhouse, respectively, (%);

$k_{t.gr.}$ is the coefficient of heat transfer for a greenhouse enclosure (W/K);

V is the full geometric volume of a greenhouse, (m^3);

V_t, V_r is the volume of air that is heated and moistened, respectively (m^3).

It is typically 60-70 % of the total volume of a greenhouse.

ρ is the air density (1.2 kg/m^3);

C_a is the heat capacity of air (1.005 $kJ\text{-}kg^{-1}\text{-}K^{-1}$);

Q_h is the power of air heating system in a greenhouse, (W);

Q_f is the performance of a fogging system, (g water/s);

S_a is the solar radiation absorbed by a greenhouse (W);

λ is the heat of vaporization, (2,256 kJ/kg);

v_υ is the air exchange, provided by a system of ventilation, (m^3/s);

$E[S_a(t), \varphi_{ins}(t)]$ is the evapotranspiration of plants as a function of the absorbed solar radiation and air humidity in a greenhouse (g water/s);

α, β are scale ratios.

By assessing the performance, one can conclude that the system is non-linear in nature. To study such a system (6.3), (6.4) and to define optimal control over it, it is necessary to use the method of analytical construction of aggregated controllers.

$$\frac{dT_{ins}(t)}{dt} = M_1 \cdot [M_2 \cdot Q_h(t) + S_a(t) - M_3] - (\frac{v_\upsilon(t)}{M_4} + M_5)[T_{ins}(t) - T_{out}(t)], \quad (6.3)$$

$$\frac{d\varphi_{ins}(t)}{dt} = M_6 \cdot Q_f(t) + M_7 \cdot [E(S_a(t), \varphi_{ins}(t))] - \frac{v_\upsilon(t)}{M_8}[\varphi_{ins}(t) - \varphi_{out}(t)] \quad (6.4)$$

where M_1–M_8 are the model's parameters that take into account design features of a greenhouse.

According to the method of analytical construction of aggregated controllers, it is necessary to define control laws u_i, which ensure optimal control over the modes of greenhouse operation. The chosen control u_1 is the value for air temperature inside a greenhouse $T_{ins}(t)$, the chosen control u_2 is the value for humidity of inside air in a

greenhouse φ_{ins}.

In accordance with the method of analytical construction of aggregated controllers, control laws depend on:

$$\begin{aligned} &u_1(Q_h, S_a, T_{ins}, T_{out}) \\ &u_2(Q_f, \nu_\upsilon, \varphi_{ins}, \varphi_{out}) \end{aligned} \tag{6.5}$$

Such laws are executed when the optimal values for temperature and humidity of inside air in a greenhouse are provided. To this end, it is necessary to ensure the power of the system that heats air in a greenhouse, the air exchange, which is provided for by a ventilation system. Important parameters also include the output of a fogging system and the solar radiation absorbed by a greenhouse. In addition, the temperature and humidity of air inside a greenhouse are dramatically affected by the temperature and humidity outside the greenhouse.

According to the method of analytical construction of aggregated controllers, we have defined managing actions shown in Fig. 6.1. To proceed with the study, we must consider invariant manifolds.

$$\begin{aligned} &\psi_1(Q_h, S_a, T_{ins}, T_{out}) = 0 \\ &\psi_2(Q_f, \nu_\upsilon, \varphi_{ins}, \varphi_{out}) = 0 \end{aligned} \tag{6.6}$$

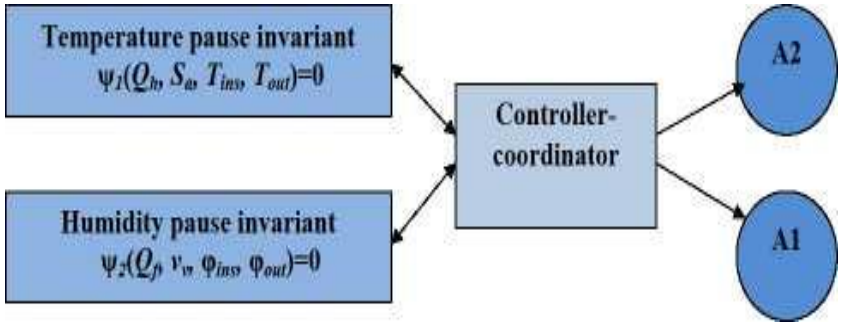

Fig. 6.1 Synergistic principle of hierarchy (A1 — temperature pause attractor; A2 — humidity pause attractor)

Parallel sequential consideration of invariant manifolds allows us to examine the invariants as attractors with pulling zones when applying control laws u_1=(Q_h, S_a, T_{ins}, T_{out}); u_2 = (Q_f, ν_υ, φ_{ins}, φ_{out}).

The system floats across a phase space until intersecting the manifolds ψ_1=0,

ψ_2=0. Since the output of a fogging system and the solar radiation absorbed by a greenhouse do not directly influence control u_1, u_2, it is necessary to provide this connection via ψ_i.

$$\begin{aligned} \psi_1 &= T_{ins} + (Q_h, S_a, T_{out}) \\ \psi_2 &= \varphi_{ins} + (Q_f, v_\upsilon, \varphi_{out}) \end{aligned} \tag{6.7}$$

Considering dependences (6.5) and (6.6), we obtain:

$$\begin{aligned} T_{ins} + (Q_h, S_a, T_{out}) &= 0 \\ \varphi_{ins} + (Q_f, v_\upsilon, \varphi_{out}) &= 0 \end{aligned} \tag{6.8}$$

To employ the method, it is necessary to apply (6.8):

$$T_{ins} \cdot \psi_{ins}(\tau) + \psi_{ins}(\tau) = 0 \tag{6.9}$$

where τ is time, (s).

It follows from the model's equation and equation (6.8) that

$$\begin{aligned} &T_1\left[\frac{dT_{ins}}{dt} + \frac{dv}{dQ_h}\cdot\frac{dQ_h}{dt} + \frac{dv}{dS_a}\cdot\frac{dS_a}{dt} + \frac{dv}{dT_{out}}\cdot\frac{dT_{out}}{dt}\right] + T_{ins} + v + (Q_h, S_a, T_{out}) = 0 \\ &T_2\left[\frac{d\varphi_{ins}}{dt} + \frac{dv}{dQ_f}\cdot\frac{dQ_f}{dt} + \frac{dv}{dv_\upsilon}\cdot\frac{dv_\upsilon}{dt} + \frac{dv}{d\varphi_{out}}\cdot\frac{d\varphi_{out}}{dt}\right] + \varphi_{ins} + v + (Q_f, S_a, \varphi_{out} = 0 \end{aligned} \tag{6.10}$$

where v is some dependence function of actual technological parameters. Control laws over technological pauses will be equal:

$$\begin{aligned} u_1 &= \frac{T_{ins} + v}{\varphi_{ins} T^1} + \frac{\frac{Q_h}{M^2 + Q_h}\cdot M^2 \cdot \frac{M^3}{M^4 + S_a \cdot M^4}}{\varphi_{ins}} + \frac{dv}{vS_a}\cdot\frac{\frac{v_\upsilon}{M^5 + v_\upsilon}\cdot\frac{M^5}{M^4 + T_{out}\cdot M^4}}{\varphi_{ins}} + \frac{dv}{vT_{out}}, \\ u_2 &= \frac{\varphi_{ins} + v}{T_{ins} T^2} + \frac{\frac{Q_f}{M^6 + Q_f}\cdot M^7 \cdot \frac{M^6}{M^8 + E}}{T_{ins}} + \frac{dv}{vE}\cdot\frac{\frac{v_\upsilon}{M^5 + v_\upsilon}\cdot\frac{M^5}{M^4 + \varphi_{ins}\cdot M^4}}{T_{ins}} + \frac{dv}{v\varphi_{out}}, \end{aligned} \tag{6.11}$$

where T_1, T_2 are the synergistic controller's parameters.

A structural diagram of the considered control system for a greenhouse complex, executed in the software environment MATLAB Simulink 16, is shown in Fig. 6.2.

In a given scheme, functional unit fun_block1 simulates the resulting synergetic dynamic controller, it contains computation of macro-variable ψ_1, ψ_2, (6.6) and implements control law (6.11). Input signals to the unit are temperature and

humidity. The output signal from the unit is control law u_1.

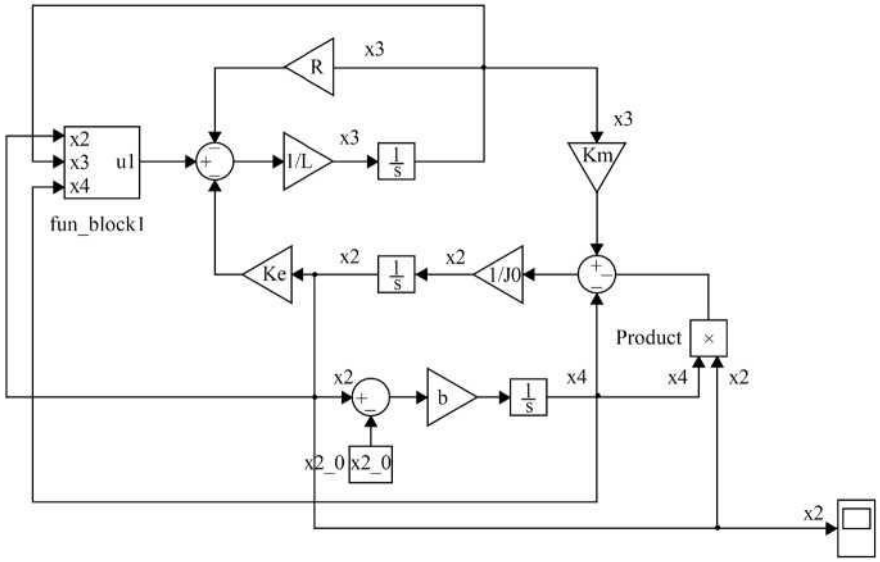

Fig. 6.2 Structural diagram of control system for a greenhouse complex

In order to achieve the set goal (for the derived control law), we shall synthesize a neural network controller by training it to functions implemented by unit fun_block1.

6.2 Synthesis of a neural network controller based on the synergetic control law

In a general case, solving the task set for the designed neural network controller reduces to synthesizing a multi-layer artificial neural network of direct propagation, trained to approximate the required function.

When building a neural network controller of this kind, it is important to determine:

- dimensionality of the neural network (the number of layers in the network and the number of neurons at each layer, required to ensure the required accuracy of functioning);

- the applied activation functions in neurons.

Determining the dimensionality of a neural network for solving a particular task very often depends on the experience of the developer. However, as noted by authors in [2], a network that consists of at least two layers and which has, in the

hidden layer, an arbitrary number of neurons, could approximate almost any nonlinear function. This, in most cases, underlies the use of artificial neural networks to solve control tasks. Owing to their architecture, such networks make it possible to supplement an artificial neural network with *a priori* knowledge about the desired law of signal processing within the network.

Based on this, to solve the set problem, it is advisable to choose a double-layer artificial neural network of direct propagation. Because the chosen input signals to the network are ψ_1, ψ_2, the chosen output signal - control law u_1, then the number of neurons in the input layer is 2 (the number of input components), in the output layer - 1 neuron. In this case, the number of neurons in the hidden layer is considered to equal 40. A given number is selected considering the provision of a reserve redundancy in the structure of the neural network.

We shall apply, as an activation function in neurons at the hidden and output layer, a sigmoidal activation function, which:

- satisfies the conditions for the input data range (0, 1);
- makes it possible to implement the full range of values for input signals;
- does not limit a solution that employs the neural network with discrete values.

In the process of learning, inside an artificial neural network, its own algorithm-solution is generated, according to which the information that enters the network is generalized. That is why, it is expedient to form, as a training sample, the sets of signals that most fully capture the entire range of possible input signals and corresponding solutions at the output. In this case, to produce an optimal solving algorithm, we shall train the neural network in the form not explicitly dependent on time.

6.3 Practical application of resource-efficient control strategies in synergetic automation systems

Our research based on artificial neural networks for a greenhouse complex has made it possible to “teach” a neural network controller. At the next stage, it is

necessary to calculate parameters for the units that will scale the input and output signals in order to ensure the proper functioning of the intelligent system.

The accepted parameters for a control system whose structure employs a neural network controller take the form shown in Fig. 6.3.

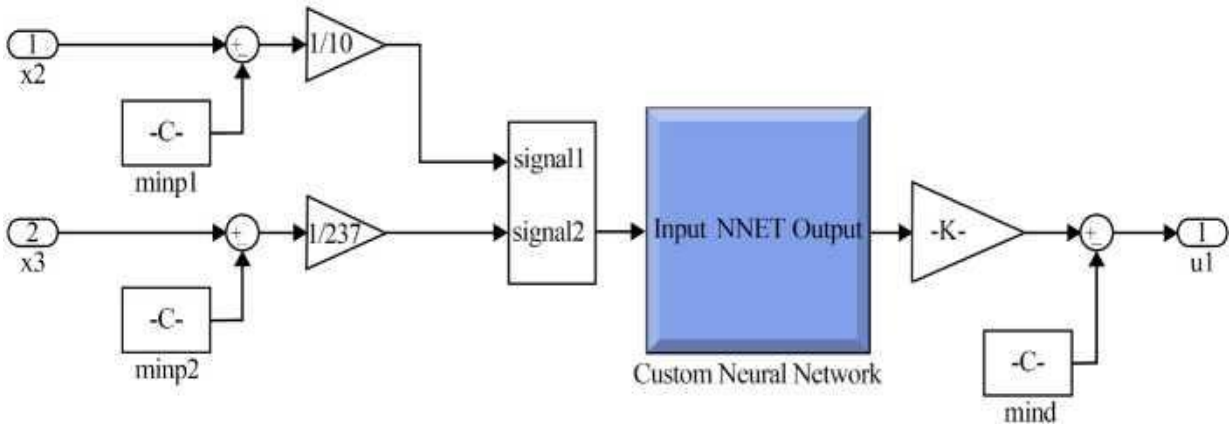

Fig. 6.3 Structure of the neural network controller for a greenhouse complex

Having synthesized a neural network controller in this fashion and by placing it inside a closed control system, we shall evaluate its functioning.

To do this, we shall assign the above-presented parameters for the control system and simulate system operation at different values for temperature and humidity at a greenhouse complex. Fig. 6.4 shows simulation charts for a temperature inside a greenhouse of 24 °C.

Fig. 6.5 shows simulation charts of air humidity inside a greenhouse (humidity value=60 %).

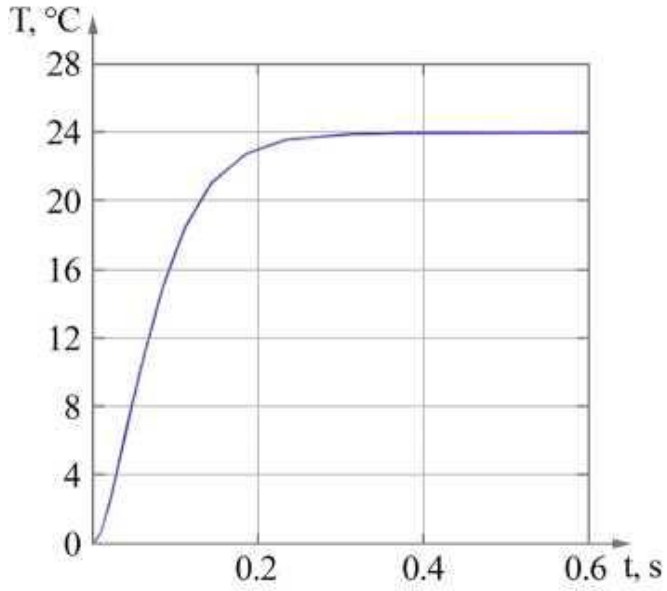

Fig. 6.4 Charts of temperature change inside a greenhouse, at T=24 °C

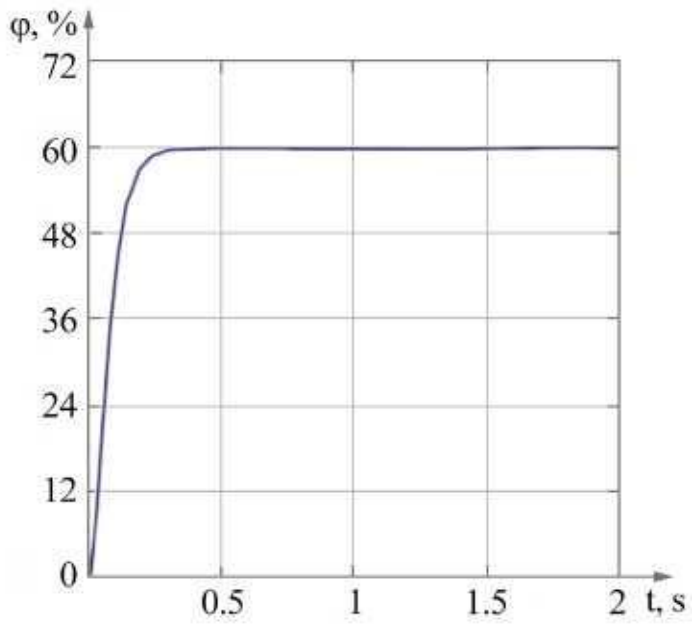

Fig. 6.5 Charts of change in humidity inside a greenhouse, at φ=60 %

Next, we shall simulate, by employing the Simulink programming tools, external disturbing effects on a neural network system for two cases:

1) random disturbance that generates a signal that is filled according to the Gaussian distribution;
2) the disturbance of harmonic character.

Simulation results for random disturbances are shown in Fig. 6.6.

Simulation results for harmonic disturbances are shown in Fig. 6.7.

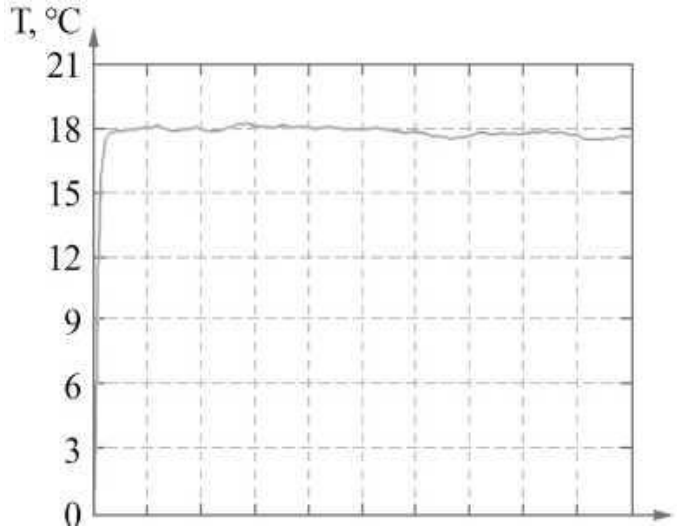

Fig. 6.6 Chart of change in temperature when a system is exposed to random disturbances

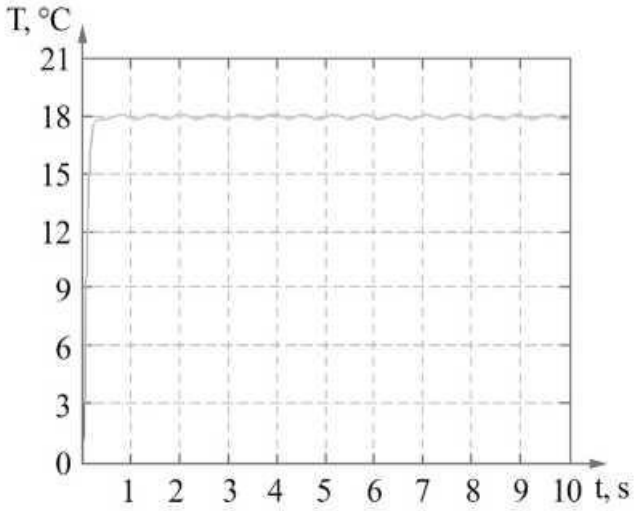

Fig. 6.7 Chart of change in temperature when a system is exposed to harmonic disturbances

In general, the simulation results show (Fig. 6.6, 6.7) that a neural network controller, synthesized based on the synergetic dynamic controller (6.9), demonstrates, compared with conventional approaches, better quality indicators for transients. As well as over a wide range of changes in parameters: temperature, air humidity in a greenhouse, greenhouse air heating system capacity, the output of a fogging system, solar radiation absorbed by a greenhouse, heat of vaporization, air exchange that is enabled by a ventilation system; it possesses capability to adapt to

parametric and external disturbances.

Practical value of the research results obtained when applying a synergistic approach to artificial systems is in that such systems are characterized by ideology of unification in the processes of targeted self-organization and control. According to the method of analytical construction of aggregated controllers, we have defined managing actions for a greenhouse complex, shown in Fig. 6.1. In addition, the considered invariant manifolds have made it possible to construct the laws controlling the temperature and air humidity in a greenhouse (6.11), which ensure the optimal management of the greenhouse operating modes. Owing to this, there is the possibility to generate predictive information that would allow the design of a variety of systems.

The use of artificial neural networks for a greenhouse complex (namely, their features - learning on the experimental sample and parallel information processing) provides high performance (Fig. 6.6, 6.7). The performed synthesis of a neural network controller for a greenhouse complex produces its own solving algorithm, according to which the information about a value for temperature and humidity inside a greenhouse that enters the network is generalized. We have formed the sets of signals (6.10) to use as a training sample, which most fully capture the entire range of possible input signals and corresponding solutions at the output. Construction of the optimal solving algorithm to train a neural network is given in the form not explicitly dependent on time. It should also be noted that our study makes it possible to simultaneously monitor processes that occur at an actual facility. This becomes possible through the distributed processes of internal functioning.

Having synthesized the neural network controller and by placing it inside a closed system of management, we estimated its functioning. The assigned parameters for the control system (6.11) and simulation results at different values for temperature and humidity at a greenhouse complex are shown in Fig. 6.4-6.7.

Thus, the integrated use of the synergistic approach (6.6) and neural network structures (6.11) has made it possible to synthesize an intelligent control system for a greenhouse complex, whose feature is parallel computation of patterns in functioning

and accounting of the principles of inner self-organization.

The disadvantage of the current research is an insufficiently high degree of examining the artificial neural network redundancy, which ensures the safety of functioning at disruption of a connection or at loss of controlling influences.

In the future, we plan to undertake a research into a greenhouse complex using the synergistic approach and artificial neural networks for the entire set of technological parameters and material flows.

Conclusions to chapter 6

1. The laws to control the air temperature and humidity in a greenhouse according to the analytical construction of aggregated controllers that ensure optimal control over the greenhouse operation modes were constructed. The proposed synergistic controller for a greenhouse complex possesses a kind of “intelligence” and so successfully adapts to non-controlling disturbances (disturbing effects on a neural network system that form a Gaussian-distributed signal and the disturbances that are harmonic in character) that act on the system.
2. A neural network controller was synthesized and trained on functions that are implemented by unit fun_block1 to derive the control laws for temperature and humidity inside a greenhouse. This enabled the development of effective systems of synergetic control that ensure maximal utilization of own resources of the controlled object owing to the phenomena of self-organization.
3. The synergistic synthesis of controller for a greenhouse complex has been performed. The simulation results showed that the neural network controller, synthesized on the basis of a synergetic dynamic controller, demonstrates, when compared to conventional approaches, better quality indicators of transient processes and adaptation to parametric and external disturbances.

References to chapter 6

1. Dudnyk, A., Lysenko, V., Zaets, N., Komarchuk, D., Lendiel, T., Yakymenko, I. (2018). Intelligent Control System of Biotechnological Objects with Fuzzy Controller and Noise Filtration Unit. 2018 International Scientific-Practical Conference Problems of Infocommunications. Science and Technology (PIC S&T). doi: https://doi.org/10.1109/infocommst.2018.8632007.
2. Lysenko, V., Dudnyk, A., Yakymenko, I. (2017). Design peculiarities of neuro-fuzzy control system of energy consumption in greenhouses. Enerhetyka i avtomatyka, 4. P. 60-69.
3. Loveikin, V. S., Romasevych, Y. O. (2017). Dynamic optimization of a mine winder acceleration mode. Naukovyi Visnyk Natsionalnoho Hirnychoho Universytetu, 4, P. 55-61.
4. Gao, A., Chen, H., Hou, A., Xie, K. (2019). Efficient antimicrobial silk composites using synergistic effects of violacein and silver nanoparticles. Materials Science and Engineering: C, 103, 109821. doi: https://doi.org/10.1016/j.msec.2019.109821.
5. Vogeling, H., Plenagl, N., Seitz, B. S., Duse, L., Pinnapireddy, S. R., Dayyoub, E. et. al. (2019). Synergistic effects of ultrasound and photodynamic therapy leading to biofilm eradication on polyurethane catheter surfaces modified with hypericin nanoformulations. Materials Science and Engineering: C, 103, 109749. doi: https://doi.org/10.1016/pmsec.2019.109749.
6. Hossine, G., Katia, K. (2017). Improvement of vector control of Dual Star Induction drive using synergetic approach. 2017 14th International Multi-Conference on Systems, Signals & Devices (SSD). doi: https://doi.org/10.1109/ssd.2017.8167006.
7. Prophet, S., Atman, J., Trommer, G. F. (2017). A synergetic approach to indoor navigation and mapping for aerial reconnaissance and surveillance. 2017 International Conference on Indoor Positioning and Indoor Navigation (IPIN). doi: https://doi.org/10.1109/ ipin.2017.8115919.

8. Chernetski, N., Kishenko, V., Ladanyuk, A. (2015). An upgrade of predictor functions based on the analysis of line- series for mashing beer wort. Eastern-European Journal of Enterprise Technologies, 4 (2 (76)), 57-62. doi: https://doi.org/10.15587/ 1729-4061.2015.47350.
9. Li, K., Qi, X., Wei, B., Huang, H, Wang, J, Zhang, J. (2017). Prediction of transformer top oil temperature based on kernel extreme learning machine error prediction and correction. Gaodianya Jishu/High Voltage Engineering, 43 (12) , 4045-4053, doi: http://dti.ttg/10.13336/j.1003-6520.hve.20171127032
10. Zhou, J. Adaptive Backstepping Control of Uncertain Systems Nonsmooth Nonlinearities, Interactions or Time-Variations / J. Zhou, C. Wen // SpringerVerlag Berlin Heidelberg, 2008. – 241 p.
11. Prophet, S., Atman, J., & Trommer, G. F. (2017). A synergetic approach to indoor navigation and mapping for aerial reconnaissance and surveillance. Paper presented at the 2017 International Conference on Indoor Positioning and Indoor Navigation, IPIN 2017, 2017-January 1-8. doi:10.1109/IPIN.2017.8115919 Retrieved from www.scopus.com.
12. Gao, Q., Zribi, M., Escorihuela, M. J., & Baghdadi, N. (2017). Synergetic use of sentinel-1 and sentinel-2 data for soil moisture mapping at 100 m resolution. Sensors (Switzerland), 17(9) doi:10.3390/s17091966.
13. Zhang, X., Che, L., Shahidehpour, M., Alabdulwahab, A. S., & Abusorrah, A. (2017). Reliability-based optimal planning of electricity and natural gas interconnections for multiple energy hubs. IEEE Transactions on Smart Grid, 8(4), 1658-1667. doi:10.1109/TSG.2015.2498166.
14. Dudnyk, A. (2018). Method of designing a resource-effective control system for vegetable growing modes in greenhouses. Scientific Gerald of National University of life and environmental sciences of Ukraine. Vol. 283, P. 81-88.

TABLE OF CONTENTS